The Importance of the Natural Transmission of Rift Valley Fever Virus for Its Infection in the Mammalian Host

Dissertation

to obtain the degree Doctor of Philosophy
from the Faculty of Mathematics, Informatics and Natural Sciences
Department of Biology
University of Hamburg

submitted by

András Bencsik

Hamburg
2023

The present work was performed under the supervision of Prof. Dr. Esther Schnettler and Prof. Dr. César Muñoz-Fontela at the Bernhard Nocht Institute for Tropical Medicine (BNITM) in Hamburg.

Evaluators

1st Reviewer: **Prof. Dr. Esther Schnettler**
Bernhard Nocht Institute for Tropical Medicine
Research Group Mosquito-Virus Interaction
Bernhard-Nocht-Straße 74, 20359 Hamburg

2nd Reviewer: **Prof. Dr. Minka Breloer**
Bernhard Nocht Institute for Tropical Medicine
Research Group Helminth Immunology
Bernhard-Nocht-Straße 74, 20359 Hamburg

Date of oral defence: 05.03.2024

Eidesstattliche Versicherung - Declaration on oath

Hiermit erkläre ich an Eides statt, dass ich die vorliegende Dissertationsschrift selbst verfasst und keine anderen als die angegebenen Quellen und Hilfsmittel benutzt habe.

I hereby declare, on oath, that I have written the present dissertation by my own and have not used other than the acknowledged resources and aids.

Hamburg, den 18.12.2023 Unterschrift/Signature

Acknowledgement

I would like to thank the following people without whom I would not have been able to complete this dissertation. Firstly, I would like to thank all the past and present members of the virus immunology and mosquito virus interaction groups at the Bernhard Nocht Institute for Tropical Medicine. I owe special thanks to my supervisors, Prof. Esther Schnettler, who has helped me over the years not only with her insightful knowledge but also with her kind and encouraging mentorship, and Prof. César Muñoz-Fontela whose expertise and guidance kept me on track and inspired me to look for the bigger picture. I am eternally grateful to my former mentor Dr. Zoltán Pós; without your teaching in the past, I could never have succeeded in this project. I also owe my gratitude to the Joachim Herz Foundation for funding this project.

I would like to thank Sergio Gómez Medina for the BSL-3 training and Dr. Mayke Leggewie and Dr. Mine Altinli for showing me how to work with mosquitoes. I owe my gratitude to Dr. Dániel Cadar for his help with the sequencing, and to Dr. Susanne Krasemann for preparing the histology sections.

I would like to thank Dr. Catherine Awuor Olal for encouraging me to pursue experiments I had given up on before even trying, also for her input and moral support together with Dr. Emily Nelson and Monika Rottstegge. Your friendship helped me to see this through to the end.

I am thankful to Pedro Neira for always helping me with my molecular biology questions, and to Dr. Beatriz Escudero-Pérez for her help with the TVAs and for training me for BSL-4 work. Thank you to all the Herzis for helping me navigate life in Germany and, most importantly, for all the great times we have spent together.

I would like to thank my friends in Hungary, Barbara Gellén, Dr. Barbara Molnár-Érsek, Krisztián Tóth and Dr. Erik Zajta for their endless efforts to remain my friends despite the great distances this project has created between us. Your support meant a lot to me while I was so far from home. Of course, I would like to thank my family. Köszönöm, hogy hittetek bennem és erőtökön felül támogattatok ezen a hosszú és embert próbáló úton!

Finally, and most importantly, to my partner, Matthijs Van Daele, for being my rock and solid ground during these difficult years. Thank you for your love, your support and the sacrifices you have made, enabling me to pursue my calling. I could not have done it without you.

Table of contents

List of figures

List of tables

Abbreviations

Abl2	Abelson murine leukaemia viral oncogene homolog 2
ADCC	antibody-dependent cell cytotoxicity
AECI	type I alveolar epithelial cell
AECII	type II alveolar epithelial cell
ALN	auricular lymph node
AMf	alveolar macrophage
APC	antigen-presenting cell
arbovirus	arthropod-borne virus
BBB	blood-brain barrier
BCR	B cell receptor
BNITM	Bernhard Nocht Institute for Tropical Medicine
CCL	C-C motif ligand
CD	cluster of differentiation
cDC	classical dendritic cell
CLR	C-type lectin receptors
CNS	central nervous system
CPE	cytopathic effect
DC	dendritic cell
DC-SIGN	dendritic cell-specific ICAM-grabbing non-integrin
ds	double-stranded
ELISA	enzyme-linked immunosorbent assay
EMA	European Medicines Agency
Fc	fragment crystallizable
FDA	US Food and Drug Administration
FSC	forward scatter
Gc	glycoprotein C
Gn	glycoprotein N
H&E	haematoxylin-eosin
ICAM	intercellular adhesion molecule
ID	intradermal
IFN	interferon
Ig	immunoglobulin
IL	interleukin
IMf	interstitial macrophage
IN	intranasal
IRF	interferon regulatory factor
kDa	kilodalton
KO	knock-out
LC	Langerhans cell
LD	lethal dose
LDL	low-density lipoprotein
Lrp1	LDL receptor-related protein 1
L-SIGN	liver/lymph node-specific intercellular adhesion molecule-3-grabbing integrin
Ly-6C	lymphocyte antigen 6 complex
Mf	macrophage

MHC	major histocompatibility complex
mL	millilitre
MLN	mediastinal lymph node
moDC	monocyte-derived dendritic cell
MOI	multiplicity of infection
moLC	monocyte-derived Langerhans cell
mRNA	messenger ribonucleic acid
NHP	non-human primate
NK cell	natural killer cell
NLR	nucleotide-binding oligomerisation domain (NOD)-like receptor
NOD	nucleotide-binding oligomerisation domain
Np	nucleoprotein
NSm	non-structural protein of M segment
NSs	non-structural protein of S segment
PAMP	pathogen associated molecular pattern
PBS	phosphate-buffered saline
pDC	plasmacytoid dendritic cell
PFA	paraformaldehyde
PFU	plaque-forming unit
PRR	pattern recognition receptor
RdRp	RNA-dependent RNA polymerase
RIG-1	retinoic acid inducible gene-I
RLR	retinoic acid inducible gene-I (RIG-I)-like receptor
RNA	ribonucleic acid
RNP	ribonucleoprotein
RT-PCR	reverse transcription polymerase chain reaction
RVF	Rift Valley fever
RVRF	Rift Valley fever virus
SC	subcutan
SEM	standard error of mean
Siglec-H	sialic-acid-binding immunoglobulin-like lectin-H
SIRPα	Signal regulatory protein α
ss	single-stranded
SSC	side scatter
Tc cell	T cytotoxic cell
TCR	T cell receptor
TFIIH	transcription factor IIH
TGF	tumor growth factor
Th cell	T helper cell
TLR	toll-like receptor
TNF	tumor necrosis factor
Treg	T regulatory cell
tSNE	t-distributed stochastic neighbour embedding
VCAM1	vascular cell adhesion molecule 1
WHO	World Health Organisation
WT	wild type
XCR1	X-C motif chemokine receptor 1

Summary

The objective of this study was to provide a better understanding on viral and host factors that influence the outcome of Rift Valley fever virus (RVFV) infection in mammalian host.

The main aim was to focus not only on one factor – as it usually were in previous studies – but to investigate how these multiple factors – which occur in natural infections – together determine the disease course.

The results of infecting wild type (WT) laboratory mice with RVFV, isolated either from a human patient (huRVFV) or from a mosquito (mosRVFV), emphasize the infection route as a major determinant in pathogenesis. Importantly, the effect of the infection route was directly opposite depending on the virus isolate. While intradermal (ID) infection with the human isolate resulted in higher mortality rate compared to the intranasal (IN) route, disease symptoms also occurred earlier following the dermal route. On the contrary, more animals succumbed to the disease after IN infection with the mosquito isolate.

Investigation of the viral dissemination revealed further, unexpected differences: huRVFV was widely disseminated throughout the body and was uniformly present in all investigated organ samples except the brain for most cases. Furthermore, accelerated dissemination was observed following ID infection. Strikingly, mosRVFV was detectable only in the skin following ID infection or in the brain of infected animals with fatal disease. Causes of death were linked to either the swift, haemorrhagic form following huRVFV infection or the late-onset neuropathic form following mosRVFV infection.

Administration of mosquito saliva at the time of ID infection with mosRVFV did not increase the mortality, nor did it accelerated or enhanced viral dissemination. Immunohistochemical analyses of the brain gained from individual succumbed to RVF encephalitis following ID infection with mosRVFV, suggested that virus travelled to the brain via retrograde axonal transport through peripheral neurons, rather than crossing the blood-brain barrier.

In vitro viral growth kinetics revealed that both virus isolates are able to infect different cell types, in most cases with comparable efficacy, suggesting that a so far unidentified factor is present in the *in vivo* system that may be responsible for the different viral dissemination profile.

Flowcytometric analyses indicates that the two isolates target the same cell types in the skin; however, huRVFV infects the cells with higher efficacy. Characterization of the infected cells showed that dermal non-leukocytes are infected with the highest frequency, and that the most permissive immune cell type is a monocyte-like or monocyte-derived cell population, which expresses medium level of Langerin, yet they are different from classical Langerhans cells. The detection of infected cells in the lung after IN infection was unsuccessful, maybe due to the inappropriate timing of sampling or because the primary target cells after intranasal infection may not be located in the lung.

Additional research is needed to better understand why the IN route with huRVFV sometimes lead to abortive infection, focusing on the barrier function of the airway mucosa.

Furthermore, this study lacks hard evidence to explain how mosRVFV could remain undetectable in the host even when the animals were symptomatic. The collection of additional sample types together with cytokine analysis may help to answer this question. Nevertheless, the dissemination of mosRVFV was confined exclusively to the brain; therefore, this isolate may open new avenues for Rift Valley fever encephalitis research.

Zusammenfassung

Ziel dieser Studie war es, ein besseres Verständnis der Virus- und Wirtsfaktoren zu erlangen, die den Ausgang einer Infektion mit dem Rifttalfiebervirus (RVFV) in einem Säugetierwirt beeinflussen.

Das Hauptziel bestand darin, sich nicht nur auf einen Faktor zu konzentrieren - wie es in früheren Studien üblich war -, sondern zu untersuchen, wie diese vielfältigen Faktoren - die bei natürlichen Infektionen auftreten - zusammen den Krankheitsverlauf bestimmen.

Die Ergebnisse der Infektion von Wildtyp (WT)-Labormäusen mit RVFV, das entweder von einem menschlichen Patienten (huRVFV) oder aus einer Mücke (mosRVFV) isoliert wurde, unterstreichen den Infektionsweg als eine wichtige Determinante der Pathogenese. Wichtig ist, dass die Auswirkungen des Infektionsweges je nach Virusisolat direkt entgegengesetzt waren. Während die intradermale (ID) Infektion mit dem menschlichen Isolat zu einer höheren Sterblichkeitsrate führte als die intranasale (IN) Infektion, traten die Krankheitssymptome auch früher auf, wenn die Infektion über die Haut erfolgte. Im Gegensatz dazu erlagen mehr Tiere der Krankheit nach einer IN-Infektion mit dem Mückenisolat.

Die Untersuchung der Virusverbreitung ergab weitere, unerwartete Unterschiede: huRVFV war im ganzen Körper weit verbreitet und in allen untersuchten Organproben mit Ausnahme des Gehirns in den meisten Fällen gleichmäßig vorhanden. Darüber hinaus wurde nach einer ID-Infektion eine beschleunigte Ausbreitung beobachtet. Auffallend ist, dass mosRVFV nur in der Haut nach einer ID-Infektion oder im Gehirn infizierter Tiere mit tödlicher Erkrankung nachweisbar war. Die Todesursachen wurden entweder mit der schnellen, hämorrhagischen Form nach huRVFV-Infektion oder der spät einsetzenden neuropathischen Form nach mosRVFV-Infektion in Verbindung gebracht.

Die Verabreichung von Moskitospeichel zum Zeitpunkt der ID-Infektion mit mosRVFV erhöhte weder die Sterblichkeit, noch beschleunigte oder verstärkte sie die Virusverbreitung. Immunhistochemische Analysen des Gehirns von Individuen, die nach einer ID-Infektion mit mosRVFV einer RVF-Enzephalitis erlagen, deuteten darauf hin, dass das Virus über einen retrograden axonalen Transport durch periphere Neuronen in das Gehirn gelangte, anstatt die Blut-Hirn-Schranke zu passieren.

Die Kinetik des Viruswachstums in vitro zeigte, dass beide Virusisolate in der Lage sind, verschiedene Zelltypen zu infizieren, in den meisten Fällen mit vergleichbarer Wirksamkeit, was darauf hindeutet, dass im In-vivo-System ein bisher nicht identifizierter Faktor vorhanden ist, der für das unterschiedliche virale Verbreitungsprofil verantwortlich sein könnte.

Durchflusszytometrische Analysen zeigen, dass die beiden Isolate auf die gleichen Zelltypen in der Haut abzielen; das huRVFV infiziert die Zellen jedoch mit höherer Wirksamkeit. Die Charakterisierung der infizierten Zellen zeigte, dass dermale Nicht-Leukozyten mit der höchsten Frequenz infiziert werden und dass der permissivste Immunzelltyp eine monozytenähnliche oder von Monozyten abgeleitete Zellpopulation ist, die ein mittleres Maß an Langerin exprimiert, sich aber von klassischen Langerhans-Zellen unterscheidet. Der Nachweis infizierter Zellen in der Lunge nach einer IN-Infektion war nicht erfolgreich, was möglicherweise auf den ungeeigneten Zeitpunkt der Probenahme oder darauf zurückzuführen ist, dass sich die primären Zielzellen nach einer intranasalen Infektion möglicherweise nicht in der Lunge befinden.

Um besser zu verstehen, warum der IN-Weg mit huRVFV manchmal zu einer abortiven Infektion führt, sind weitere Forschungsarbeiten erforderlich, die sich auf die Barrierefunktion der Atemwegsschleimhaut konzentrieren.

Darüber hinaus fehlen in dieser Studie stichhaltige Beweise, um zu erklären, wie mosRVFV im Wirt unnachweisbar bleiben konnte, selbst wenn die Tiere symptomatisch waren. Die Sammlung zusätzlicher Probentypen zusammen mit einer Zytokinanalyse könnte helfen, diese Frage zu beantworten. Nichtsdestotrotz war die Verbreitung von mosRVFV ausschließlich auf das Gehirn beschränkt; daher könnte dieses Isolat neue Wege für die Erforschung der Rifttalfieber-Enzephalitis eröffnen.

1. Introduction

1.1. Rift Valley Fever Virus

1.1.1. Taxonomy

Rift Valley fever virus (RVFV) received its latest scientific name by the International Committee on Taxonomy of Viruses in 2023 as *Phlebovirus riftense* (International Committee on Taxonomy of Viruses, 2023). The virus currently belongs to the *Bunyavirales* order, *Phenuiviridae* family, and *Phlebovirus* genus after its reclassification in 2016 by the same committee (Gaudreault et al., 2019).

Members of the *Phenuiviridae* family infect three different kingdoms: animals, plants, and fungi, which is uncommon among known viral families. Many of them are highly pathogenic to humans, animals and plants, posing heavy burden to global health care, livestock industry, and agriculture (Sun et al., 2022). The largest genus in this family is *Phlebovirus*. Viruses belonging to this genus are circulating between arthropod vectors and mammalian hosts. The most common vector for this genus is *Phlebotominae* sandflies - hence the genus name -, however RVFV is primarily transmitted by *Aedes spp.* and *Culex spp*. mosquitoes (Calisher & Calzolari, 2021).

1.1.2. Ecology and veterinary relevance

RVFV was originally discovered in Kenya during an epidemic among lambs and sheep in the Great Rift Valley, giving the name of the virus (Daubney et al., 1931). Since its discovery in 1930 the virus has spread across the continent and now it is not only endemic in multiple African countries but also in Madagascar, Yemen, and Saudi-Arabia (Rissmann, Stoek, et al., 2020). Serological screenings of humans along with animals indicate RVFV infection in Turkey (Tezcan-Ulger et al., 2019) and Iran, too (Fakour et al., 2017). Figure 1. represents the distribution of RVFV in 2020.

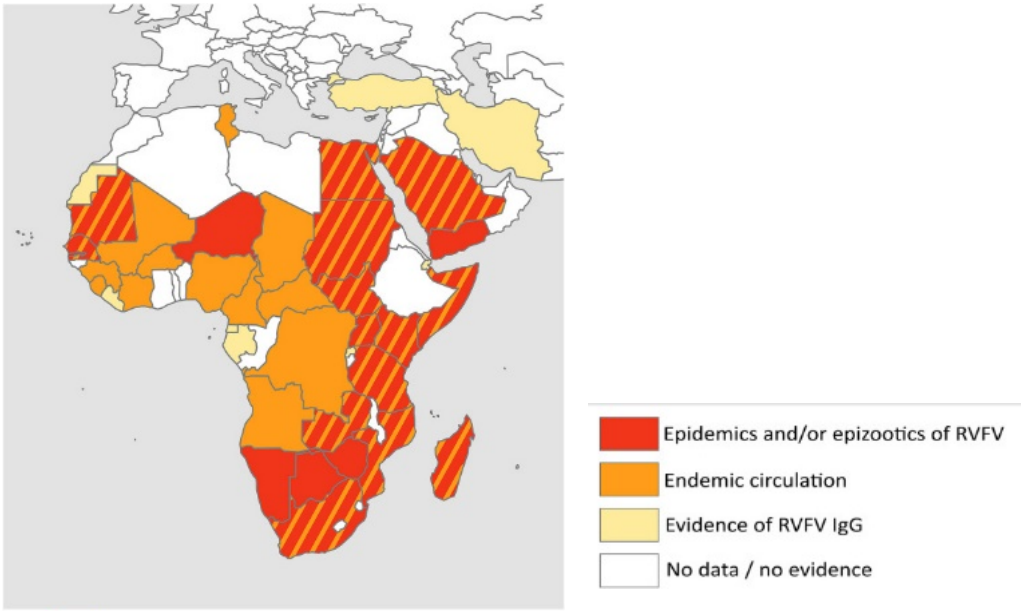

Figure 1. Distribution of RVFV in 2020.
The geographical map shows the distribution of RVFV infections in humans or animals by 2020, based on confirmed cases or seroconverted individuals (Rissmann, Stoek, et al., 2020).

The epidemiology of RVFV is not yet completely understood; however, two different transmission cycles are known. The enzootic – or inter-epizootic – cycle, which takes place

during the dry season; here the virus is believed to be maintained mostly by *Aedes spp.* via vertical transmission (Wright et al., 2019).
The second cycle – called epizootic cycle – starts after the freshly hatched floodwater *Aedes spp.* initiate the infection of wildlife and domesticated animals following extremely high amount of rain and subsequent floodings. Once the ruminants are infected, several other *Arthropod* species can transmit the virus (Rostal et al., 2017; Wright et al., 2019).
Beside the evidence for vertical transmission in some mosquito species, it is not clear whether wild animals have a role maintaining the virus population during the epidemics. Several species of wild ungulates have been verified as host for RVFV infection (Evans et al., 2008) yet there is no evidence that these animals would produce sufficient viremia for a successful transmission to mosquitoes (Wright et al., 2019). The role of amphibians and reptiles as putative reservoirs has also been investigated, since cell-lines from these organisms were permissive for RVFV infection (Rissmann et al., 2021), however *in vivo* experiment could not support the *in vitro* data (Rissmann, Kley, et al., 2020).
While Aedes and Culex mosquitoes are mainly responsible for RVFV transmission in nature, other blood-sucking insects - including mosquitoes of other genera, sandflies and midges - have also been found to carry the virus during the epidemic cycle. (Linthicum et al., 2016). Some sandfly species were able to transmit RVFV to rodents in laboratory settings (Dohm et al., 2000; M. J. Turell & Perkins, 1990),
RVFV infection in wild animals is typically asymptomatic or mild; however, it is highly pathogenic in domesticated ruminants. These animals are considered as amplifying hosts, meaning they produce viremia high enough to infect blood feeding mosquitoes that may potentially infect the next host. No direct animal-to-animal infection has been reported, nor has it occurred in laboratory set-ups either, but vertical transmission between mother-to-foetus occurs in all livestock species. Beside ruminants, RVFV can infect camels, pigs, and pets, such as dogs and cats, as well. (Hartman, 2017; Lubisi et al., 2023; Wichgers Schreur et al., 2016; Wright et al., 2019).
Humans get infected mostly through the respiratory mucosa via aerosols generated during handling infected animals or carcasses. Infection can also occur through micro- or macro damages on the skin or by consuming unpasteurized milk of infected animals. It is less frequent, but transmission via the mosquito vectors (mostly Culex spp. and Mansonias spp.) is possible, too. Human-to-human infection has not been documented, however there is evidence for mother-to-foetus transmission (Hartman, 2017; Wright et al., 2019). The schematics of RVFV transmission cycles are represented in Figure 2.

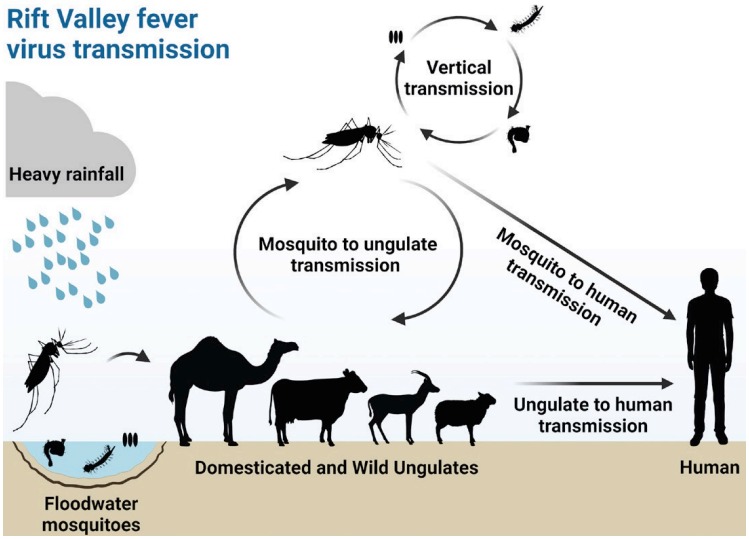

Figure 2. Rift Valley fever virus transmission cycles

Outside the time of RVFV epidemics, the virus is maintained through vertical transmission in floodwater mosquitoes. During periods of heavy rainfall and the subsequent increase in water surfaces, infected mosquitoes hatch and infect available ungulates. These infected mammals serve as amplifying hosts, providing the next generation of the virus for further dissemination by other mosquito species. Humans become infected either through contact with infected domesticated ruminants or by being bitten by infected mosquitoes, from (Alomar et al., 2023).

As mentioned earlier, domesticated ruminants are extremely susceptible for RVFV infection. Young offsprings are more susceptible to death then their adults, and adult sheep and goats are more prone to lethal disease than cattle. Interestingly, difference in mortality and morbidity of different breeds of sheep has also been described. Embryos and foetuses almost always succumb to the infection, which can result in a phenomenon called abortion storm, referring to multiple, sometimes hundreds of miscarriages at the same time. This is a common sign of the epizootic cycle of the virus (Hartman, 2017; Ikegami & Makino, 2011; Wright et al., 2019).

The disease course and symptoms vary among different species, but the virus primarily targets the liver in all animals. This often results in (per)acute hepatitis, the most common cause of death. Infected livers frequently exhibit widespread necrotic lesions often accompanied by haemorrhages. Additionally, subcutaneous, visceral, and serosal haemorrhages, along with tissue necrosis, which may affect the spleen, lung, stomach, and distal part of the intestine. These haemorrhages occasionally lead to the discharge of blood from the nose or result in bloody diarrhoea. The brain and the eyes are usually spared in contrast to severe infections in humans (Bird et al., 2009; Hartman, 2017; Ikegami & Makino, 2011; Odendaal et al., 2021; Wright et al., 2019).

1.1.3. RVFV in humans

In most cases, RVFV is a self-limiting, febrile illness in humans, however around 1-2% of the cases develop a severe form of the disease. The overall case fatality rate is estimated between 0,5-2%, but higher mortality rates for example 18% and 28% have been recorded by the Saudi Health Ministry in 2000 or by Tanzania in 2007, respectively (Javelle et al., 2020a).

Incubation period is typically 2-6 days. Clinical symptoms of RVFV include fever, headache, backache, generalized pain in the joints and muscles, vertigo, anorexia, gastrointestinal

syndromes including nausea, and vomiting. In the uncomplicated and majority of the cases these symptoms last for 4-7 days (Anywaine et al., 2022; Javelle et al., 2020a). A schematic timeline about the development of RVFV disease from (Bird et al., 2009) is represented on Figure 3.

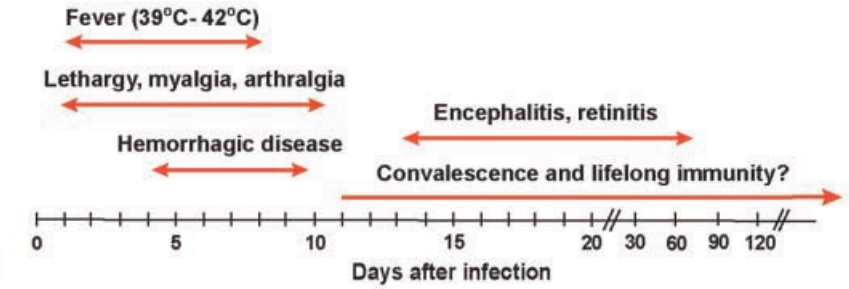

Figure 3. The development of RVF disease in humans
Human RVF disease development over time from (Bird et al., 2009)**.**

As mentioned earlier, a minority of the cases can develop into severe form of the disease. Factors that may drive RVF to severe form is not fully understood, however some factors have been already identified. Such determinants are: 1. touching, handling, consuming or generally being in very close contact with infected animal(parts) possibly linked to being exposed to more viral particles and having higher inoculation dose. 2. co-infections with malaria or positive HIV-status. 3. single nucleotide polymorphisms in genes associated to innate immune pathways (Hise et al., 2015; Javelle et al., 2020b; Mohamed et al., 2010).

Severe cases of RVF can manifest in the following forms:
Ocular syndrome: the most common severe form of RVF with up to 10% of RVF cases. Symptoms may include retro-orbital pain, photophobia, impaired vision, even transient or permanent blindness.
Hepatic syndrome: severe hepatic manifestation is less frequent (1-2% of total cases) comparing to the ocular form, yet 10% of these cases result in death. Most common symptoms are jaundice, and liver failure. Almost all patients with hepatic syndrome require hospitalization.
Haemorrhagic fever: as the result of acute hepatitis and the consequent imbalance in the coagulation system, patient can present bleeding from the nose and gums. Other haemorrhagic symptoms include vomiting blood, blood in the urine or faeces and purple skin rashes. The most severe form with the highest mortality rate (~65% of all patients with haemorrhagic symptoms).
Meningoencephalitis: usually a late-onset form of RVF. As with other forms its incidence rate varies among outbreaks, but it is estimated around 5% in total RVFV infection. Clinical symptoms may include severe headache, neck rigidity, amnesia, hallucination, confusion, paralyses, and coma. This form can be fatal in more than 50% of the cases, meanwhile survivals may experience long-term or even permanent consequences. Underlying mechanism behind the development of this form of RVF is not yet understood and is currently under intensive research.
Renal syndrome: most common symptom of this form is acute renal failure, which can lead to multiple-organ dysfunction. 60% of the patients during the outbreak in Saudi Arabia in 2000 represented renal impairment leading to a 31% case fatality rate (Anywaine et al., 2022; El et al., 2009; Hartman, 2017; Javelle et al., 2020b; Wright et al., 2019).

1.1.4. Molecular biology of RVFV

1.1.4.1. Virion structure

RVFV has a spherical shape with a 90-100 nanometre diameter (Figure 4.). The genetic material is coded on three viral RNA segments, all of which are associated with the nucleocapsid protein (Np) and the RNA-dependent RNA polymerase (L), and together they form the ribonucleoprotein (RNP) complexes. These RNP complexes are packed in a lipid bilayer envelope gained during the budding process. The envelope is built of glycoprotein heterodimers, composed of glycoprotein N (Gn) and glycoprotein C (Gc), which are further organized into pentameric or hexameric structures, forming the cylindrical spikes on the surface of the virion (Calvo-Pinilla et al., 2020; Gaudreault et al., 2019).

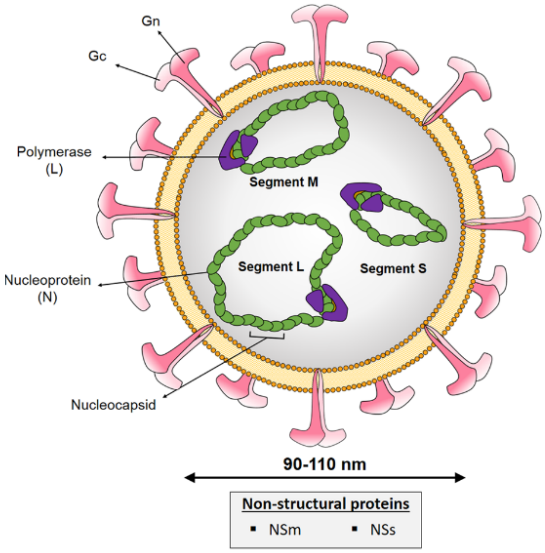

Figure 4. Diagrammatic representation of RVFV

Enveloped virion of RVFV contains a tri-segmented RNA genome, which is encapsidated by the nucleoprotein (N) and is associated with the viral polymerase (L) to form the nucleocapsid. The surface of the virion carries the two glycoproteins (Gn and Gc) in a heterodimer form, from (Calvo-Pinilla et al., 2020).

1.1.4.2. Genome organization

The tri-segmented negative strand RNA genome of RVFV is coding for two to three non-structural (depending on the cells) and five structural proteins (Figure 5.). The largest, (L) segment encodes only the RNA-dependent RNA polymerase (RdRp).

The medium (M) segment has only one open reading frame, despite it encodes for the two glycoproteins (Gn, Gc), two forms of a non-structural protein (NSm, NSm') and a fusion protein called 78-kDa protein composed of the NSm and Gn. These proteins are produced by alternative cleavage of the polyprotein precursor, which events are determined by the differential usage of the start codons located on the 5' end of the mRNA. While Gc is always expressed regardless of which start codon is used, Gn is only produced when translation does not start from the first start codon. NSm or the truncated NSm' are produced – together with the other two glycoproteins – in case of the usage of the second or the third start codon, respectively. While the NSm and Gn is expressed in the form of 78-kDa protein when the first AUG codon is utilized. Interestingly, researchers found that the 78-kDa protein was only incorporated into the virion when the virus was propagated on mosquito cells, but not when on mammalian cells. The selective usage of the AUG codons is believed to be the result of leaky scanning; however, the exact mechanism is not yet understood (Weingartl et al., 2014).

The small (S) segment encodes the nucleoprotein (Np) and a non-structural protein (NSs) in an ambisense fashion divided by a hairpin structure, whereas the Np is in genomic and the NSs is in antigenomic orientation.

All three segments bear flanking short untranslated regions which hybridize, hence forming the panhandle shape of the RNPs (Gaudreault et al., 2019).

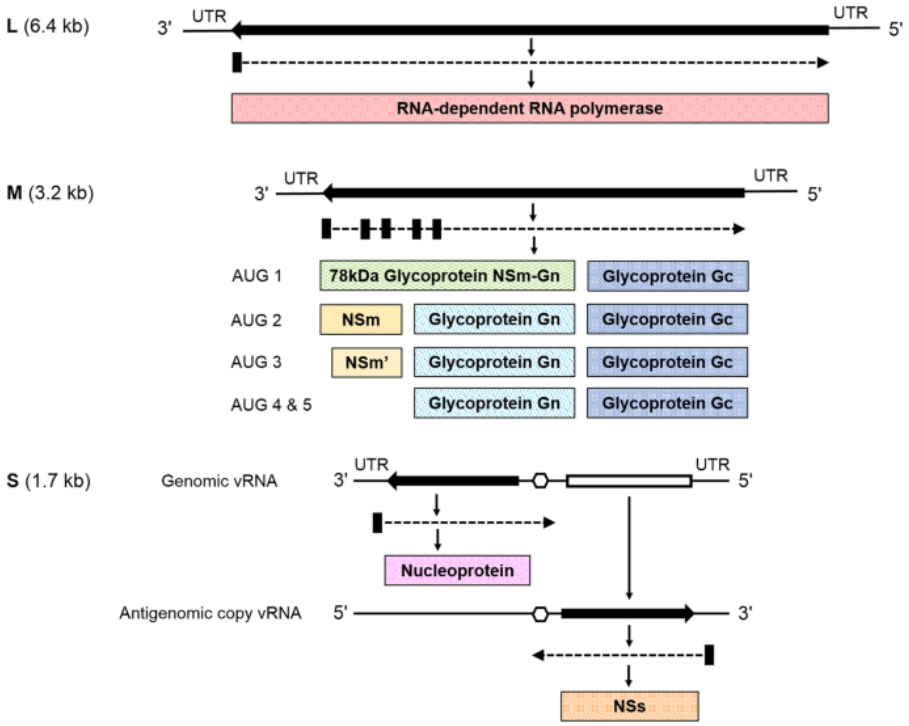

Figure 5. The genomic organization of RVFV
RVFV genome consists of three segments. The large (L) segment encodes the RNA-dependent RNA polymerase. The medium (M) segment encodes the glycoproteins (Gn and Gc), two non-structural proteins (NSm and NSm'), and the 78-kDa protein in a polyprotein fashion. The final proteins are generated by a splicing mechanism determined by the position of the start codon used for translation initiation. The mall (S) segment encodes the nucleoprotein and a non-structural protein (NSs) in an ambisense fashion, from (Gaudreault et al., 2019).

Whole genome analyses of 33 isolates collected throughout Africa and Saudi Arabi for over 56 years revels low genetic diversity with 5% difference at nucleotide and about 2% at amino acid level (Bird et al., 2007).
Despite its low genetic diversity, the analyses of partial sequence of Gn produced 95 unique sequences that separate RVFV isolates into 15 lineages (Lineage A-O), yet these lineages have only one serotype (Grobbelaar et al., 2011).

1.1.4.3. Functions of viral proteins

RdRp (sometimes also called the L protein) is an RNA-dependent RNA polymerase and is responsible for the transcription and the replication of the viral genome (Malet et al., 2023; X. Wang et al., 2022). Glycoprotein **Gn** and **Gc** heterodimers form pentameric or hexameric capsomers, with Gn located on the outer surface of the capsomer and positioned on top of Gc (Figure 6. A). This arrangement of Gn and Gc glycoproteins allows Gn to serve as the receptor-binding protein responsible for the attachment and entry of the virus into the host cell. Conformational change is triggered by the acidic pH of the phagolysosome inducing the insertion of the Gc into the host cell membrane (Figure 6. B) (Rusu et al., 2012).

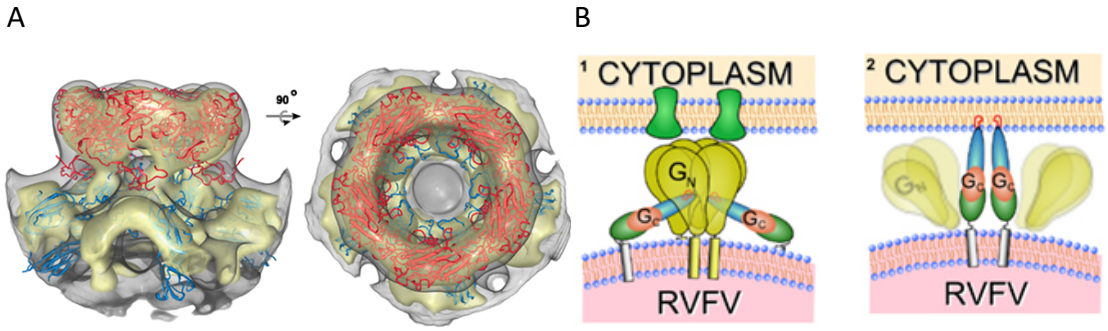

Figure 6. Overview of the RVFV glycoprotein shell
Glycoprotein arrangement of pentameric RVFV capsomer was reconstituted from cryogenic electron microscope density, in which Gn is indicated in red and Gc is indicated in blue (A). Model illustrating the attachment (1) and penetration (2) of RVFV into the host cell (B), from (Rusu et al., 2012).

There are three types of cell surface entry receptors that have been identified for RVFV to date: 1. Heparan sulphate (a type of glycosaminoglycan), is abundantly expressed by most cell type. 2. C-type lectin, for example dendritic cell-specific ICAM-grabbing non-integrin (DC-SIGN) which can be found on dermal dendritic cells (DC), or liver/lymph node-specific intercellular adhesion molecule-3-grabbing integrin (L-SIGN) expressed on the endothelial cells of the liver and lymph nodes. 3. The most recently discovered entry receptor belongs to the low-density lipoprotein receptor family and called low-density lipoprotein (LDL) receptor-related protein 1 (Lrp1). Lrp1 is ubiquitously expressed in the liver, placenta, and brain, and on both, innate and adaptive immune cells. (Ganaie et al., 2021; Koch et al., 2021; Sizova et al., 2023).Beside the attachment to host cells, Gn has another crucial role in viral assembly. Since RVFV lacks a matrix protein, which serves as an anchor between the viral envelope and RNP in other viruses, the N-terminal part of the cytoplasmic tail of the Gn takes over this role. The cytoplasmic tail of Gn is responsible for the recruitment and incorporation of RdRp and Np into the forming virion (Piper et al., 2011; Spiegel et al., 2016).
In cell culture experiments both NSm and the 78-kDa protein were dispensable for viral replication (Won et al., 2006). However, **NSm** has an anti-apoptotic effect on infected cells and therefore increases virulence in mammalian hosts (Won et al., 2006, 2007). The role of **78-kDa protein** is not fully understood. It has been showed that it was indispensable for viral dissemination in mosquitoes (Kreher et al., 2014), but its role in the mammalian host remains to be less obvious. Indirect evidence suggests that the 78-kDa protein may influence the disease course of RVFV infection in goats, however it does not affect mortality (Nfon et al., 2012). Also, knocking out of 78-kDa protein did not influence the mortality in mice either (Kreher et al., 2014).
One of the main roles of the nucleoprotein (**Np**) is to create a protective coating along the negative strand-RNA genome, and with that forming the nucleocapsid (Raymond et al., 2010). Additionally, it has a crucial role in the viral cycle through its interaction with the L protein, as it determines the transition between transcription and replication (Guu et al., 2012; Le May et al., 2005). It has also been shown that the C-terminal of the Np can induce autophagy in macrophages subsequently dampening their antiviral IFN-response (Zhu et al., 2023).
NSs is the main virulence factor of RVFV in the mammalian host. Total or partial lack of NSs results in an avirulent form of the virus in immune competent hosts (Bird et al., 2008; M. Turell et al., 1995). NSs demonstrates multiple strategies for immune evasion: 1. by binding to Sin3A Associated Protein 30 (SAP30) and interacting with the transcription factor Ying Yang 1, NSs

blocks the activation of interferon (IFN) -β (Le May et al., 2008). 2. by preventing the eukaryotic transcription factor IIH (TFIIH) complex recruitment to the nucleus, it shuts off the host's transcription process (Le May et al., 2004). 3. dsRNA-dependent protein kinase R (PKR) is responsible to prevent translation in a virus infected host. However, NSs can induce the degradation of PKR, hence the viral translation remains unaffected (Ikegami et al., 2009). NSs can also induce nuclear abnormalities (e.g., micronuclei and lobulated nuclei) via interacting with pericentromeric regions of the DNA leading to chromosome cohesion and segregation defects (Mansuroglu et al., 2010). This can also induce cell cycle arrest (Baer et al., 2012). Furthermore, NSs was directly linked to the virus' cytopathic effect by affecting the host's actin cytoskeleton system via targeting its key regulator, the Abelson murine leukaemia viral oncogene homolog 2 (Abl2) (Bamia et al., 2020).

1.1.5. Therapy

Until today, the primary treatment for RVF patients remains solely supportive care. Despite numerous research efforts focusing on the molecular aspects of the RVFV lifecycle, no therapeutics that are approved by the US Food and Drug Administration (FDA), or the European Medicines Agency (EMA) are currently available. The following two antiviral drugs have been tested *in vivo* for RVFV treatment:

Ribavirin is a nucleoside analogue. *In vitro* experiments suggested antiviral effect of ribavirin on RVFV (Kirsi,' et al., 1983), however its effect in mouse experiment was less promising, as mice exposed to the virus SC were partially protected from lethal infection, meanwhile ribavirin-treated mice infected with aerosolized RVFV were not protected at all (Reed et al., 2013). Ribavirin was evaluated in clinical trials during the 2000 epidemic in Saudi Arabia. The drug was administered intravenously to patients with moderate disease at various stages, however the trial was suspended due to suspicion of increased risk for neurological symptoms caused by the drug, according to a World Health Organisation (WHO) report (WHO, 2019).

Favipiravir is a non-nucleoside inhibitor originally developed against influenza viruses (Furuta et al., 2005), yet it resulted as a potent antiviral drug against various viruses (Furuta et al., 2009), such as arenaviruses and bunyaviruses among others, including RVFV based on *in vitro* tests (Gowen et al., 2007). However, in the hamster model, favipiravir was protective only against the acute but not the late-onset form of RVF (Scharton et al., 2014). The effect of favipiravir in rats following inhalational RVFV challenge showed a remarkable 92% survival rate even when administrated 48 hours after infection. The animal succumbed to the disease died due to late-onset encephalitis (Caroline et al., 2014).

Other (non-)small molecules targeting viral, or host components are under development and investigation, yet these compounds have not reached the pre-clinical phase, hence no *in vivo* results are currently available (Atkins & Freiberg, 2017).

1.1.6. Vaccines

Currently there is no licensed vaccine against RVFV available for human use. However, RVFV has been identified by the WHO research and development blueprint as one of the top 10 pathogens for its future outbreak potential, which may grant priority for future vaccine development (WHO, n.d.).

Immunological aspects of RVFV vaccines

A later chapter provides a comprehensive overview of the immune response to RVFV. The information presented here primarily highlights key aspects of the immunology related to RVFV vaccine approaches.

In most vaccines against viral pathogens, the gold standard for evaluating vaccine efficacy is determined by the production of neutralising antibodies. These antibodies typically recognise the glycoproteins or other key elements of viruses, that are responsible for their attachment and uptake into the host cell. Gn and Gc of RVFV have been the main targets for vaccine development. Interestingly, IgM and IgG antibodies against the Np, produced during RVFV infection, are at a comparable level to the ones against Gn or Gc (Pepin et al., 2010). A study showed that antibodies against the nucleoprotein may not be neutralizing, yet still provide protection, probably via antibody-dependent cell cytotoxicity (ADCC) or complement mediated cell lysis (Jansen van Vuren et al., 2011). Np is also proved to be a potent $CD8^+$ - cytotoxic - T cell antigen, inducing protective T cell response against RVFV infection (Xu et al., 2013). Furthermore, a study analysing peripheral blood mononuclear cells from a cohort of former RVFV vaccinees, found that despite the waned neutralization antibody titer, the individuals still possessed RVFV-reactive memory T cells up to 24 years after immunization (Harmon et al., 2020). All of these suggest the need for the assessment of T cell response alongside neutralizing antibodies for future RVFV vaccine development strategies.

Live attenuated vaccines

The **Smithburn strain** is the first and most widely used vaccine for livestock. It has been developed from the Entebbe strain via serial passage in mouse brains. Despite its low cost and the potency to induce long-lasting immune protection even after a single administration, there have been several concerns about its safety. It has been reported that the vaccine induced high rate of abortion in pregnant animals, furthermore in some cases it induced pathological malformations in internal organs, particularly in the liver (Botros et al., 2006; Kamal, 2009). Due to its known safety concerns, it has not been tested in humans (Ikegami, 2019).

MP-12 was developed from the pathogenic strain ZH548 by serial passage in the presence of a chemical mutagen. The strain MP-12 carries a total of 11 amino acid changes located on all the three segments of the virus, compared to the original ZH548 strain (Vialat et al., 1997). Vaccination with MP-12 resulted in a high neutralising antibody titer that was maintained over the period of 5 years without booster vaccination. However, some of the vaccinee developed viremia, and sometimes the virus carried new mutations (Ikegami, 2019). Its administration to livestock generated effective immune protection. However, similarly to Smithburn, MP-12 was also reported to cause liver necrosis in some vaccinated calves and to have teratogenic and abortion-inducing effect in sheep when administered during the first trimester (Kamal, 2009; Kitandwe et al., 2022).

Clone 13 has a natural 69% deletion of its NSs gene. This attenuated strain is another widely used vaccine for livestock, however it is less effective in cattle. It is highly immunogenic and safe, yet in case of overdose, Clone 13, is able to cross the placenta and cause foetal infection with the potential for miscarriage (Makoschey et al., 2016).

One major concern regarding the use of live attenuated vaccines is their potential to reassort with their wild counterparts and consequently regaining their virulence. Reassortment is a phenomenon in which two or more virus strains co-infect the same cell and exchange genetic material. While reassortment between vaccine and wild type RVFV strains in nature has not yet been detected, there is ample evidence of such scenarios occurring under experimental

conditions. Additionally, reassortments of wild type virus strains have also been observed in field isolates. (Gaudreault et al., 2019).

Formalin inactivated vaccines
Two formalin-inactivated vaccine **NDBR-103** and **TSI-GSD-103** were tested in humans. Both induced neutralizing antibodies, but their titer declined rapidly with time, and they required repeated booster shots to maintain their neutralizing effect. Furthermore, they require BSL-3 laboratories for the production of the virus batches. All of these making them suboptimal for commercial use (Ikegami, 2019).

There are several further vaccine development strategies, including DNA plasmid, viral vector, subunit, viral replicon and virus-like protein (VLP), however none of these are licensed yet (Alhaj, 2016; Kitandwe et al., 2022).

1.2. Immune response to RVFV

The immune system is a complex, tightly regulated system consisting of cells, tissues, and soluble components. Its main task is to maintain the organism's homeostasis and to protect it from pathogenic invaders or cancerous malformations, while its pathological operation may lead to autoimmune diseases and hypersensitivity reactions.
Historically the immune system was divided into two major arms, the innate and adaptive immune system. Meanwhile the basis of this type of distribution still stands, with the discovery of the innate lymphoid cells, the border between the two arms became elusive. Regardless, in general, the innate immune system consists of cells (such as granulocytes, monocytes, dendritic cells (DC), macrophages and natural killer (NK) cells) that are able to recognise pathogens or danger signals based on their common molecular compositions and provide a rapid response to them. However, their rapid response is usually followed by a steep decline in their numbers. In contrast, the adaptive immune system (consisting of T cells and B cells) is slower to activate and usually requires the help of innate components, but it can recognise invaders by their specific motifs, also called antigen epitopes, and can provide long-term protection against recurrent infections by forming so-called memory cells (McComb et al., 2019).

As mentioned earlier, RVFV enters the body through the respiratory tract, through breaks and abrasions in the skin, or through the proboscis of a mosquito that penetrates the skin during its blood meal. Once inside the body RVFV encounters local immune cells, which start the virus-specific immune response of the host. While some immune cells directly attack the pathogen, others – most importantly, dendritic cells and other antigen-presenting cells (APCs) – phagocyte and process them resulting in its presentation on their major histocompatibility complex (MHC) molecules.

1.2.1. Pattern recognitions receptors (PRR)

The adequate immune response is a complex, well-coordinated process, in which humoral and cellular components mutually regulate each other's behaviour. At the site of infection, local phagocytic cells recognize the different pathogens via their pattern recognition receptors (PRRs). Together with the surrounding infected cells, they begin to produce pro-inflammatory

cytokines and chemokines, which in turn induce the recruitment of other local and circulating immune cells (Herbert & Panagiotou, 2022).
PRRs are key components of the innate immune system, as they are able to recognize molecular patterns that are characteristic of pathogens but are absent in the host, also called pathogen-associated molecular patterns (PAMPs). These PAMPs cab be, for example double-stranded (ds) or single-stranded (ss) RNA, common genetic materials of viruses (Chan & Gack, 2016). PRRs can be located either on the cell surface or intracellularly. Later ones can be cytoplasmic, or membrane bound within the endosomes. The wide-spread distribution of PRRs allows the recognition of both, intra- and extracellular pathogens. Intracellular PRRs are usually present in all nucleated cells (Herbert & Panagiotou, 2022).
There are four main groups of PRR: Toll-like receptors (TLRs), Nucleotide-binding oligomerisation domain (NOD)-like receptors (NLRs), retinoic acid inducible gene-I (RIG-I)-like receptor (RLRs), and C-type lectin receptors (CLRs).

Our knowledge about the relationship between RVFV and certain PRRs is limited, however, genetic polymorphism of TLR3, 7, 8 showed correlation with RVFV severity in human patients (Hise et al., 2015). Furthermore, some CLRs may play a role in viral uptake. These receptors recognise carbohydrate structures on the glycoproteins of various viruses. They are predominantly expressed on the cell membrane of DCs and macrophages. Internalization via CLRs can lead to degradation via lysosomes and subsequent antigen presentation via MHCs, or it can induce autophagy (Bermejo-Jambrina et al., 2018). DC-SIGN is an important member of the CLRs, as it has a pivotal role in the pathogenesis of numerous viral pathogens. Viruses can exploit the internalization via DC-SIGN by hijacking the degradation in the lysosome making them possible to use the phagocytic cells for their replication and further dissemination. Such mechanism has been described for RVFV, too (Phoenix et al., 2016). Another CLRs, called L-SIGN expressed mainly on hepatocytes have also been identified as entry receptor for RVFV (Léger et al., 2016).

1.2.2. Antigen presenting cells

One crucial cell type of the immune system called T cells (will be discussed in detail in the followings) are unable to recognize antigens on their own. The antigens must be presented to them by a special protein complex called the MHC.
The expression “antigen-presenting cells” may be somewhat convoluted as MHC I is expressed on all nucleated cells in the body, hence technically they also present antigens, however the term APC are usually applied to cells that are capable of presenting antigens to T cells via MHC II. These cells are DCs, macrophages and B cells, and are referred to as professional antigen presenting cells (Eiz-Vesper & Schmetzer, 2020). Recent data indicates that other immune cells such as granulocytes or even non-hematopoietic cells - such as endothelial cells, stromal cells, or hepatocytes – can also express MHC II, yet their T cell priming capability is debated, hence they are called as atypical APCs (Kambayashi & Laufer, 2014; Lin & Loré, 2017). For the proper activation of a naïve, peripheral T cell at least three signals are required: 1. antigen presented to the T cell receptor (TCR) via MHC molecules. 2. Co-stimulatory receptor-ligand interaction (e.g CD27-CD86/86). 3. cytokines produced by the APC, which can polarise the following immune response based on the type of pathogenic invader.

1.2.2.1. Monocytes and macrophages

Monocytes and macrophages are both mononuclear phagocytic cells playing crucial roles in immunity and tissue homeostasis (van Furth & Cohn, 1968; Wynn et al., 2013).

Monocytes can be divided into two main types defined as $CD14^{+}$ or $CD14^{-}$ in humans and lymphocyte antigen 6 complex $(Ly\text{-}6C)^{high}$ or $Ly\text{-}6C^{low}$ as their mouse counterparts. $Ly\text{-}6C^{low}$ monocytes' main function is to survey the endothelial integrity. They can respond to local danger signals via TLR7 and initiate the recruitment of neutrophil granulocytes. This usually leads to local endothelial necrosis followed by the clearance of the subsequent cell debris by $Ly\text{-}6C^{low}$ monocytes. In contrast, the role of $Ly\text{-}6C^{high}$ monocytes is less well-defined, but they are known for their high phagocytic capacity and the ability to rapidly access to inflamed tissues, where they can differentiate into DCs or macrophages (Ginhoux & Jung, 2014). Despite their role in immunity, it has been shown that many viruses can directly infect them (Ströher et al., 2001), and use them as a "trojan horse" for entering the central nervous system (Gras & Kaul, 2010). Although, animal experiments suggests that monocytes have a preventive role in RVFV encephalitis (Harmon et al., 2018).

Macrophages can arise from precursors during embryogenesis or by differentiation from monocytes. They are exquisitely heterogen. Macrophages can be found in almost every part of the body having a role in development, homeostasis, immunity and pathology. Based on their roles during immune response we differentiate M1 and M2 macrophages with pro-inflammatory or anti-inflammatory properties, respectively. M1 macrophages are armed with various PRRs and upon tissue injury or infection they produce pro-inflammatory cytokines such as tumor necrosis factor (TNF), interleukin (IL)-1 and reactive oxygen or nitrogen radicals to eliminate pathogens and initiate a sufficient immune response. On the other hand, M2 macrophages are counterbalancing the work of M1 macrophages. They are secreting potentially anti-inflammatory cytokines, such as tumor growth factor (TGF)-β and IL-10. They also have an important role in wound healing and tissue-repair, and they can serve as APCs to recruited T cells (Murray & Wynn, 2011).

1.2.2.2. Dendritic cells

While DCs are considered as members of the innate immune system, they play a crucial role in creating a bridge between the innate and adaptive immune system. As mentioned earlier APCs are indispensable for T cell activation, and while macrophages and B cells do present antigens to T cells, DCs are considered superior in T cell priming as they are the only cell types which can prime naïve T cells (den Haan et al., 2014). Since their discovery in 1973 (Steinman & Cohn, 1973) multiple subsets of DCs have been characterized with various location, development, differentiation markers, and function, yet they all have the ability to activate naïve T cells in lymphoid tissues. They can all be characterized by the expression of CD45 leukocyte marker, MHC II and CD11c integrin, with various density (Merad et al., 2013).

Classical DCs (cDC)

cDCs can be divided into two main subsets: type 1 cDC (cDC1) and type 2 cDC (cDC2). Both subpopulations can be found in lymphoid tissues, as well as non-lymphoid or peripheral tissues. cDC1 located in lymphoid tissues and carries CD8a meanwhile its peripheral-tissue counterpart expresses CD103 integrin. Their unified marker is the X-C motif chemokine receptor 1 (XCR1) chemokine receptor (Crozat et al., 2010; Dorner et al., 2009). cDC1 are the main cross-presenters among the DCs. Cross-presentation is the phenomenon when an APC uptake antigen from the environment, but instead of MHC II presentation, the antigen is being presented via MHC I molecules. This is a vital process for activating cytotoxic T cells via DCs

which are not infected with the virus (Theisen & Murphy, 2017). cDC2 can be distinguished from cDC1 by their expression of CD11b integrin. They are not known for their cross-presenting ability but, they are superior in the induction of $CD4^+$ immunity, partially because of their increased MHC II expression (Dudziak et al., 2007).

Monocyte-derived DC (moDC)
As mentioned earlier, monocytes are recruited to sites of inflammation where they can differentiate into dendritic cells. This cell population has multiple ways to contribute to both innate and adaptive immune response: 1. they promote local antimicrobial actions 2. they induce $CD4^+$ T cell response with Th1 and Th17 polarization 3. they can also cross-present external antigens, and with that, activate $CD8^+$ T cells (Chow et al., 2016, 2017; Domínguez & Ardavín, 2010; Le Borgne et al., 2006; Qu et al., 2009; Shin et al., 2019). As they differentiate from inflammatory monocytes, the two cell types share multiple cell surface markers – such as, CD11b, CD11c, signal regulatory protein α (SIRPα) = CD172a, CD64, Ly-6C, however MHC II expression is a key differential marker for moDCs (DiPiazza et al., 2017; Dong et al., 2016). It has been shown that RVFV can infect moDCs *in vitro* (Lozach et al., 2011; Nfon et al., 2012).

Plasmacytoid DC (pDC)
While most of the DCs including cDC and moDC develop from common myeloid progenitor, pDCs are a result of a unique developmental pathway as they rise from the common lymphoid progenitor (Naik et al., 2005). pDCs are usually accumulate in the blood and lymphoid tissue. They are key members of antiviral immune response, as their main PRRs are TLR7 and TLR9 (both recognise intracellular viral nucleotides) and can produce an exceptional amount of Type I and Type III IFN, which have direct inhibitory effect on viral replication. (Merad et al., 2013; Naik et al., 2005; Yin et al., 2012). Murine pDCs can be identified by their unique expression of sialic-acid-binding immunoglobulin-like lectin (Siglec)-H (J. Zhang et al., 2006).

1.2.2.3. B cells

B cells or B lymphocytes can recognise antigens via their B cell receptor (BCR) and undergo activation with or without the help of T cells. Activation without T cell help (also called as T cell-independent B cell activation) leads to proliferation and differentiation into either memory B cells or short-lived antibody-producing cells. Antibodies are the soluble form of BCRs secreted by transformed B cells, called plasma cells (Lam et al., 2020).
Activation with T cell help (T cell-dependent B cell activation), however, provides further advantage in terms of immunity, including isotype-switching, affinity maturation, production of long-lived plasma cells and memory B cells (Akkaya et al., 2020).
BCR belongs to the immunoglobulin (Ig) superfamily and has five isotypes: IgA, IgD, IgE, IgG and IgM. Naïve B cells express either IgM or IgD by default and change in the Ig isotype requires T-cell-dependent activation. Antibody isotypes determine the downstream immune cell-mediated processes, based on their selective expression of fragment crystallizable (Fc) receptors. The isotype to which the B cells switch is largely determined by the local cytokine milieu, which is the consequence of the activation signal that the helper T cells have previously received from the antigen-presenting cells during their priming or during their interaction with the B cells in the germinal centres. (Higgins et al., 2019; Lam et al., 2020).
Meanwhile production of IgG antibodies requires several days to a couple of weeks, therefore B cells are most likely less important during acute RVFV pathogenesis. However, RVF encephalitis and ocular disease usually manifest after two weeks of exposure, which provides

a window for antiviral adaptive immune response. The role of RVFV-specific antibodies in viral clearance was indeed confirmed in mice by using attenuated (delta-NSs) RVFV strain, whereas B cell knock-out (KO) mice failed to clear the virus in the liver, spleen and brain 21 days after infection Another publication also reported that vaccination followed by depletion of T cells provided immunity in challenged mice, indicating that humoral response alone was sufficient to provide protection against RVFV re-infection (Doyle et al., 2022).

1.2.3. T cells

T cells, too, belong to the adaptive arm of the immune system and are sometimes called conductor of the immune system, as they are key player in orchestrating adequate immune response against any type of pathogens (Wan & Flavell, 2009). As written earlier, T cells are unable to recognise antigens on their own, they require APCs to present processed antigens via MHC I or MHCII to them. TCR recognises the presented antigen-peptide, meanwhile the co-receptors are stabilizing the interaction, by attaching to the side of the MHC molecules. CD4 can only attach to MHC II, while CD8 can only attach to MHC I. $CD4^+$ T helper (Th) cell and $CD8^+$ T cytotoxic (Tc) cells have distinct effector functions during the immune response: Th cells mediate the immune response by secreting the required activating or repressing cytokines, while Tc cells eliminate infected cells via direct cell lyses (Majumdar et al., 2018). Regulatory T cells (Treg) are a special types of Th subsets. Their function is based on inhibition rather than activation. Tregs hinder previously activated T cells, thereby preventing an uncontrollable immune reaction causing more harm in the body than necessary (Kempkes et al., 2019). The cytokines that DCs secrete during priming are greatly influenced by the PRRs, which initially recognized the pathogen along with the local cytokine milieu. Cytokines later secreted by the polarised Th cells will influence the isotype-switching of the B cells in the germinal centers, as well as the activation of other innate and lymphoid cells at the site of infection (Cintolo et al., 2012; Herbert & Panagiotou, 2022; Padovan et al., 2007). Figure 7. summarizes the main cytokines involved in T cell polarization and the effector function of the Th subpopulation.
The role of T cells during RVFV infection is less obvious than expected. As discussed before, RVFV infection often leads to rapid death before the activation of the adaptive immune system, therefore the proper activation of the innate immune system is critical to fight the disease. However, experiments conducted on mice confirmed the indispensable role of the adaptive immune system. Using the delta-NSs strain of RVFV, researchers found that mice failed to clear the virus and developed RVF encephalitis when CD4 cells were depleted (this was in association with impaired antibody production). Interestingly viral clearance was not affected by $CD8^+$ T cell depletion. (Dodd et al., 2013). The same group reported the role of Th1, Tfh, Tc, B cells and monocytes as key players to prevent RVF encephalitis (Barbeau et al., 2021; Harmon et al., 2018). T cell influx to the brain was also reported in encephalitic form of RVFV, however results suggest that pathological findings are due to direct virus-mediated damage and not because of uncontrolled immune response (Dodd et al., 2014a).

1.2.4. Other immune cells

Currently available publications on other immune cells - such as neutrophils (Albe et al., 2019; Gommet et al., 2011; Lathan et al., 2017; Odendaal et al., 2019) and NK cells (Harmon et al., 2018; Hum et al., 2022) - have not identified a definitive role in the pathogenesis of RVFV.

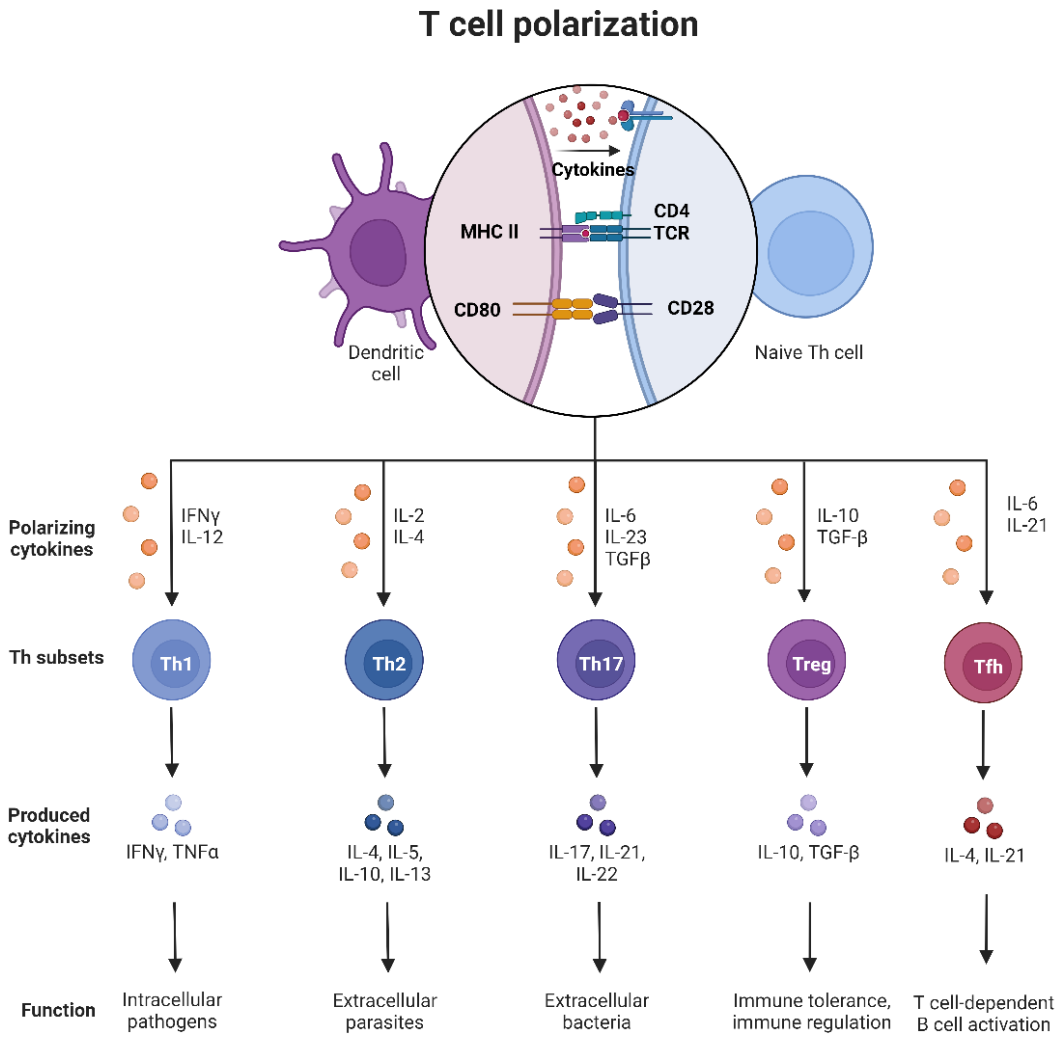

Figure 7. Diagram depicting cytokines involved in the polarization of different Th cell subsets and their subsequent effector functions.
Activated DCs can prime naïve T helper (Th) cells by providing antigen-specific stimulus in context of MHC II molecules, together with co-stimulation via CD28 and cytokines. These cytokines will induce the polarization of the naïve Th cells into different subsets, each required for successful elimination of different types of pathogen. Th, helper T cell; Treg, T regulatory cell; Tfh, T follicular helper cell. Image created with BioRender.

1.3. RVFV pathogenesis

This chapter aims to describe the pathogenesis of RVFV in a chronological manner, focusing on the virus-host interactions. It is important to note that pathogenesis varies between hosts (see Chapter Animal models) and virus strains (Bird et al., 2007).
For this doctoral thesis, laboratory mice were used as model animal, therefore this chapter follows the stages of RVFV pathogenesis in mice as it was described by Darci Smith and her colleagues. They used BALB/c mice infected subcutaneously (SC) with 1000 PFU of RVFV, strain ZH501. The infection was lethal to all animals, which succumbed to the disease either due to early onset hepatitis or late onset encephalitis (D. R. Smith et al., 2010).

1.3.1. Early stage

This phase confines to the early event of infection including the invasion of the host, the initial replication cycles and dissemination.

As mentioned earlier RVFV enters the body either through the skin or through mucosal surfaces, most commonly through the respiratory tract in case of humans. As the anatomy of these two organs on both, tissue and cellular level, is fairly different, it requires the discussion of the early events in these organs separately.

1.3.1.1. Skin route

The virus can enter through the skin following the bite of an infected mosquito or via direct contact with infectious materials through broken skin. It is generally believed that for most arthropod-borne (arbo-) viruses the skin serves as the initial replication site before dissemination (Visser et al., 2023). The skin consists of three layers: epidermis, dermis, hypodermis. Mosquitoes can probe during their blood meal deep to the hypodermis (Choumet et al., 2012). Cells in the epidermis and dermis can be divided into two groups based on their origin: the non-hematopoietic skin cells, like keratinocytes and stromal cells, and skin-resident immune cells. It has been reported that several arboviruses can infect both, keratinocytes (Hamel et al., 2015; Lim et al., 2011; Surasombatpattana et al., 2011), as well as dermal stromal cells (Bustos-Arriaga et al., 2011; Hamel et al., 2015; Wichit et al., 2017). Surprisingly, keratinocytes may be the initial target for many arboviruses, however they have also been reported to exhibit immuno-regulatory properties, despite their non-hematopoietic origin and they express various TLRs and RLRs, as well (Lebre et al., 2007; Piipponen et al., 2020). Stimulation upon PRRs, keratinocytes can secrete various pro-inflammatory cytokines, chemokines and MHC II; factors that are necessary for the recruitment and activation of immune cells. (Cristina Lebre et al., 2003; Nickoloff & Turka, 1994; Piipponen et al., 2020; Visser et al., 2023).

The skin is heavily loaded with various immune cells (Figure 8.). The epidermis hosts mainly Langerhans cells (LC) and $CD8^+$ T resident memory cell (Trms). LCs form a net-like structure in the epidermis and are one of the first immune cells to come into contact with pathogens. The role of LCs in viral dissemination via their migration to the draining lymph node has been confirmed in arbovirus infections e.g., equine encephalitis viruses (MacDonald & Johnston, 2000). $CD8^+$ Trms are also among the firsts to recognize pathogenic invaders, however their presence requires previous encounter with the pathogen (Nestle et al., 2009). The dermis — in contrast to the epidermis — contains a much diverse immune population, including mast cells, cDC1 and cDC2, macrophages, Tregs and $CD4^+$ Trms in steady-state. Dermal DCs and macrophages were shown to be the initial targets for example for dengue virus (Schmid & Harris, 2014a). The chemokines produced by the activated keratinocytes, immune- and stromal-cells lead to the recruiting of neutrophils and inflammatory monocytes. The later ones can further differentiate into moDC. These cell types were also reported to be permissive for many arboviruses (Bai et al., 2010; Schmid & Harris, 2014b). There is a paradoxical role of the immune cells in arboviral infection in terms of viral clearance and dissemination as they can contribute to both processes. It has been shown that preventing uncontrollable viral replication through Th1 immune response is necessary to avoid neuroinvasion and subsequent death caused by arboviruses (Bai et al., 2010; Bryden et al., 2020; Chambers & Diamond, 2003; Nestle et al., 2009; Ong et al., 2014).

Till date, no multiparametric analysis of the initial target cells of RVFV in an *in vivo* setting has been reported, therefore we can only speculate on the initial target cells of this virus based on *in vitro* experiments and indirect data. Gommet and her colleagues characterized RVFV

infected immune cells via flow cytometry, however the analysed samples were collected from the spleen of immunodeficient (IFN-α receptor KO) mice, which were infected with delta-NSs RVFV strain expressing GFP. They detected GFP signals from macrophages, CD11b$^+$ DCs and granulocytes (Gommet et al., 2011). However, since the samples were collected from the spleen, it is not evident whether these cells were initial or subsequent targets of the virus following dissemination.

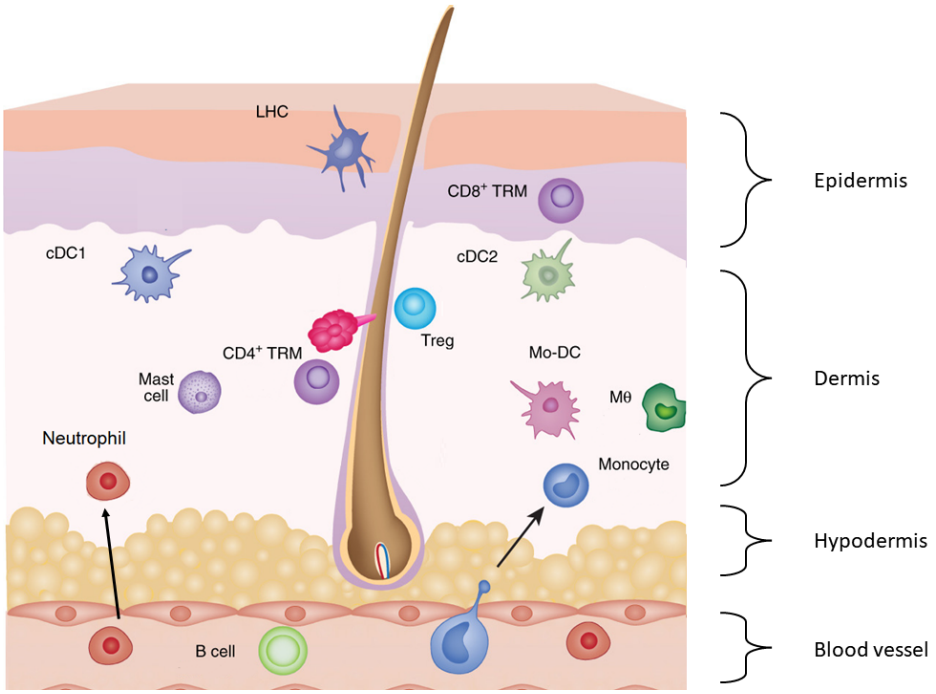

Figure 8. Immune cell populations in the skin
Schematic section of the skin highlights the most important immune cell populations and their location during arbovirus infection. LHC, Langerhans cell; Mo-DC, monocyte-derived DC; Mθ, macrophage; Treg, Regulatory T cell; TRM, tissue resident memory T cell; cDC, classical dendritic cell, adapted from (C. Zhang et al., 2022)**.**

1.3.1.1.1. Double-trouble: arbovirus transmission through mosquito saliva

The previous section introduced the early events following arbovirus infection; however, it focused solely on the virus-host interactions, processes expected to happen for example, after an injury. However, infection via arthropod vectors — in this case mosquito — adds an additional factor to the picture. There is a growing amount of evidence about the modulatory effect of the mosquito saliva (see Figure 9.) and its role in arboviral pathogenesis.
It is important to note that the protein composition of the saliva varies between mosquito genera, and is influenced by other factors, like age, sex, previous blood meal and infection status (Argentine & James, 1995; Choumet et al., 2012; Ribeiro, 2000; Thangamani & Wikel, 2009). Proteins in the vector saliva have direct physiological effect needed to facilitate blood feeding, like anticoagulants and vasodilators. Adenosine deaminase found in the mosquito saliva can directly induce mast cell degranulation (Z. Li et al., 2022). Compounds such as histamine and serine proteases released from their granules further increase the blood vessel permeability leading to plasma leakage causing oedema. Activation of mast cells also induces neutrophil influx to the bite-site (Demeure et al., 2005). Similarly, McCimmie's group also described the influx of neutrophil granulocytes; and they showed that these cells were the main producers of IL-1β and monocyte-attracting chemokines, such as C-C motif ligand (CCL)2

and 4 (both are ligands for chemokine receptor CCR2). They showed that bone marrow-derived, CD11b^{+} myeloid cells recruited via CCR2 were targeted by Semliki Forest virus and were responsible for virus amplification (Pingen et al., 2016).
Concurrently, mosquito saliva skews the polarization towards a Th2 type immune response. Furthermore, mosquito saliva was reported to inhibit proliferation of T and B cells in *in vitro* experiments (Guerrero et al., 2020; Visser et al., 2023; Vogt et al., 2018; Wasserman et al., 2004). Unfortunately, as discussed above, a proper Th1 immune response is a prerequisite for defense against arboviruses.
The effect of mosquito saliva on arbovirus pathogenesis is intensively studied. Based on the numerous reports, it is clear that the saliva can and, in many cases, does promote transmission and pathogenesis of arboviruses (Marín-López et al., 2023; Pingen et al., 2017; Schneider et al., 2010; Visser et al., 2023; Wichit et al., 2016); either by recruiting the necessary target cells (Pingen et al., 2017), disrupting blood vessel integrity (Lefteri et al., 2022), or preventing the polarization towards the necessary immune response (Schneider & Higgs, 2008).
The effect of mosquito saliva on the pathogenesis of RVFV was tested by Choumet's group. They have found that co-injection of salivary gland extract from Aedes aegypti increased the mortality and viral load in several organs of mice infected with RVFV ZH548 (Le Coupanec et al., 2013).

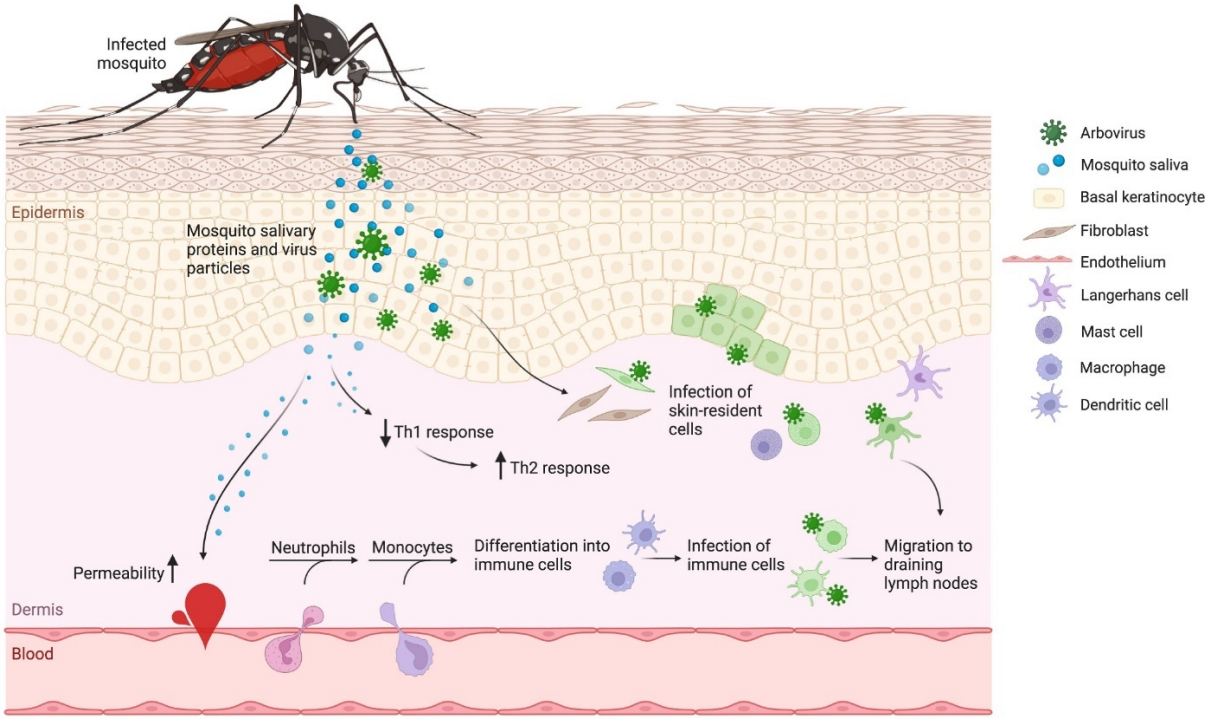

Figure 9. Arbovirus transmission and the effect of mosquito saliva
Schematic overview of the early events following the bite of an arbovirus-infected mosquito. During probing, mosquito deposits its saliva containing the virus into the dermis. The virus infects the skin-resident keratinocytes and stromal cells leading to their activation. Parallel, saliva compounds induce the degranulation of mast cells. Chemokines released by the activated keratinocytes and mast cells recruit neutrophils followed by inflammatory monocytes from the circulation. Recruited myeloid cells become infected with the virus and by migrating towards the draining lymph node, they promote its dissemination. The induction of Th2 type cytokines in the skin leads to the generation of an improper immune response aiding viral pathogenesis; from (Visser et al., 2023).

1.3.1.2. Respiratory route

The skin is constantly exposed to the environment, hence its most upper layer (*stratum corneum*) provides a physical barrier via the cornified epithelium, which is impenetrable for most pathogens, therefore successful infection through the skin usually requires the damage of this upper layer. On the contrary, the respiratory tract is covered by non-cornified epithelial cells, therefore they lack this type of protection. However, physical barrier in the form of mucus which is swiped outwards by ciliated epithelial cells is still present in the upper respiratory tract and it provides protection against less virulent pathogens. However ciliated cells are absent from the alveoli, hence alveolar epithelial cells are directly exposed to pathogens (Sato & Kiyono, 2012).

The alveolar epithelium consists of two cell types: type I (AECI) and type II (AECII) alveolar epithelial cells. Interestingly, while AECII is present in similar numbers to AECI in the lung, the latter makes up 96% of the alveolar surface. AECI are thin and flat, allowing for efficient gas exchange between the air and blood, while AECII are more cuboidal in shape and produce pulmonary surfactant, which is important for alveolar mechanical stability and gas exchange. Additionally, AECII cells have a self-renewal capacity and contribute to the maintenance of alveolar surface integrity (Guillot et al., 2013). AECII are also immunologically active, they bear numerous PRRs, they produce cytokines, chemokines and are also able to present antigens to $CD4^+$ T cells through MHC II (Debbabi et al., 2005; Hartl et al., 2018; Pechkovsky et al., 2005; Rock & Hogan, 2011).

There are two macrophage (Mf) subsets in the lung: alveolar Mf (AMf) and interstitial Mf (IMf). AMfs are unique cell types in regards that they reside in the alveolar space during steady-state. They are generally considered as anti-inflammatory cells. Their immunosuppressive nature is crucial to limit inflammation, hence, to prevent severe pneumonia, although, their anti-inflammatory properties can be exploited by pathogens. IMfs are less well-characterized Mf population as their alveolar counterpart. As their name suggests, they reside in the lung parenchyma. They constitutively express IL-10, and reactive oxygen species upon stimuli. They are believed to play a role in antigen presentation as they express MHC II (Ardain et al., 2020).

There are two subsets of cDC in the lung, which are usually distinguished by the expression of either CD103 or high amount of CD11b. As the $CD103^+$ population also expresses XCR1, they may be considered as cDC1 cells, while the $CD11b^{hi}$ population can be considered as cDC2 cells. cDC1 cells are located right below the mucosal surfaces, adjacent to the AECs, and are able to probe the lumen by their long excesses. cDC2 cells populate the lung parenchyma. Both subsets secrete proinflammatory cytokines upon activation, however cDC2 cells are the major chemokine producer subset (Ardain et al., 2020; Guilliams et al., 2013; Sato & Kiyono, 2012). pDC is another resident DC population in the lung parenchyma, and they are known for their massive IFN production upon viral infection.

The activation of AECs, interstitial macrophages and DC population followed by their production of pro-inflammatory cytokines and chemokines results in the influx of granulocytes and monocytes. Monocytes can differentiate into moDCs upon arrival to the lung and together with the granulocytes, they express their effector functions, as described earlier (Alshammary & Al-Sulaiman, 2021; Braciale et al., 2012; GeurtsvanKessel et al., 2008; GeurtsvanKessel & Lambrecht, 2008; Guilliams et al., 2013).

Immune response to respiratory viruses is summarised in Figure 10. Similarly to the skin, local and recruited immune cells may provide further pool for virus replication, and migratory APCs may be – at least partially – responsible for viral dissemination.

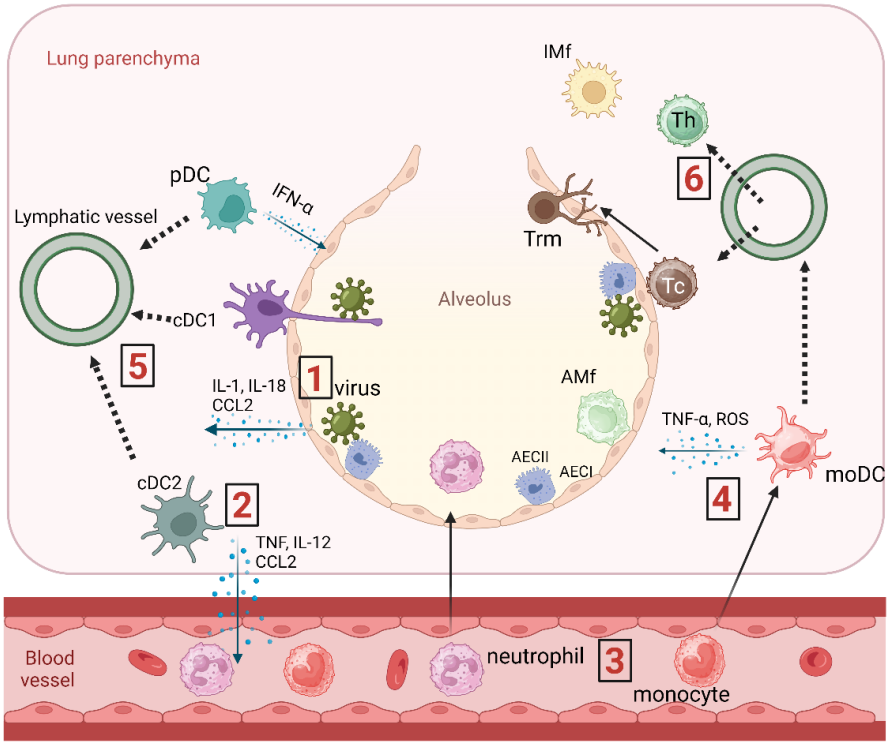

Figure 10. Immune response following virus infection in the lung.
Viruses reaching the alveoli of the lung, may infect AEC. Upon infection AECs begin to secrete pro-inflammatory cytokines and chemokines (1). Cytokines produced by AECs activates the local dendritic cell populations, enhancing their effector function (2). Chemokines produced by activated cDC2 – along with AEC – recruit neutrophils and monocytes from the circulation into the lung via CCR2-dependent manner (3). Monocytes differentiate into moDCs and produce further pro-inflammatory molecules (4). DCs migrate to the mediastinal lymph node following antigen uptake, where they activate virus-specific T cells (5). Activated T cells arrive to the lung, where they contribute to viral clearance (6). AEC, alveolar epithelial cell; AMf, alveolar macrophage; IMf, interstitial macrophage; pDC, plasmacytoid dendritic cell; cDC, classical dendritic cell; moDC, monocyte-derived dendritic cell; Th, helper T cell; Tc, cytotoxic T cell; Trm, tissue-resident memory T cell; ROS, reactive oxygen species. Image created with BioRender.

It is important to note that both the skin and the respiratory tract are interwoven with peripheral nerves, which can be targets for neurotropic viruses. There are several viruses reported to effectively infect neurons and some of them are able to travel towards the central nervous system via a process called retrograde axonal transport (Bearer et al., 2000; Davis et al., 2015; Maximova et al., 2016; J. Wang & Zhang, 2021). While viruses entering through the skin must make their way via peripheral neurons, through the spinal cord just to reach the brain eventually; viruses transmitted via aerosols may use the olfactory nerve as a shortcut to reach the central nervous system (Riel et al., 2015). Utilizing the nervous system, viruses can travel inside the body, sometimes without being detected by the immune system. RVFV was reported to be able to exploit both pathways (Boyles et al., 2021; Reed et al., 2012).

1.3.2. Middle stage

RVFV enters the blood circulation after its transport to the draining lymph nodes. With the blood, it disseminates rapidly in the body and undergoes replication in broad range of organs, especially in the liver. Microscopic analysis of RVFV infected liver tissues is characterized with multifocal necrosis affecting mostly hepatocytes, together with endothelial disruption leading to haemorrhage and infiltration of various immune cells (Odendaal et al., 2019).

This organ may not be a so-called barrier organ, however, it is equipped with potent immune surveillance against pathogens present in the blood, provided mostly by its resident macrophage population, also called as Kupffer cells. These cells reside in the liver sinusoid and extend their processes into the extracellular space between the sinusoid endothelial cells and hepatocytes. Kupffer cells become activated following the detection of viral antigen or the demise of hepatocytes. Upon activation Kupffer cells release pro-inflammatory cytokines as well as chemokines (Liaskou et al., 2012). These cytokines activate the sinusoidal endothelial cells, which subsequently upregulate their adhesion molecules and in combination with the cytokines produced by the Kupffer cells can promote the recruitment and extravasation of neutrophils and monocytes. (Méndez-Sánchez et al., 2021; Protzer et al., 2012).

Infection of hepatocytes and Kupffer cells followed by neutrophil and monocyte influx during the middle stage of RVFV infection have been described in several publication (Ahmed K, 2018; Odendaal et al., 2019; D. R. Smith et al., 2012). Gray et al. investigated the cytokine and chemokine production in the liver (among other organs) during RVFV infection, where they found that elevated pro-inflammatory cytokine and chemokine) production correlated with liver pathology (Gray et al., 2012). It has also been observed by Batista et al., that during the late-onset RVF encephalitis, mice exhibited liver repair characterized by a sharp decrease in cytokine and chemokine production (Batista et al., 2020). On the other hand, while Th1-dependent viral clearance has been reported during RVFV infection (Dodd et al., 2013), high level of IL-10 contributed to viral escape in mice (Jansen van Vuren et al., 2011). Furthermore, proinflammatory cytokine showed positive correlation with survival in human patients (McElroy & Nichol, 2012a). All of these suggest the need for proper control of pro- and anti-inflammatory cytokine production to balance between immune-mediated pathology and effective viral clearance (Lau & Thomson, 2003; Liaskou et al., 2012; Terasaki & Makino, 2015).

1.3.3. Late stage

Severe meningoencephalitis in humans and ruminants following RVFV infections is relatively rare, however, it is associated with 50% lethality in humans. The exact mechanisms and factors that drive RVFV infections towards the encephalitic form are not fully understood, and intensively investigated in these current days. This form has a late-onset characteristic with or without prior liver-stage (Hartman, 2017).

There are two major routes how RVFV and generally other viruses can enter the brain: 1. either through the blood-brain-barrier (BBB), or 2. via retrograde axonal transport through peripheral neurons (McGavern & Kang, 2011a).

1.3.3.1. Blood-Brain-Barrier

The role of the BBB is to shield the central nervous system (CNS) from uncontrolled diffusion of cellular and vascular components. This shield has multiple layers composed by various cellular and molecular elements (see Figure 11.). Blood vessels entering the CNS are lined by endothelial cells that use tight junctions to restrict the transmigration of circulating immune cells. They also produce *lamina basalis* to create additional physical barrier. The vascular tone

is regulated by smooth muscle cells and pericytes surrounding the blood vessels. The endfeet of astrocytes create a dense network forming the outermost layer of the BBB, called *glia limitans*. Macrophages on both sides of the glia limitans play the role as immunological sentinels (McGavern & Kang, 2011b).

BBB is a complex and usually well-regulated system during homeostasis, however various viruses evolved to be able to cross it. One possible way to do so is by directly infecting the endothelial cells. Infection can subsequently alter the function of these cells, including the promotion of increased chemokine and adhesion molecule production, such as CCL2 and vascular cell adhesion molecule 1 (VCAM1), respectively; altered expression of tight junction proteins. These events may lead to increased permeability of the endothelial layer, which not only promotes passive diffusion of viral particles, but also aids the other pathway called "Trojan horse" mechanism, in which the pathogens infect immune cells, which are able to cross the BBB. Monocytes and macrophages are the most common cell types used as "Trojan horses" by encephalitic viruses. Excessive production of CCL2 by infected endothelial cells further increase the recruitment of monocytes and their migration to the brain parenchyma (McGavern & Kang, 2011a).

Interestingly, RVFV is believed not to utilize the disruption of BBB for its entry to the brain, although other viruses (e.g., human T lymphotropic virus) may use the same entry receptor – heparan sulphate proteoglycan – for their infection of cerebral endothelial cells (Afonso et al., 2008). Dodd et al. could not detect BBB disruption in their mouse model following IN or ID infection with RVFV despite the presence of high proinflammatory responses in the CNS (Dodd et al., 2014b). Walters and his colleagues found that increased vascular permeability found in rats following RVFV infection was a consequence of inflammation, but the virus was replicating in the CNS days prior the BBB damage (Walters et al., 2019). Both results suggest that CNS invasion by RVFV does not require the disruption of the BBB.

Furthermore, up until today there is no direct evidence for RVFV using infected leukocytes as "Trojan horses" for their CNS invasion. In addition, Harmon and her colleagues reported that monocytes – which are the most commonly used leukocyte population as "Trojan horses" by other viruses – had a preventive role in RVF encephalitis (Harmon et al., 2018).

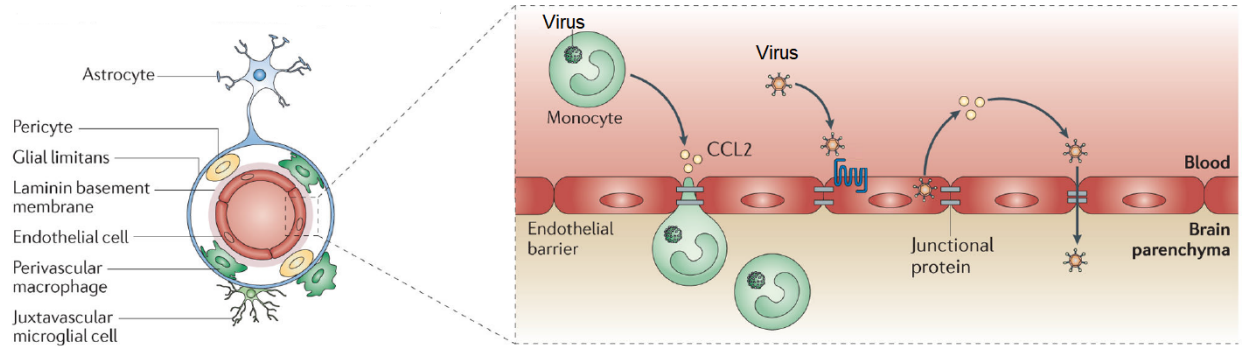

Figure 11. Schematic structure of the BBB and strategies for viruses to cross it

The BBB consists of various cellular and molecular barriers to prevent free diffusion of cells or humoral elements from the blood towards the CNS. Viruses with brain tropism evolved to cross this barrier via several ways: 1. By infecting immune cells that are able to pass through the BBB using them as a "Trojan horse"; 2. Infecting the endothelial cells directly and being released into the cerebrospinal fluid; 3. Free diffusion in case of inflammation and consequent disruption of the BBB, adapted from (McGavern & Kang, 2011a).

1.3.3.2. Accessing peripheral nerves

The second strategy for invading the CNS is through the infection of peripheral nerves and hijacking the axonal transport system to travel in a retrograde manner. Utilizing the retrograde axonal transport of the olfactory nerves by RVFV following IN infection and its migration towards the olfactory bulb through the cribriform plate has been well characterized in a rat model (Boyles et al., 2021). The migration of RVFV towards the brain followed by dermal inoculation is not understood in detail, however the ultrastructural description of RVFV infection in mouse models following SC administration showed intensive virus budding in neurons and neuroglial cells located in the spinal cord and brain stem, which suggests that the virus may have infected peripheral sensory or motor neurons and travelled via retrograde axonal transport (Reed et al., 2012).

1.3.3.3. Different cell types in the brain

Viruses reaching the CNS are provided with various types of susceptible cells. The brain is covered by the meninges which consists of three layers, from outside to inside: dura mater, arachnoid mater, and pia mater (see Figure 12.). Viruses targeting the meninges are usually arriving through the BBB and are present in the liquor, also known as cerebrospinal fluid. Liquor is produced at the choroid plexus, which is the only part of the BBB, which lacks astrocytes. Infection of the meninges causes meningitis, which usually results in a less severe form of disease, partially because the meninges are easily accessible to immune cells. Besides meningeal cells are self-renewable; therefore, they can recover from the damage caused during the infection. On the other hand, infection of the brain parenchyma is usually associated with encephalitis, which is more likely to cause fatal disease (Griffin, 2003; McGavern & Kang, 2011b).

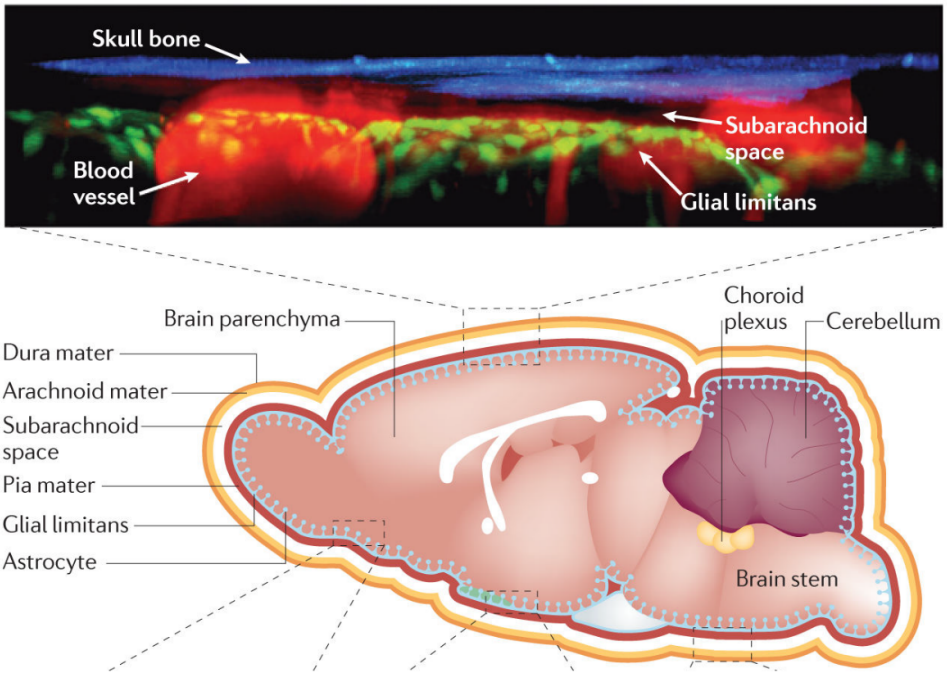

Figure 12. Diagrammatic section of the mouse brain

Beneath the skull bone sits the outer lining of the brain, consisting of the dura mater, arachnoid mater and pia mater, collectively referred to as the meninges. Between the arachnoid and the pia mater lies the subarachnoid space, in which flows the cerebrospinal fluid, and it contains blood vessels. The pia mater is separated from the brain parenchyma by the glia limitans, which is consists of astrocytes endfeet and basal lamina, from (McGavern & Kang, 2011b).

The two major cell types in the brain parenchyma are neurons and glial cells (see Figure 13.). There are numerous types of neuron in the brain, and while the characterization of all is not within the scope of this dissertation, it is worth noting that they are not equally susceptible to viral infections, and their ability to get infected depends on the virus tropism and the route of entry. In addition to neurons, the brain is also composed of multiple different types of glial cells. Astrocytes were previously described at the BBB. Beside their role played in forming and maintaining the BBB, they also support neuronal growth, regulate synaptic transmission, and remove toxic materials (Sofroniew & Vinters, 2010).
Oligodendrocytes are the most abundant cells in the CNS. They are responsible for the myelination of the axons, which is crucial and indispensable for the adequate functioning of the neurons and, therefore, the entire CNS. It is easy to see, that damage or death of these cells leads to neurological disfunction or even irreplaceable neuronal loss. Unfortunately, oligodendrocytes are a particularly vulnerable cell population. They are sensitive to oxidative damage and prone to mitochondrial injury, both are common during pro-inflammatory immune response with the presence of oxygen and nitric oxide radicals. In addition, TNFα can directly induce apoptosis in oligodendrocytes, whereas IFNγ is highly toxic to these cells during their proliferation (Bradl & Lassmann, 2010).
The third major glial cell population is the microglia. They are the resident macrophage population in the brain. They can grow processes through the pia limitans to monitor the BBB environment for pathogens. Together with astrocytes, they can produce chemokines to recruit other immune cells in the presence of pathogenic invaders. Beside their role during immune activation, they are responsible for controlling synaptic density and connectivity (Colonna & Butovsky, 2017).

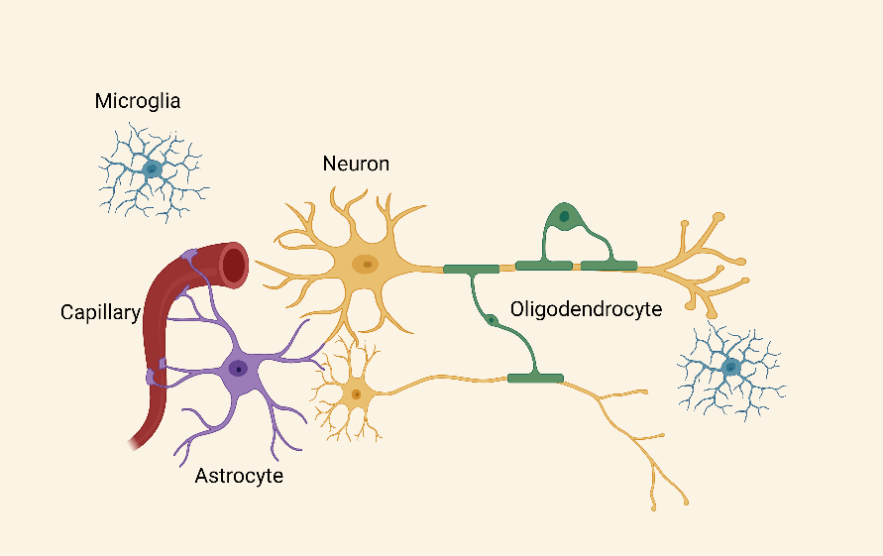

Figure 13. Major cell types of the CNS.
The two main cell types in the brain parenchyma are neurons and glial cells. Glial cells include astrocytes, oligodendrocytes and microglia. Astrocytes are found around brain capillaries and are part of the BBB. Oligodendrocytes are responsible for myelination of neurons. Astrocytes are scattered throughout the brain parenchyma. Image created with BioRender.

As the brain is particularly sensitive for inflammatory stress, the immune system is kept in an anti-inflammatory stage through the production of TGF-β by astrocytes and meningeal cells.

In case of infection, neurons and glial cells rapidly produce IFN-β. The body of the damaged or stressed neurons can signal to nearby astrocytes and microglia cells even if the neuronal damage occurs at the distant axons. Activated astrocytes and microglia produce various pro-inflammatory cytokines and chemokines which increase the adhesion molecules on the endothelial cells promoting leukocyte recruitment. The following events are a balancing act between viral clearance and immune regulation for the sake of preventing further neuronal damage.
As pointed out previously, the neuropathogenesis of RVFV is still not deciphered. The potential neurotropism of certain RVFV strains is evident, so is their direct cytopathic effect on infected cells. There is no consensus on the contribution of immune cells to the pathogenesis of RVFV. Infiltration of various immune cells together with elevated pro-inflammatory cytokines in lethal cases have been reported. However, selective depletion of certain immune subsets either had no effect or was detrimental to disease outcome (Albe et al., 2019; Dodd et al., 2013, 2014b; Harmon et al., 2018).

1.4. Animal models

Several animal models of RVFV infection have been developed and described over the years to study pathogenesis or to test potential antivirals or vaccines; however, all these models have their limitations regarding their sensitivity to RVFV or their ability to reproduce the symptoms of natural infections. It is important to keep in mind that pathogenesis is influenced by the virus strain and the administration route, furthermore, natural human and livestock infections have different disease courses as well, therefore, previous considerations must take place before choosing the appropriate model. This chapter briefly summarises our current knowledge about different animal models of RVFV emphasising their advantages and disadvantages (see Table 1.).

Table 1. Animal models for RVFV infection

Different animal models are listed, highlighting their advantages and disadvantages, adapted from (Ikegami & Makino, 2011).

Model	Advantages	Disadvantages
Mouse	Highly susceptible to RVFV	No haemorrhagic fever
	Acute hepatitis and lethal meningoencephalitis at late stage	No ocular disease
	Cost-effective	No time to generate adaptive immune response using WT virus
Rat	Similar pathogenesis to mice	Different susceptibility of the same strain from different breeding colonies
	Reproducible encephalitis	
	Occasional ocular involvement	
	Cost-effective	
	Varied susceptibility of different inbred strains	
Hamster	Highly susceptible to RVFV	No haemorrhagic fever
	Similar pathogenesis to mice	No ocular disease
		Limited research resources

Gerbil	Encephalitis with minimum liver disease	
	Age-dependent difference in susceptibility	
		Limited research resources
Macaques	Lethal haemorrhagic fever	No ocular disease
	Similar susceptibility to humans	Lack of reproducibility of severe symptoms
		Requirement of BSL3 lab for NHPs
		Expensive
Marmosets	Highly susceptible to RVFV	Requirement of BSL3 lab for NHPs
	Similar and reproducible symptoms to severe human cases	Expensive
Ferret	Reproducible lethal encephalitis	Limited research resources
	Less expensive compared to NHPs	Only IN infection route causes disease
Sheep and goat	Suitable for veterinary studies	Susceptibility varies among different breeds and age
	Highly susceptible to RVFV	Limited research resources
	Lethal hepatitis	Expensive
		Requirement of BSL3 lab for large animals

1.4.1. Mouse

Mice are probably the most frequently used animal models for RVFV due to their cost effectiveness and exceptional susceptibility to RVFV infection. The lethal dose 100 (LD_{100}) was determined as little as 1 plaque forming unit (PFU) for most inbred mouse strains, in case of footpad administration of RVFV ZH501. These mice died within 3-5 days post infection. There are only minor differences in the pathogenesis between the inbred mouse strains, which mainly related to the time of death (Cartwright et al., 2020; Connors & Hartman, 2022; Ikegami & Makino, 2011). The vast majority of mice succumb to the disease due to acute liver failure characterized by elevated levels of liver enzymes in the blood, prolonged blood clothing time and disseminated haemorrhages throughout the body affecting multiple organs. The virus antigen or infectious virus particles can be detected in various tissues, with the highest level in the liver. Mice that survive the liver phase usually manage to clear the virus from these organs; however, they later succumb to meningoencephalitis (D. R. Smith et al., 2010). Pathogenesis of RVFV in mice mimics the pathogenesis in lambs making them ideal to use in laboratories, which do not have access to BSL-3 laboratories designed for large animals. On the other hand, virus is undetectable in the eyes of infected mice, making mice unsuitable to study the ocular form of RVFV, which is the most common serious form in humans. They also do not develop fever, on the contrary, many times mice have hypothermia by the progression of the disease, which is uncharacteristic to most infection in other species (Ikegami & Makino, 2011). Due to their fast disease course, studying the adaptive immune response is often impossible using wild type (WT) mice and virus. Furthermore, their sensitivity and consequent mortality making mice unsuitable for immunological memory studies in a WT system. Lastly, while mice can develop meningoencephalitis, it is not possible to predict which individual would survive the liver phase, and enter the late phase, hence using them for solely studying

the encephalitic form of RVF disease is unpractical. Some of the disadvantages may be overcome by using gene-modified models, but one should always consider the pitfalls of such systems, considering that altered genetic makeup could lead to conclusions that may not hold true for non-modified viruses. For example, disposal of the NSs not only circumvent its IFN antagonistic property, but also eliminates its effect on cell cycle arrest, direct cytopathy and general halt of translation, which may interfere with the findings when using the delta-NSs strain of RVFV.

1.4.2. Rat

Rats are also frequently used animals investigating RVFV infection. They reproduce many of the symptoms occurring in natural infections similarly to mice, with the extension of occasional ocular involvement after aerosol challenge. However, in contrast to mice, inbred laboratory rat strains represent distinct disease course: Wistar-Furth and Brown Norway rats usually die quickly to acute hepatitis, meanwhile August-Copenhagen-Irish and Lewis rats are more resistant to subcutaneous infection route. However, these rat strains develop lethal encephalitis reproducibly, following aerosol exposure to RVFV, making them excellent model for investigating RVF encephalitis (Bales et al., 2012; Connors & Hartman, 2022). Limitations of these animals include the known genetic variability of the US and European colonies and their marked differences in susceptibility to RVFV infection (Ritter et al., 2000).

1.4.3. Hamster

Hamsters, just like mice, are exceptionally susceptible for RVFV infection. They usually succumb to the disease after 2-3 days due to extended liver necrosis. They show similar spectrum of symptoms than mice. Febrile and ocular disease have not been observed in hamsters either. The lack of hamster-specific reagents further narrows the applicability of this species (Ikegami & Makino, 2011; Scharton et al., 2015).

1.4.4. Gerbil

Gerbils are great candidates to study RVF encephalitis as these animals are uniformly succumb to encephalitis following RVFV infection with minimal liver involvement. Gerbils also show disease severity in an age-dependent manner, which was observed in domesticated ungulates too (Anderson et al., 1988). Similarly to hamsters, the available gerbil-specific reagents are limited.

1.4.5. Non-human primate (NHP)

While *Rhesus* and *Cynomolgus* macaques can be infected with RVFV, they are far less susceptible to RVFV infection than rodents. RVF disease in NHPs are usually mild and accompanied by fever; but occasionally it can develop into fatal haemorrhagic fever or meningoencephalitis. The lack of reproducibility of severe symptoms makes these species difficult to use for pathogenesis studies; especially when considering the cost-ineffectiveness and the ethical aspects of using these animals. However, NHPs do reproduce human RVF cases and pathogenesis better than other animal models (Connors & Hartman, 2022; Ikegami & Makino, 2011).

A novel NHP model involves SC or IN infection of common marmosets. These animals are not only more susceptible to RVFV infection and show higher morbidity and mortality rates than macaques, but exhibit acute-onset hepatitis with haemorrhagic fever, and delayed-onset encephalitis, which are characteristics to severe RVF in humans (D. R. Smith et al., 2012).

However, these models require high containment laboratories suitable for NHPs.

1.4.6. Ferret

Ferrets are good models for RVF encephalitis studies as they develop febrile illness with lethal encephalitis following IN but not ID exposure to RVFV. The virus is transiently present in other organs, and induce temporally elevation of liver enzymes, which can be detected in blood (Barbeau et al., 2020). However, the available reagents specific for ferrets are limited.

1.4.7. Sheep and goat

As sheep and goats are natural hosts of RVFV infection and are responsible for the amplification of the virus during enzootic period, they represent a very good animal model for this disease. However, genetic variance and consequent susceptibility to RVFV between breeds has been described, similar to that in rats. (Faburay et al., 2016; A. Kroeker et al., 2018). Using these animals requires BSL-3 facilities suitable for large animals, which increases the costs and narrows the accessibility of these models.

1.5. Aim of the study

While RVFV shows high mortality in several domesticated farm animals, human infections are described as self-limiting febrile illnesses. However, RVFV infections can sometimes develop into severe forms with fatal outcome. Mortality is very variable among outbreaks with 0,5-28% case fatality rate. Our understanding about how different factors - such as, the route of infection and the viral source - influence the disease outcome remains incomplete and somewhat elusive. This is, in part, is due to the exceptionally high virulence of the most commonly used virus strains, such as ZH501 and ZH548. This excessive virulence can limit the potential of these models and often requires scientists to resort to gene-modified systems, both for the virus and/or hosts.

The aim of this study was to expand our current knowledge on how different factors, both on the virus and host sides, influence the outcome of RVFV infection using only wild-type hosts and virus isolates obtained from the field, which have never been reported in *in vivo* tests before.

The three main objectives are:

1. To assess whether host susceptibility to RVFV infection and disease depends on the infection route
2. To determine whether RVFV pathogenesis and organ tropism in our model varies between virus isolates of different origin (e.g. mosquito vs mammalian isolates).
3. To characterize the primary target cells of RVFV at the natural portals of virus entry (e.g. skin vs mucosae)

In order to accomplish these goals, pathogenesis and phenotyping studies will be performed in the BSL-3 laboratory at the Bernhard-Nocht-Institute for Tropical Medicine in Hamburg. These expereiments will include entomologic, virologic and immune assays.

The ultimate goal is to better understand RVFV infection and its multifaceted disease progression, with the hope to provide additional, more suitable animal models for future studies requiring *in vivo* models.

2. Materials

2.1. Reagents

Table 2. List of reagents

Reagent	Company
DNase I	Sigma
Dulbecco's Modified Eagle Medium (DMEM)	Sigma
Dulbecco's Phosphate Buffered Saline (PBS)	Sigma
Ethylenediaminetetraacetic acid (EDTA)	Roth
Fetal calf serum (FCS)	Gibco
Isoflurane	Abbvie
L-Glutamine (200 mM)	Gibco
Methyl cellulose	Roth
Paraformaldehyde (PFA)	Biocyc GmbH CO & KG
Penicillin/Streptomycin	Gibco
RBC lysis buffer	BioLegend
Roswell Park Memorial Institute medium (RPMI) 1640	Gibco
Sodium hydroxide	Roth
Trypsin TrypLE TM	Gibco
Liberase TM	Roche
Tryprtose Phosphate Broth (TPB)	Gibco
Rompum	Bayer
Ketamine	WDT
Fructose	Sigma
Crystal violet	Serva
Buffered PFA/Formalin	Biocyc
Triton-X100	Roth
Glutamax	Gibco
Bovine serum albumin	Sigma
4-(2-hydroxyethyl)-1-piperazineethanesulfonic acid (HEPES)	Gibco
Crystal violet	Sigma
0,33% neutral red solution	Sigma
NaHCO3	Sigma
Minimum essential medium (MEM)	Gibco
10X DMEM	Gibco
Non-essential amino acid solution	Gibco
Cell culture grade water	Gibco

2.2. Buffers and media

2.2.1. Media

Table 3.List of media

Media	Component
Vero E6 growing medium	in DMEM
	5% FCS
	1% Penicillin/Streptomycin
	1% Glutamax-100
A549-Npro growing medium	in DMEM
	10% FCS
	10% TPB
	1% Penicillin/Streptomycin
	1% Glutamax-100
Infection medium	in DMEM
	2% FCS
	1% Penicillin/Streptomycin
	1% non-essential amino acids
	10mM HEPES
2X Minimum essential medium (MEM)	in 10X MEM
	1% Glutamax-100
	1% Penicillin/Streptomycin
	10mM HEPES
	0,42% Bovine Serum Albumin (BSA)
	0,24% $NaHCO_3$
	68% cell culture grade H_2O
Skin and lung digestion media	in RPMI 1640
	0,2 mg/mL Liberase TM
	50µg/mL DNase I

2.2.2. Buffers

Table 4. List of buffers

Buffer	Components
FACS buffer	in PBS
	2% FCS
	2mM EDTA

2.2.3. Solutions

Table 5. List of solutions

Solution	Components
Mosquito feeding solution	in H_2O
	10% fructose
Neutral Red Solution	in 10X MEM
	4% neutral red (which is already in 0,33% solution)
	86% cell culture grade water H_2O
Agarose gel	in PBS
	1,2% agar
Crystal violet solution	in H_2O
	20% ethanol
	1% crystal violet

2.3. Cell lines

Human lung carcinoma A549 cell line expressing N-terminal protease fragment (Npro) of Bovine Viral Diarrhea Virus (in the following: A549-Npro) cells were used for virus plaque purification and plaque assays (Hilton et al., 2006). Vero E6 cell line, previously isolated from African green monkey kidney, was used for virus amplification. The human neuroblastoma cell line SH-SY5Y and the human hepatoma cell line Huh7 were used for the virus growth kinetics experiment.

Cell lines were kept at 37°C with 95% relative humidity and 5% CO_2.

2.4. Viruses

The two natural isolates of Rift Valley Fever Virus used in these experiments were a generous gift from Prof. Matthias Niedrig's lab at the Robert Koch Institute. The isolates were amplified on Vero76 followed by a second amplification on VeroE6 cells. After this the isolates were plaque purified on A549-Npro cells followed by a last amplification on VeroE6 cells. Supernatant from the last amplification steps were collected and centrifuged at 700 RCF, 4°C for 5 minutes to remove any cell debris. The supernatant was aliquoted and stored at -80°C until further use. The virus batches were titered and sequenced.

For the sake of readability, I will refer to isolate CAR R1662 as human isolate (huRVFV) and to isolate Ar20364 as mosquito isolate (mosRVFV). Table 6. contains general information about the two RVFV isolates.

Table 6. General information on the RVFV isolates used in this study

Isolate	Lineage	Species of origin	Country of Origin	Year of Isolation
CAR R1662	G	human	Central African Republic	1985
Ar20364	F	mosquito	South Africa	1981

2.5. Mice

Mice were originated from Jacksons Laboratory and were housed in the animal facility of the Bernhard-Nocht-Institute for Tropical Medicine (BNITM). The animals were kept in individually ventilated cages and were fed and watered *ad libitum*. The experiments were taken place in a room with controlled temperature and humidity, with a 12-hours day-night cycle. All animal

experiments were performed on female C57Bl/6J laboratory mice with the age of 6-12 weeks. Animals were transferred into the BSL-3 laboratory, 5-7 days before the beginning of experiments for the sake of their acclimatisation to the new environment.

2.6. Mosquitoes

Aedes aegypti PAEA strain mosquitoes (obtained through INFRAVEC2 from Prof. Failloux, Institute Pasteur) is a colony from French Polynesia. The mosquitoes were kept at 28±5°C and 80% humidity with a 12-hour light/dark cycle. They were hatched and raised in the insectary at BNITM. Mosquitoes were fed with 10% fructose solution *ad libitum*. Female mosquitoes were separated and starved one-day prior saliva collection.

2.7. Antibodies

For a list of antibodies used for flow cytometry, see Table 11 in the Flow Cytometry section. Polyclonal rabbit anti-RVFV Gn antibody - used for IHC analyses - was a kind gift from Prof. Martin Groschup from Friedrich Loeffler Institute.
Monoclonal mouse anti-RVFV Np IgG2bκ antibody (clone R3-1D8-1-1) - was obtained from the Joel M. Dalrymple - Clarence J. Peters USAMRIID Antibody Collection through BEI Resources, NIAID, NIH – was used as a positive control for ELISA analysis for testing seroconversion.

2.8. RNA probes

Target probes detecting the mRNA of RVFV S segment via flow cytometry was designed with the collaboration of Thermo Fisher's bioinformatics team.
Probes complementary to mouse beta-actin mRNA (catalog number: PF-204) was used as positive control.

2.9. Kits

Table 7. List of kits

Kit	Company
QIAamp Viral RNA Mini Kit	Qiagen
ID Screen® Rift Valley Fever Competition ELISA	Innovative Diagnostics
LIVE/DEAD™ Fixable Blue Dead Cell Stain Kit	Invitrogen
Fixation and permeabilization (Cytofix/Cytoperm) kit	BD Biosciences
PrimeFlow™ RNA Assay Kit	Thermo Fisher
QIAseq FX DNA Library Kit	Qiagen
UltraView Universal DAB Detection Kit	Roche

2.10. Equipment

Table 8. List of equipment

Machine	Company
Cytek SpectroFlo Aurora	Cytek Biosciences
MRX^{e} microplate reader	Dynex
FastPrep-24 5G	MP Biomedicals
Fuji DRICHEM Analyzer	Fujifilm
NextSeq550	Illumina
Ventana BenchMark XT	Ventana

2.11. Computer softwares

Table 9. List of computer programs

Program/Software	Company/Developer
BioRender	BioRender
ChimeraX	UCSF ChimeraX
Clustal Omega	EMBL-EBI
Expasy	SIB
FlowJo, V10.9	FlowJo LLC
GraphPad Prism	GraphPad Software, Inc
Mendeley	Elsevier
Microsoft Office	Microsoft Corporation
CLC Main Workbench	Qiagen

3. Methods

3.1. Plaque purification

A549-Npro cells were seeded into 6-well plates in 2 mL the day prior to the experiment. Plates with ~85% confluent cell monolayer were taken into the BSL-3 laboratory. The virus isolates were serially diluted 10-fold in infection medium and 300µl was added to each well. Plates were placed for an hour into an incubator with 37°C, 95% humidity and 5% CO_2. During incubation, agarose gel was melted and mixed with 2x MEM medium in 1:1 ratio. After incubation, plates were decanted, and the agarose overlay was gently administered onto the monolayers. After the overlay solidified, plates were kept in the incubator for 5 days with the same conditions mentioned before. On day 4, a second overlay, prepared with the mixture of 1,2% melted agarose and 4% neutral red solution in 1:1 ratio, was layered onto each well. Neutral red overlay was used to enhance the visibility of the forming plaques. On the same day VeroE6 cells were seeded onto T75 flasks. After 5 days of infection, cells around the visible plaques were collected via pipette tips piercing through the agar layer. The content of each pipette tips was washed into separate T75 flasks. The flasks were incubated for an additional 5 days at 37°C, 95% humidity and 5% CO_2. Supernatant from flasks with visible cytopathic effect (CPE), was collected into 50mL centrifuge tubes, followed by centrifugation for 5 minutes at 4°C and 600 RCF. Sediment-free virus stocks, gained after centrifugation, was aliquoted into cryotubes and stored at -80°C until further use.

3.2. Viral RNA isolation

Randomly selected tubes from viral stocks were thaw and RNA was isolated by using QIAamp Viral RNA Mini Kit following the manufacturer's protocol. Final RNA was eluted in 60µl using the kit's elution buffer and aliquoted in 30µl. Eluted RNA was stored at -80°C until further processing.

3.3. Viral genome sequencing

Viral genome sequencing was performed by the BNITM's Next-Generation Sequencing Core Facility. RNA samples were used for a reverse transcription polymerase chain reaction (RT-PCR) with random primers to amplify viral RNA. The amplified viral RNA samples were subjected to library preparation using a QIAseq FX DNA Library Kit. After library preparation, the samples were normalized to ensure equal representation and then pooled together. The pooled sample was sequenced using NextSeq550 platform. The generated raw sequencing reads were first checked for quality using Phred quality scores. Reads with a quality score below 20 were trimmed and filtered to remove low-quality or polyclonal reads that may interfere with downstream analysis. The remaining filtered raw reads were then subjected to *de novo* assembly, where overlapping reads were assembled into longer contiguous sequences using Trinity v2.6.64239 and CLC workbench. Amino acid sequences were generated by using the online platform Expasy (web.expasy.org/translate) (Duvaud et al., 2021). Amino acid sequences of reference strain (ZH-501) were gained from GeneBank (ID: ABD51510.1, ABD38813.1, ABD38728.1, ABD38729.1) (Bird et al., 2007). Pairwise analysis was performed by using Clustal Omega Multiple Sequence Alignment tool (https://www.ebi.ac.uk/Tools/msa/clustalo/).

3.4. Collection of mosquito saliva

Female mosquitoes were placed at -20°C for 2 minutes or until no movement could be observed. Paralysed mosquitoes were transferred onto glass petri-dish cooled and kept on ice. Wings and legs were removed from all the insects to prevent locomotion during salivation. 10-µl pipette tips were filled earlier with microscope immersion oil. The proboscis of immobilized mosquitoes was gently inserted into an oil-loaded pipette tip. After one hour the mosquitoes were collected and humanely euthanized via 96% ethanol. The content of pipette tips containing mosquito saliva was pooled into a 1,5mL microcentrifuge tube. 1µl PBS/10 salivated mosquitos were added to the tube, vortexed and spun at 4°C for 15 minutes at 1000 RCF. The water-based portion was collected and stored at -80°C until usage.

3.5. Ethics statement

All animal experiments were performed in accordance with the prescribed rules and regulations of the German Society for Laboratory Animal Science. The experiments were approved by the Committee on the Ethics of Animal Experiments of the federal state of Hamburg. Animal experiments were performed as described in permit number N079/2020 in strict adherence with the ethical regulations outlined by the animal welfare authorities.

3.6. Humane endpoint criteria

To prevent extended suffering of experimental animals following infection, their well-being – indicated by their body weight, body temperature (measured by rectal probe), general condition and spontaneous behaviour – was scored according to the scale shown in table 10.

Animals that reached the endpoint criteria (score 3) in any category were humanely euthanized via isoflurane overdose.

Table 10. Humane endpoint criteria

Observation/finding	Score
Body weight	
Unaffected or increase	0
Reduction > 5%	1
Reduction > 10%	2
Reduction > 20%	3
General condition	
Smooth, glossy coat; clean body openings	0
Dull, ruffled coat; cloudy eyes	1
Sticky or moist body openings; abnormal posture; high muscle tone; dehydration	2
Seizures; paralysis; respiratory sounds; animal feels cold	3
Spontaneous behaviour	
Normal behaviour (sleeping, response to blowing and touching, curiosity, social interactions)	0
Unusual behaviour, limited mobility, or hyperactivity	1
Isolation; vocalization of pain; apathy; pronounced hyperactivity or stereotypies; coordination disorders	2
Self-mutilation, moribund	3
Body temperature	
36.1 - 37.9 °C	0
38.0 - 38.9 °C	1
33.0 - 36.0 °C	1
30.1 - 32.9 °C	2
>40 °C	2
<30 °C	3

3.7. Mouse infection

3.7.1. Intradermal (ID)

Intradermal injection of the virus requires perfectly still animals, not just because of the fine manipulations needed for the procedure but because of the high-risk nature it possesses to the experimenter. To ensure immobilisation of the mice for the required time, ketamine-xylazine mixture in PBS was used intraperitoneally as a sedative at a dose of 80 mg/kg and 5 mg/kg, respectively. Anesthetised animals were placed onto their abdomen and 2 µl of the virus or vehicle control was administered into the dorsal dermal layer of the ear. A high-precision glass syringe (from Hamilton) and custom-made 15 mm long, 33-gauge needles were

used to ensure accurate administration of such low volume and to minimise the potential adverse effects caused by the needle damage, as well.

3.7.2. Intranasal (IN)

For the sake of comparability of the two infection routes, the same anaesthesia was applied here as well. Sedated mice were placed onto their back and 20 µl of virus or vehicle control was dropped onto both of their nostrils. After complete inhalation of the liquid, the mice were held upright for one minute to prevent airway obstruction.

3.8. Organ shredding

The determination of the viral load in different organs requires, as a first step, the homogenisation of the organs of interest. Organs collected and stored in 2mL microcentrifuge tubes at -80°C were thaw, weighed* and transferred into 2 mL shredder tubes containing ceramic spheres Lysing Matrix D (MP Bio) and 1 mL of DMEM. Organs were mechanically homogenized by FastPrep24 5G device using the programs with the factory default settings for the corresponding organs. To sediment cell debris, the homogenates then were centrifuged at 17000 RCF for 10 minutes at 4°C. After centrifugation the supernatants were aliquoted and stored at -80°C until further processing.

*Some organs – such as the lymph nodes and the ears – were too light to be measured by the scale available in the BSL-3 laboratory. In these cases, the viral load was determined for the entire organ.

3.9. Virus titer determination from organs

The organs' viral load was determined by plaque forming assay. A549-Npro cells were seeded into 24-well plates one day prior the start of the assay. The following day - when the cell confluency was at 95-100% - the plates were transferred into the BSL-3 laboratory. 10-fold dilution of the organ homogenates were prepared using DMEM without supplements. The plates containing 200µl of tissue homogenate/well were placed for an hour into an incubator with 37°C, 95% humidity and 5% CO_2. After the incubation, the inoculums were discarded, and the cells were covered with a semi-solid overlay media prepared from cell growing media and 2% of methylcellulose in 2:1 ratio.

After four days of incubation the overlay was discarded, and the samples were inactivated for an hour by 4% of paraformaldehyde (PFA). After inactivation, the plates were taken out of the BSL-3 laboratory and were washed with water to remove any PFA residues. The cell monolayer was stained with 1% crystal violet for 15 minutes on room temperature. After the incubation the crystal violet stain was removed, and the plates were washed with water. Infectious virus particles cause disruption on the cell monolayer, which represents as a light plaque on the violet cell layer. Since each plaque corresponds to a single virus particle, the viral load in a gram of tissue sample can be calculated by multiplying the plaque numbers with the dilution factor and dividing it with the organ weight.

3.10. Virus titer determination from blood plasma

Blood was collected from either the tail vein followed by a minor incision with a surgical scalpel or - in case of the endpoint sample collections - from the *vena cava inferior* using a 1mL syringe with a 27G needle. The samples were collected into tubes containing heparin/lithium gel as anticoagulant. Blood plasma was prepared via the centrifugation of the blood at 10000 RCF

for 5 minutes at room temperature. The separated plasma was collected into 1,5mL microcentrifuge tubes and stored at -80°C until further processing.
The following steps of the plaque forming assay were performed as previously described, except that the viral load was calculated for 1 mL of plasma (instead of one gram of tissue).

3.11. (Immuno-)histochemistry

Histology samples were prepared and co-analysed by Dr. Susanne Krasemann from the Core Facility for Mouse Pathology at the University Hospital Hamburg-Eppendorf. Freshly harvested organs were placed into buffered fixation solution containing 4% of PFA and 10% of formalin and were stored at room temperature in the dark for four weeks prior taken out from the BSL-3 laboratory. After fixation, samples were briefly rinsed with water to remove fixative residue and were stored in PBS at 4°C until paraffin embedding. Prior paraffin embedding, samples were dehydrated in ascending ethanol row (70%, 80%, 96%, 100%) followed by immersion into xylol. Subsequent sections were cut at 3µm and deparaffinized by heat at 65°C for 20 minutes followed by 20 minutes in xylol and a descending ethanol row (100%, 96%, 80%, 70%) for 5 minutes each, finished by PBS. Deparaffinized sections were subjected to haematoxylin-eosin (H&E) staining according to standard procedures (see below) or processed for immuno-histochemical staining as follows: endogenous peroxidase was inactivated by using 3% hydrogen-peroxidase in PBS for 10 minutes at room temperature. Antibody-specific antigen retrieval was performed using the Ventana Benchmark XT machine. Sections were incubated with polyclonal rabbit anti-RVFV-Gn (1:5000) for one hour. Anti-rabbit Histofine Simple Stain MAX PO Universal immunoperoxidase polymer (Nichirei Biosciences) was used as the secondary antibody according to the manufacturer's instructions. Detection and counter-staining were performed with the ultra-view universal DAB detection kit from Ventana.
Sections for H&E staining were first stained in Harris Haematoxylin for 5 minutes rinsed with tap water and differentiated for 1 minute in 1% HCl. Bluing was done by running tap water. Slides were washed with 70% ethanol and counterstained with 1% eosin for 1 minute followed by a final rinse in 70% ethanol.
Immuno-histochemical or H&E-stained sections were dehydrated - as described above - and covered using xylol based mounting medium. Representative images were taken using a Leica DMD 108 microscope and staining was evaluated in a blinded fashion.

3.12. Assessment of plasma aspartate aminotransferase

Aspartate aminotransferase (AST) is an enzyme produced by the liver. In case of liver damage this enzyme leaks into the blood stream, therefore elevated level of this enzyme in the blood indicates and correlates with liver damage. The liver was reported as one of the main targets of RVFV, hence plasma AST level was measured as one indicator of the disease severeness. Therefore, blood was collected as mentioned earlier. Frozen plasma samples were thaw and diluted in 0,9% NaCl in 1:9 ratio. Fuji Dri-Chem GOT/AST P-III slides were warmed up to room temperature and 10µl of the diluted plasma was transferred onto them. The serum AST level was determined by FUJI DRI-CHEM analyser.

3.13. Assessment of seroconversion

Virus-specific IgG antibody in mice was detected via indirect enzyme-linked immunosorbent assay (ELISA). Bood plasma was prepared and stored as described in section "Virus titer determination from blood plasma" and was inactivated by 2% of Triton-X100 in PBS mixed in 1:1 ratio for one hour. Inactivated plasma samples were taken out from the BSL-3 laboratory

and were stored at -20°C until further processes. Plasma samples were thaw and diluted for 200-times and were loaded onto pre-coated and pre-blocked 96-well format ELISA plates (from ID-Vet) containing recombinant RVFV Np. Plates were incubated for an hour at 37°C. After incubation, plates were washed and labelled with a secondary, HRP-linked goat anti-mouse IgG antibody (Biozol) in 1:10000 dilution. Plates were incubated for 30 minutes at room temperature. At the end of the incubation, plates were washed again and TMB substrate was used for colour formation. Reaction was stopped by the addition of 2M sulfuric acid. The plates were read by an ELISA reader at 450nm. The optical density (OD) values were adjusted by subtracting the mean values measured for the blank wells.
Mouse anti-RVFV NP (clone R3-1D8-1-1) from Bei Resources was used as positive control. The pre-coated ELISA plate, washing- and dilution buffers, TMB substrate and stop solution were all part of the ID Screen® Rift Valley Fever Competition Multi-species ELISA kit (catalogue number: RIFTC-10P). Where applicable, cut-off values were determined by the sum of the mean OD450 value of samples obtained from mock-infected mice plus three times its standard deviation.

3.14. Flow Cytometry

3.14.1. Organ preparation

Single cell suspension was prepared from the ear and lung and their draining lymph nodes, auricular lymph node (ALN) and mediastinal lymph node (MLN), respectively.
The dorsal and ventral skin sheets of the ear were mechanically separated and placed into a 2 mL microcentrifuge tube containing 1 mL of RPMI. With the help of a scissors, small skin pieces were generated followed by the addition of 1mL digestion media. Tubes were placed into a heating block at 37°C with 1000 RPM shaking for 30 minutes. The digestion was stopped by adding 40 µl of 0,5M EDTA. The content of the tubes was loaded onto a cell strainer with 70 µm pore size. The digested tissue pieces were mashed through the strainer with the help of a syringe plunger. The strainer and the cells were washed with PBS and centrifuged at 500 RCF at 4°C for 5 minutes. Cells acquired from two animals were combined into pooled samples.
Single cell suspension from the lung was prepared in the same way as from the skin with an additional red blood cell lysis step due to its high vascularity. Red blood cells are lysed with 5 mL of RBC lysis solution (BioLegend) for 3 minutes followed by adding 30 mL of PBS and centrifugation at 500 RCF at 4°C for 5 minutes.
The lymph nodes were directly placed onto the cell strainer without prior enzymatic digestion and single cell suspension was created by simply mashing them through the strainer using a syringe plunger. The cell suspension was washed and centrifuged as described for the skin and lung samples above. No RBC lysis was used for the lymph nodes.

3.14.2. Cell Surface antigen staining

During flow cytometric analyses, it is crucial for being able to exclude dead cells, because they tend to bind antibodies in an aspecific manner, that would lead to false-positive staining results. One way of detecting such cells is by using so called live/dead stains. These stains are reactive with free amins, which can be found inside and outside of the cell membranes. Since live cells have an intact, non-permeable cell membrane for these dyes, their available amins are significantly less comparing to apoptotic or dead cells, which leads to a much lower staining signal. Therefore, this enables us to only include live cells during the flow cytometric analyses. Staining for dead cells with a stain takes place right after the last centrifugation of the organ preparation. Cells are resuspended in 1 mL PBS containing 1 µL of Live/Dead fixable blue

(Invitrogen) dye for 30 minutes at room temperature in dark. After 30 minutes, 1 mL PBS was added to the tubes followed by a centrifugation at 500 RCF at 4°C for 5 minutes.
The cell pellet was resuspended in 50 µl of FACS buffer containing 10 µl Fc-block. This step is necessary to reduce the aspecific binding of the antibodies used in the following step. Many immune cells - such as neutrophils, monocytes, macrophages, NK cells and DCs - bear Fc-receptors (CD16 and CD32) on their surfaces which can capture antibodies by their Fc-part, leading false-positive staining results. Fc-block is an antibody mix specific for these two receptors. Binding to their targets, Fc-block sterically prevents them capturing other antibodies.
Cells were incubated with the Fc-block for 15 minutes at 4°C in the dark. After that, 50 µl of antibody master mix containing appropriate amount (previously tittered) of fluorescently labelled antibodies. The antibodies and their concentration used for the master mix can be found in table 11. After the addition of labelling antibody master mix, the cells were vortexed and placed at 4°C for 25 minutes in a dark environment. Cells were washed with 1mL PBS and centrifugated as previously described.

3.14.3. Viral RNA staining

The PrimeFlow™ RNA assay (Invitrogen) enables the user to detect specific mRNA sequences via flow cytometry using target-specific oligonucleotide probes, followed by multiple amplification steps ending with a fluorescent dye-conjugated labelling probe.
For the viral RNA staining the manufacturer's protocol was followed with two exceptions: 1. The first fixation was performed with 2 mL of Cytofix/Cytoperm™ fixation and permeabilization buffer (BD Bioscience) for 30 minutes on room temperature instead of the kit's fixation buffer, since the former contains 4,5% of PFA - a validated inactivating agent in our BSL-3 laboratory - in contrast to the PrimeFlow RNA assay's fixation buffer which has an insufficient percentage of PFA. After fixation with BD's Cytofix/Cytoperm™ buffer the samples were taken out of the BSL-3 laboratory and the protocol was continued under BSL-2 conditions. 2. In our system four-times of the recommended amount of target probe was needed for the successful detection of RVFV RNA.
Cells were resuspended in FACS buffer and acquired on a Cytek Aurora cytometer.

Table 11. Flow cytometry panel used for determining RVFV infected cells

Antigen	Clone	Conjugate	Company	µl/sample
CD103	M290	BUV395	BD Biosciences	1.5
CD11b	M1/70	BV510	BioLegend	0.05
CD11c	N418	BV785	BioLegend	1.5
CD45R (B220)	RA3-6B2	BV650	BioLegend	2
CD3	17A2	BV650	BioLegend	2
CD326 (Ep-CAM)	G8.8	Alexa Fluor 594	BioLegend	0.75
CD45.2	104	BUV737	BD Biosciences	1.5
CD64	X54-5/7.1	BV711	BioLegend	0.15
CD8a	53-6.7	BUV615	BD Biosciences	1.5
DC-SIGN (CD209)	5H10	BV480	BD Biosciences	0.5
F4/80	BM8	BV605	BioLegend	0.05
Langerin (CD207)	4C7	PE-Cy7	BioLegend	1.5
LRP1	polyclonal	FITC	Santa Cruz	5
Ly-6C	HK1.4	BV570	BioLegend	0.15
Ly-6G	1A8	BV650	BioLegend	0.05
MHC II (I-A/I-E)	M5/114.15.2	Alexa Fluor 700	BioLegend	0.06
NK1.1	PK136	BV650	BioLegend	0.1
Siglec H	551	Pacific Blue	BioLegend	0.6
Siglec-F	E50-2440	APC-Cy7	BD Biosciences	0.5
SIRPa (CD172)	P84	BUV661	BD Biosciences	0.5
XCR1	ZET	BV 421	BioLegend	1.5
Live/Dead Fixable Blue	-	not public	Invitrogen	1
RNA probe	-	Alexa Fluor 647	Invitrogen	5 or 20* *for positive control and RVFV respectively

3.15. Viral growth kinetics

A549-Npro, SH-SY5Y and Huh7 cells were seeded 24 hours prior to infection at a concentration of $1x10^6$/5 mL/well in a 6-well plate format to achieve 95-100% confluence. Plates with confluent cell monolayer were taken into the BSL-3 laboratory, where human and mosquito isolates of RVFV were administered into the wells in multiplicity of infection (MOI) 0,01. One plate contained both isolates in parallel with 3 biological replicates. 100 µl of supernatant from each well was collected daily for four days, starting on day 0 as a baseline, with the viral load of the supernatant collected immediately after spiking. The collected supernatant was stored at -80°C until titration. The virus load was determined via plaque forming assay performed the

same way as it is described in Section “Virus titer determination from organs” using the cell culture supernatant instead of organ homogenates.

4. Results

4.1. Infection with huRVFV

The two main routes of human infection with RVFV are through micro- or macro-damage to the skin and through inhalation of viral aerosols. The latter route is common in laboratory settings or as a consequence of handling infected farm animals. Given the unique cellular composition of these organs, including both parenchymal and immune components, it is tempting to speculate about potentially different disease outcomes depending on the route of infection, as the virus may use the locally available cell types in these organs with different adequacy. This may result in a different infection rate or slower viral replication, which may lead to delayed viral dissemination and thus delayed disease onset and/or death. In order to assess the effect of the infection route, groups of mice were infected with the human isolate of RVFV, hereafter referred to as huRVFV, either intradermally or intranasally, mimicking the dermal and mucosal route of infection, together with mock control animals which received only PBS via the same routes. By applying two different infection doses (10 PFU and 100 PFU) the importance of initial viral dose can be simultaneously inquired in the same experiment. General morbidity and mortality in context of the above-mentioned factors was assessed by the daily monitoring of body weight and body temperature. These attributes are often decrease in mice during viral infections and are commonly used as indicators of disease burden (Rottstegge et al., 2022; Srivastava et al., 2009). If very severe symptoms were to manifest - refer to the humane endpoint criteria at Table 10. - subjects were humanely euthanized to prevent prolonged suffering of the animals.

As the liver has previously been identified as the primary target of RVFV (refer to Introduction chapter), liver damage was assessed as an additional sign of disease progression by measuring levels of the enzyme aspartate aminotransferase (AST) in blood, collected every two days after infection or at necropsy, as elevated plasma AST levels not only indicate but also correlate with liver damage.

The collected blood was also analysed for the presence of viral particles, as viremia is a sign for viral dissemination. As discussed above, the different infection route may manifest in distinct viral spread, which is likely to be associated with the onset of disease symptoms. The viral spread was further investigated by measuring viral load in various organs collected at necropsy, as it is possible that certain organs are more frequently and/or more extensively affected by the virus depending on the infection route.

Finally, blood samples collected at necropsy, were also tested for seroconversion in order to distinguish subclinical infections from abortive infections. As viral clearance prerequisites the activation of the immune system, thus subsequent generation of virus-specific IgG antibodies is expected. If a subject were to clear the virus before the onset of symptoms, the presence of such antibodies in the circulation would indicate a successful encounter with the virus.

The experimental design is concluded in Figure 14.

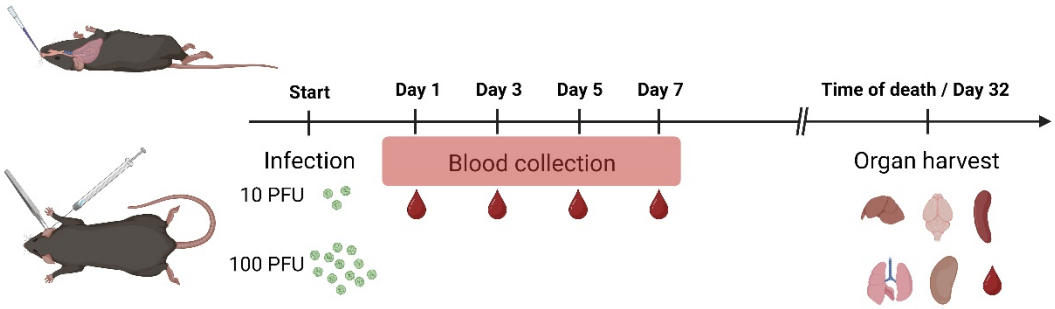

Figure 14. Experimental design for investigating huRVFV infection in mice.
Female WT mice (n=3 or 6, mock or challenged, respectively) were infected IN or ID with either 10 or 100 PFU of huRVFV. Mice were monitored daily for 32 days. Venous blood was collected every two days at the early stage of infection or at necropsy to determine viremia and liver enzyme levels. At the end of the experiment or in case mice succumb to the disease, liver, brain, spleen, lung, kidney, and blood were collected to determine endpoint viral loads. Available endpoint blood samples were also used to confirm seroconversion.

4.1.1. Intradermal infection route of huRVFV is more lethal compared to intranasal route

Striking difference in survival was observed between the two groups based on the infection route. Intradermal administration led to 100% mortality regardless of the initial infection dose, although some of the mice in group infected with the lower dose reached the euthanasia criteria one day later (at 4 DPI). In contrast, mice infected intranasally with 100 PFU started to succumb to the disease on day 4 post-infection and the group reached 66% mortality rate by 5 DPI, meanwhile only one out of six animals reached endpoint criteria on day 6 following IN infection with 10 PFU. Animals that succumbed to the disease showed symptoms of anorexia and hypothermia in both groups as shown in Figure 15. Animals euthanised due to disease severity reaching humane endpoint criteria showed signs of internal bleeding involving multiple organs, particularly the liver, small intestine and claws, as shown in Figure 16.

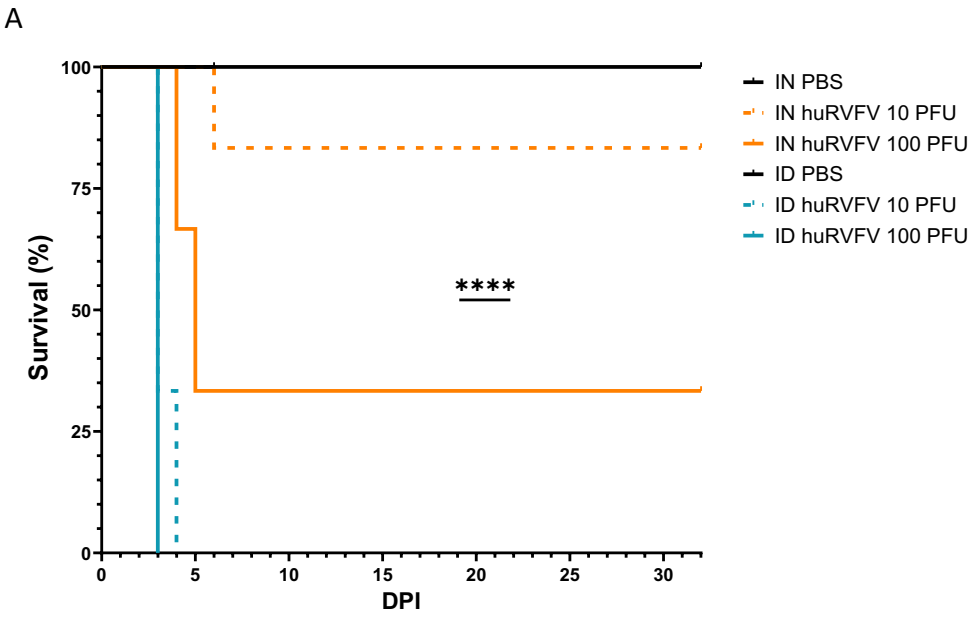

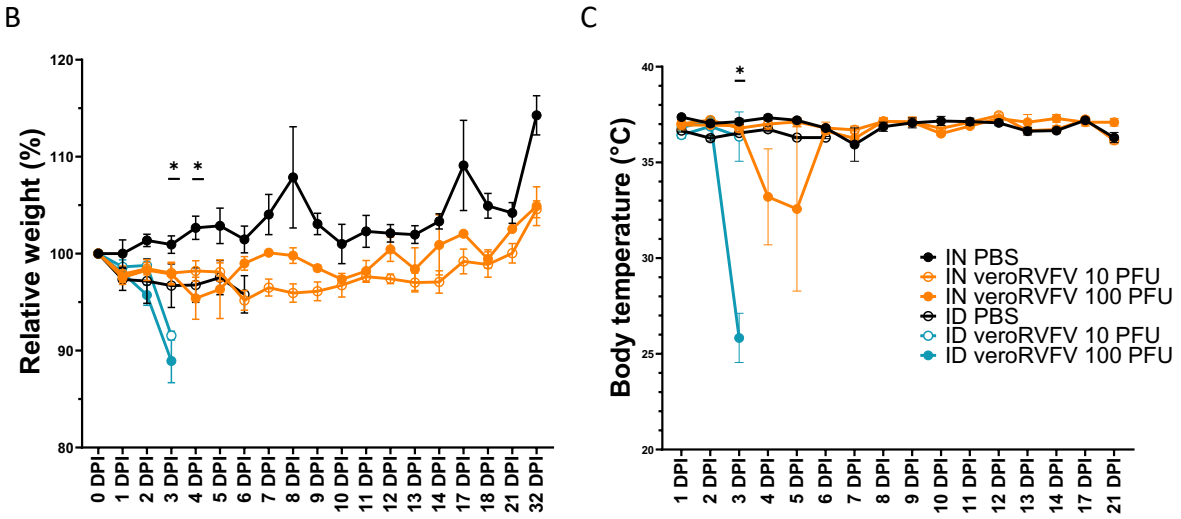

Figure 15. Infection with huRVFV via ID route results in higher mortality rate, weight loss and decreased body temperature.
Graphs show Kaplan-Meier survival curves (A), relative body weight (B) and body temperature (C) of female WT mice infected IN or ID with either 10 or 100 PFU of huRVFV. Values are reported as mean ± standard error of mean (SEM). Statistical significance was determined using Mantel-Cox test (A) or Mixed-effect model with Tukey's multiple comparisons test (B-C). (ns – not significant, *p ≤ 0.05, ****p ≤ 0.0001).

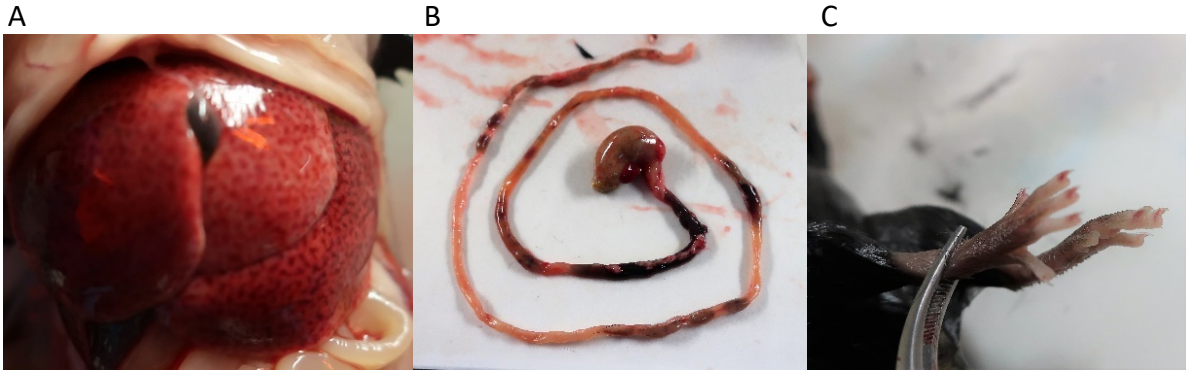

Figure 16. Infection with huRVFV led to haemorrhagic form of the disease.
Fatal cases of huRVFV were characterised by multiorgan haemorrhages. The most frequently affected organs were the liver (A), small intestine (B), and the claws (C).

4.1.2. Intradermal infection route of huRVFV accelerates disease progression but not severity

It is possible that RVFV may exploit the circulatory system to access and infect multiple organs, so viremia may be an early sign of viral dissemination. Furthermore, fulminant demise of mice following RVFV infection has been associated with acute liver failure in the past (D. R. Smith et al., 2010). The elevated level of the liver enzyme aspartate aminotransferase (AST) in the blood can be used as an early marker for liver disfunction. Analysing the serially collected blood samples for viremia and AST levels can provide information about the viral dissemination and pathogenesis of RVFV infection between the groups.

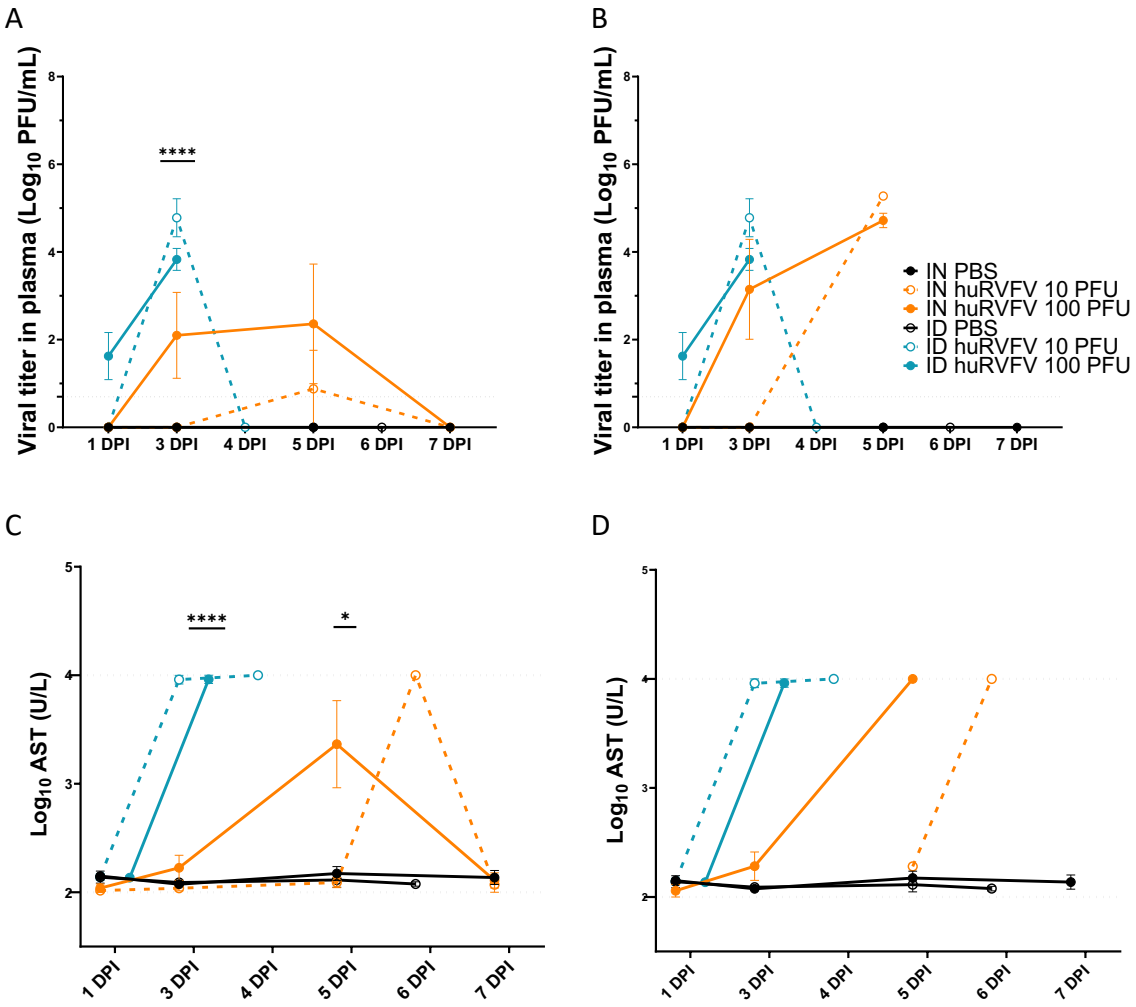

Figure 17. IN infection with huRVFV results in delayed viremia and liver damage compared to ID route.

Blood was collected from female mice every two days, or in case of death, for a week after IN or ID infection with huRVFV. Graphs show viremia titer (A-B) or plasma AST levels (C-D). Values are reported as mean ± SEM. Graph B and D represent the viremia and liver enzyme levels of the lethal cases, respectively. Dotted lines indicate viral detection limits. Statistical significance was determined using Mixed-effect model with Tukey's multiple comparisons test. (*$p \leq 0.05$, ****$p \leq 0.0001$).

ID infection with 100 PFU of huRVFV developed the earliest viremia with four out of six mice having virus in their blood as early as 1 DPI. Mice infected intradermally with 10 PFU or

intranasally with 100 PFU were positive for viremia by 3 DPI and one individual infected intranasally with 10 PFU presented virus in its blood only by 5 DPI (Figure 17. A-B). Similarly to the viremia data, both ID group reached their peak AST-levels by day 3 post-infection, meanwhile individuals infected intranasally with either 100 or 10 PFU had their peak of AST level by 5 or 6 DPI, respectively (Figure 17. C-D).

4.1.3. huRVFV shows strong preference for the liver regardless of its route of administration

To test whether the infection route had an impact on which organs are affected by the virus, several organs (liver, brain, spleen, lung, kidney) were collected at necropsy and their viral load was assessed via plaque forming assay (as shown in Figure 18.).

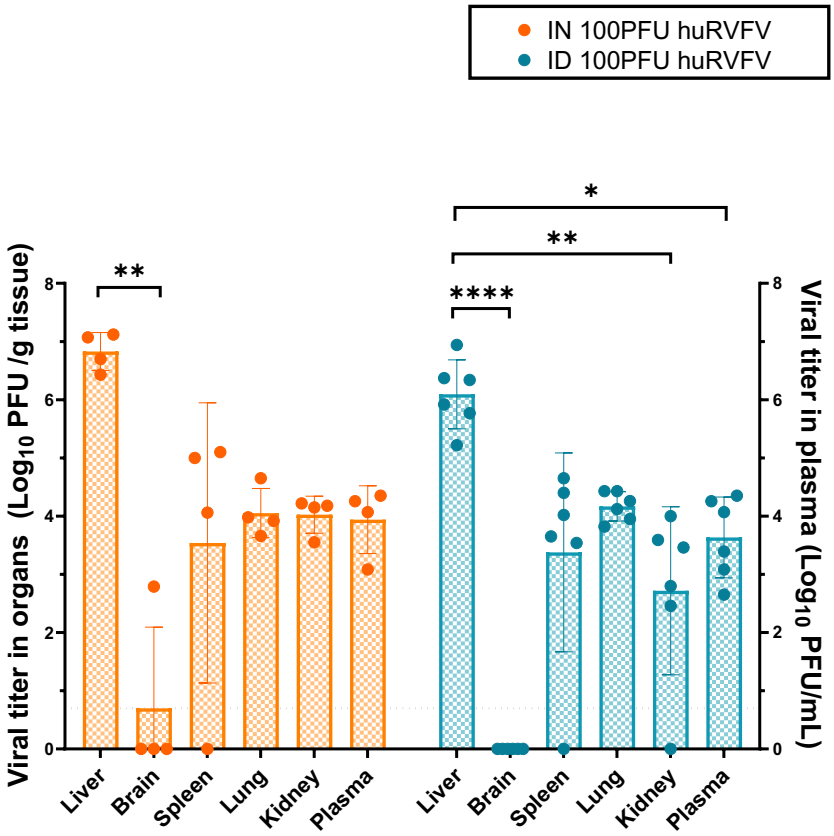

Figure 18. Viral loads in different organs are comparable in deceased animals regardless the infection route of huRVFV.

Graph represents endpoint viral titers in various organs (liver, brain, spleen, lung, kidney and blood) collected when mice deceased or reached humane endpoint criteria following IN or ID infection with 100 PFU or huRVFV. Values are reported as mean ± SEM. Dotted line indicates viral detection limit. Statistical significance was determined using Friedman test. (*p ≤ 0.05, **p ≤ 0.01, ****p ≤ 0.0001).

The virus was most abundant in the liver, but was also present in the spleen, lungs, kidneys and plasma of the animals succumbed to the disease. The brain was free of the virus, except for one animal that had been exposed to the virus intranasally.

4.1.4. There is no seroconversion following infection with huRVFV

RVFV infection in humans can be asymptomatic (Hartman, 2017), therefore mice that survived IN administration of huRVFV might have had a similar asymptomatic infection without

detectable viremia and liver damage (indicated by no elevated plasma AST levels). Successful clearance of the pathogen requires the adequate activation of the immune system which results in the production of pathogen-specific antibodies, the process also called seroconversion. To test whether these "survival" mice got infected and developed a sufficient immune response to clear the virus, their blood plasma was tested for RVFV Np-specific IgG antibodies via indirect-ELISA method, as shown in Figure 19. This test revealed that no animals that were exposed to huRVFV via IN route developed virus-specific antibodies.

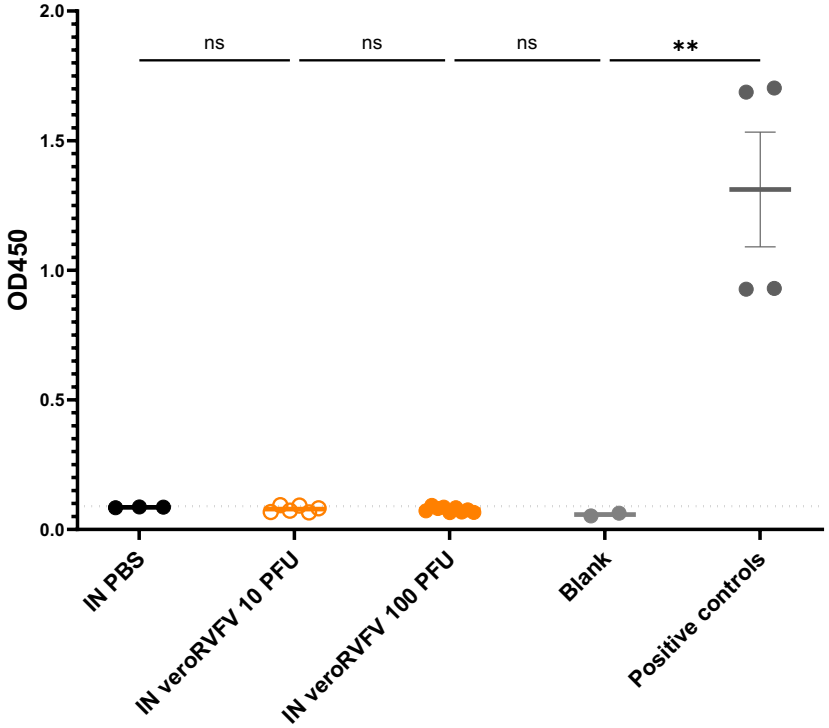

Figure 19. IN infection with huRVFV did not lead to production of virus-specific IgG antibodies.
Endpoint blood samples from groups with survival mice following IN exposure to 100 PFU of huRVFV were collected, and the presence of RVFV Np-specific IgG antibodies in their plasma was detected by indirect ELISA method. Monoclonal mouse anti-RVFV Np IgG antibody was used as positive control. Graph represents the corresponding OD450 values as mean ± SEM. Dotted line indicates cut-off value (calculation details are provided in the Materials and Methods section). Statistical significance was determined using Kruskal-Wallis test. (ns – not significant, **$p \leq 0.01$).

4.2. Infection with mosRVFV

To test whether the origin of isolation has any effect on RVFV pathogenesis, a very similar experiment was executed, in this case using a virus isolated from a mosquito (mosRVFV). Mice were exposed to mosRVFV intradermally or intranasally and their body weight and temperature were monitored daily. Blood was collected every other day during the first week of infection and blood and various organs were collected in case of reaching euthanasia criteria or at the end of the experiment at day 22 post infection.

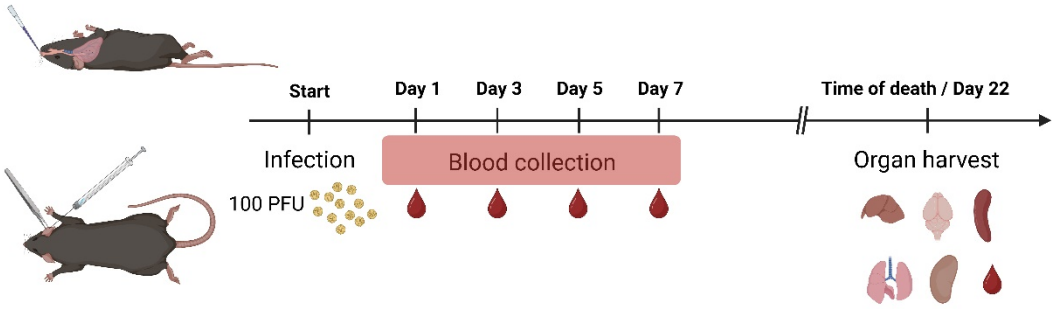

Figure 20. Experimental design for investigating mosRVFV infection in mice.
Female WT mice (n=3 or 6, mock or challenged, respectively) were infected IN or ID with 100 PFU of mosRVFV. Mice were monitored daily for over 22 days. Venous blood was collected every two days at the early stage of infection or in case of death to determine viremia. At the end of the experiment or in case mice succumb to the disease, liver, brain, spleen, lung, kidney, and blood were collected to determine endpoint viral loads. Available endpoint blood samples were also used to assess seroconversion.

4.2.1. Intranasal infection route of mosRVFV is more lethal compared to intradermal route

Mortality (Figure 21. A) and morbidity (Figure 21. B-E) results following infection with mosRVFV are noticeably different from the infection with huRVFV. No intradermally infected animals succumbed to the disease and only two out of six intranasally infected mice reached endpoint criteria resulting in a 33% mortality rate. Interestingly, there was one mouse infected intradermally and two mice infected intranasally that showed signs of illness by losing a considerable amount of weight, yet they recovered before reaching the humane endpoint criteria. This weight loss was observed in the first week of ID and in the second week of IN infection. The weight loss was accompanied by other body scoring parameters such as moderate hypothermia.

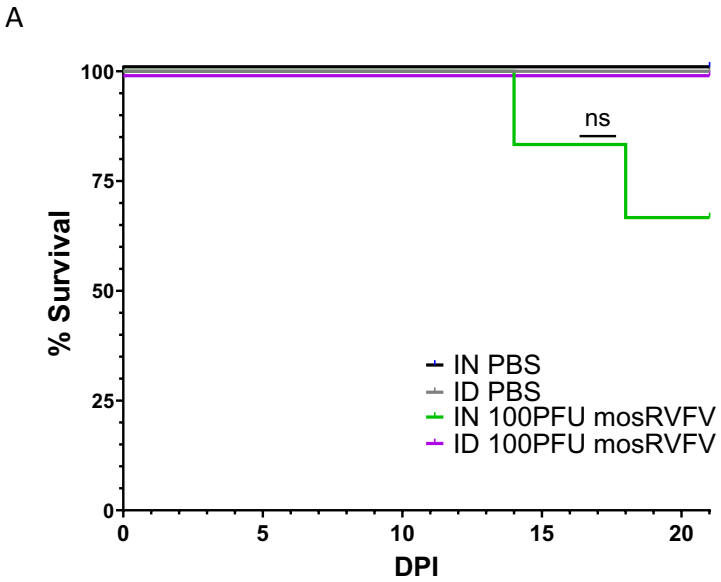

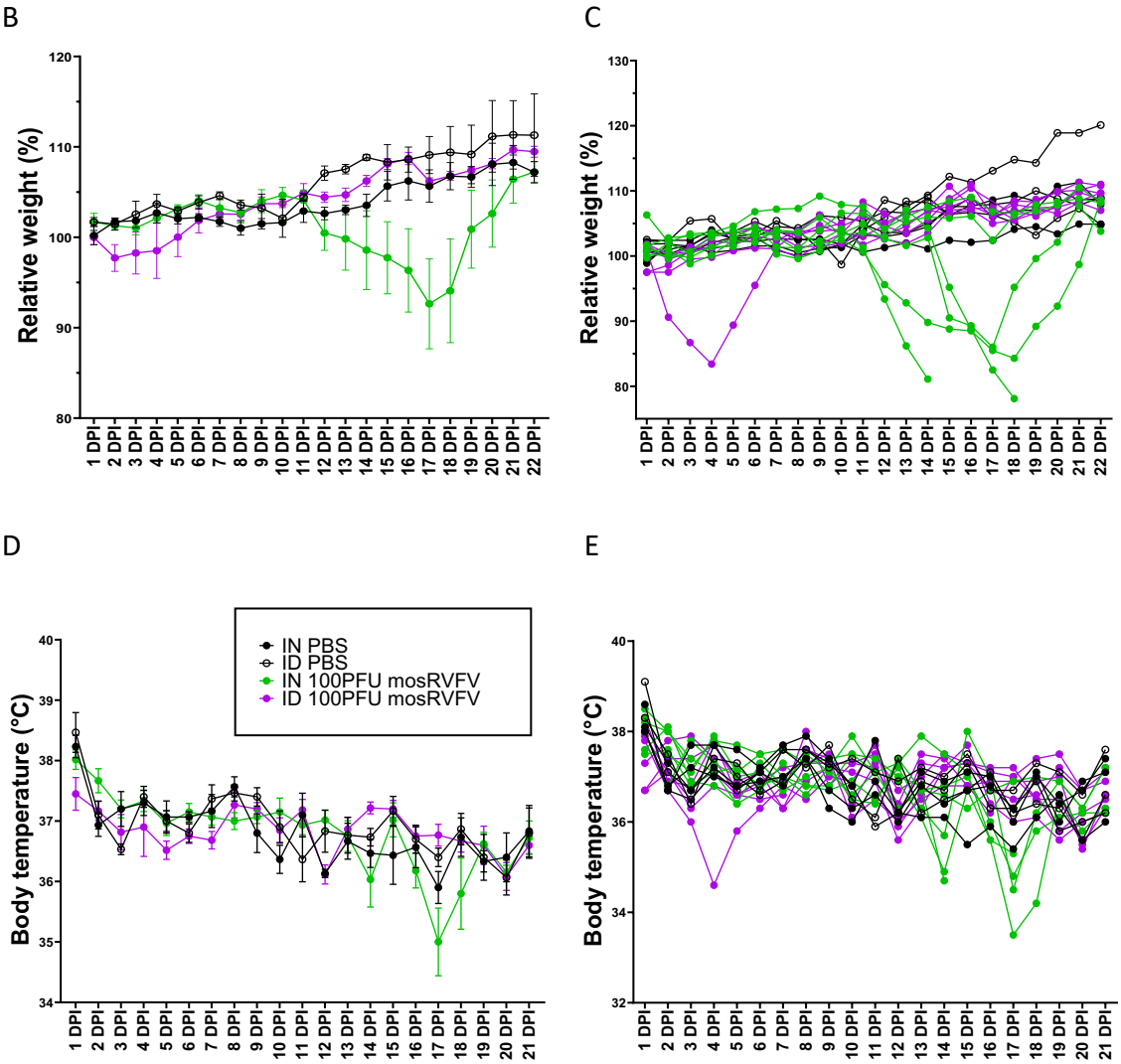

Figure 21. Intranasal infection with mosRVFV results in higher mortality rate compared to intradermal route.
Graphs show Kaplan-Meier survival curves (A), relative body weight (B-C) and body temperature (D-E) of mice after vehicle or 100 PFU of mosRVFV exposure. Values are reported either as mean ± SEM (B and D) or as individual readings (C and E). Statistical significance was determined using Mantel-Cox test (A) or Mann-Whitney test (B-E). (ns – not significant).

4.2.2. There is no early viremia in animals exposed to mosRVFV

As it was mentioned earlier, assessment of viremia can be used as an indication for viral dissemination, therefore blood plasma collected every second day up until 7 DPI was measured for viral presence via plaque forming assay. Surprisingly, no sample was found to be positive (shown in Figure 22.), whereas in the previous experiment all cases of huRVFV infection were characterised by the presence of the virus in the blood.

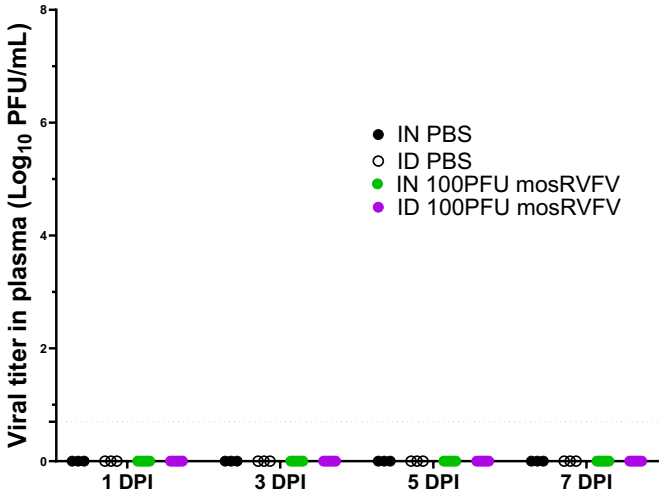

Figure 22. Neither infection route of mosRVFV leads to early viremia.
Blood was collected from female mice every two days throughout the first week of IN or ID infection with 100PFU of mosRVFV or vehicle. Graph shows viral load values as mean ± SEM. Dotted line indicates viral detection limit. Due to identical values in all groups no statistical analysis was performed.

4.2.3. The presence of mosRVFV was confined to the brain in deceased animals

To test whether mosRVFV has the same tropism as huRVFV, the same organs (liver, brain, spleen, lung, kidney and blood) were harvested as before at the time of death or at the end of the experiment (22 DPI) and assayed for viral load using a plaque-forming assay. Endpoint organ viral titers (sown in Figure 23.) revealed that mosRVFV was located only and exclusively in the brain of the deceased animals infected intranasally.

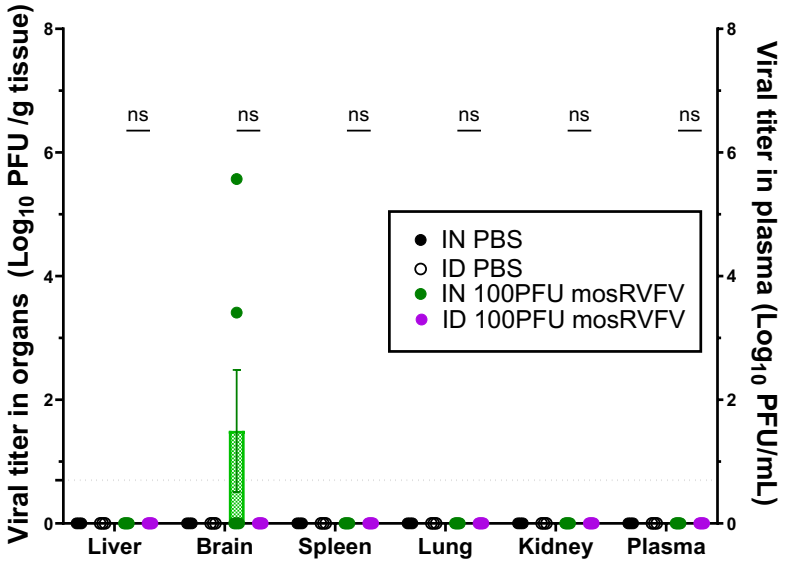

Figure 23. mosRVFV was detectable only in the brain of the individuals succumb to the disease.
Graph represents endpoint viral titers in various organs (including liver, brain, spleen, lung, kidney, and blood) collected at the end of the experiment or in case euthanasia performed, following IN or ID infection with 100PFU of mosRVFV. Values are reported as mean ± SEM.

Dotted line indicates viral detection limit. Statistical significance was determined using multiple Mann-Whitney test. (ns – not significant).

4.2.4. Infection with mosRVFV results in seroconversion in all individuals

As explained earlier the presence of virus-specific antibodies in the exposed individuals would indicate a successful immune encounter with the pathogen, therefore the presence of such, IgG class anti-RVFV Np antibodies in the blood was tested in all individuals. Results gained from the indirect ELISA test indeed confirmed the seroconversion of all virus-exposed animals (see Figure 24.) regardless of the infection route or whether they produced symptoms (such as weight loss or hypothermia) or detectable virus concentration in the blood or in other organs during the course of the experiment. Statistical analysis showed no significant difference in the amount of specific antibodies produced by the groups depending on the infection route.

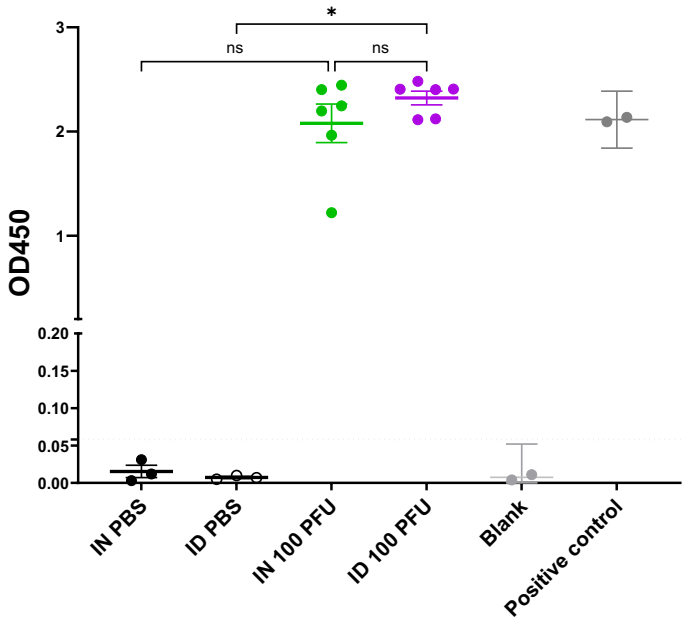

Figure 24. All animals exposed to mosRVFV developed virus-specific IgG antibodies.
Endpoint blood samples were collected from mock controls or animals infected ID or IN with 100 PFU mosRVFV and the presence of RVFV NP-specific IgG antibodies in their plasma was assessed by indirect ELISA. Monoclonal mouse anti-RVFV Np IgG antibody was used as positive control. Graph represents the corresponding OD450 values as mean ± SEM. Dotted line indicates cut-off value. Statistical significance was determined using Kruskal-Wallis test. (ns – not significant, *p ≤ 0.05).

4.3. Viral dissemination in the early phase of RVFV infection

Previous experiments have already shed light on the importance of the infection route and the virus' origin on the outcome of RVFV infection. While the data on viremia and AST levels already indicated differences in viral dissemination to the blood and liver, it is still not known how the different isolates replicate at the site of infection and how, if at all, they spread to the lymphatics in relation to the inoculation sites. In addition, the endpoint organ titers measured previously, indicated a different tropism of the two RVFV isolates, but it is not yet clear how quickly organs remote from the site of infection were affected by huRVFV, or whether mosRVFV transiently infects other organs before reaching the brain. To understand these early events, animals were infected intradermally or intranasally with one of the RVFV isolates and were serially euthanised daily for four days. The collected organs were assessed for viral load via plaque-forming assay. In parallel, immunohistochemical (IHC) analyses was performed to verify the presence of the virus in the corresponding tissue parenchyma.

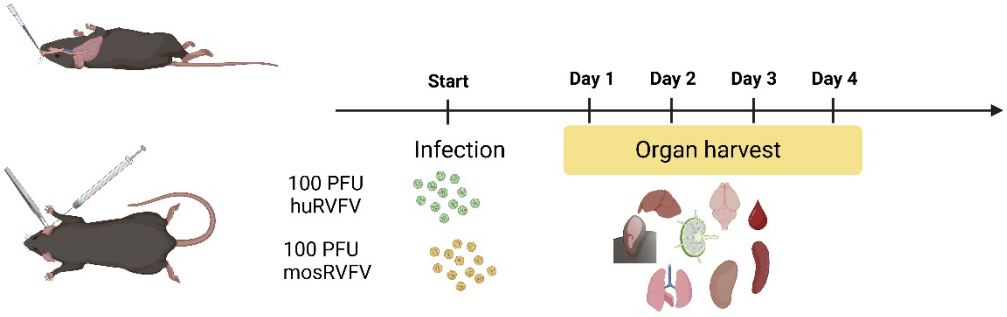

Figure 25. Experimental design for early phase serial euthanasia experiment.
Female WT mice (n=12) were infected IN or ID with 100 PFU of either huRVFV or mosRVFV. Mice were monitored daily until the end of experiment. Three mice per group were humanely euthanised and their ear, ALN, lung, MLN, liver, brain, spleen, lung, kidney and blood were collected to determine organ viral titers. Blood samples were also checked for seroconversion.

4.3.1. Different RVFV isolates have distinct dissemination profile

First, to test the viral replication at the site of the infection and the viral dissemination through the lymphatics, skin of the ears, auricular lymph nodes (ALN), lungs and mediastinal lymph nodes (MLN) were collected from intradermally or intranasally infected animals. Viral loads at the infection sites and their draining lymph nodes were determined via plaque forming assay. Viral presence in the skin was confined to intradermally infected animals only, with one exception. Viral replication in the skin is noticeably different between the two isolates. The viral load in case of ID infection with huRVFV was constantly increasing by 3 DPI and was significantly higher compared to the viral load in the animals infected with the mosquito isolate, meanwhile the viral load in the skin began to drop after 2 DPI in the animals receiving mosRVFV. It is also worth to note that all skin samples gained from the animals infected with the human isolate were positive for the virus, in contrast to some of the samples collected at day 1, 3, and 4 DPI from the animals infected with the mosquito isolate (Figure 26. A). A similar trend was observed in the ALNs, whereas RVFV was detected in all the huRVFV-infected samples, yet only one sample/day was above detection limit from the mosRVFV-infected group. The mean value of the virus titers in the skin-draining lymph nodes were steady in the first 3-days of infection with huRVFV, but it was constantly declining in case of the infection with mosRVFV. The difference in viral titer between the 2 groups was significant at 3 DPI (Figure 26. B).

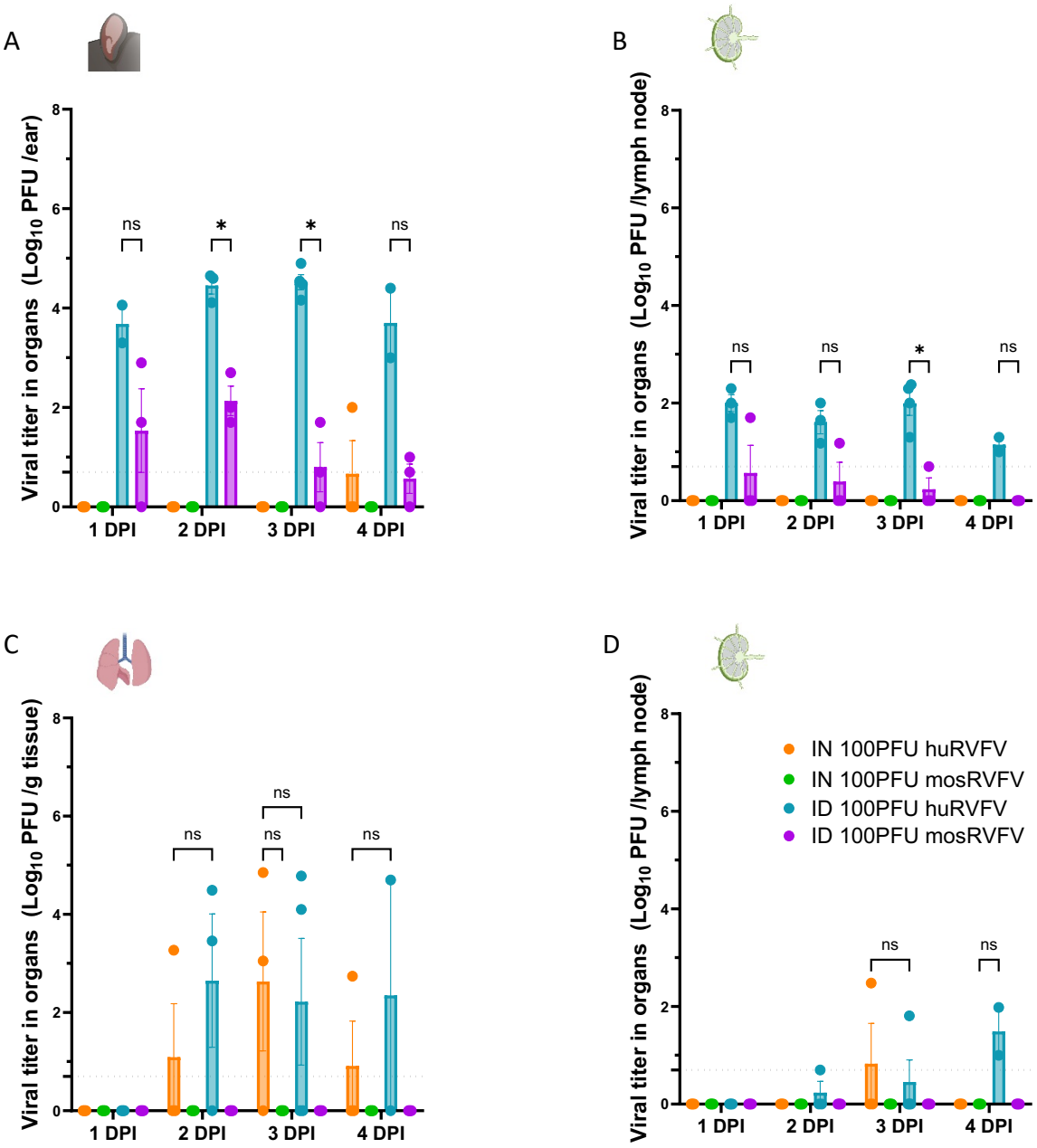

Figure 26. Skin is superior as initial replication site for both isolates.
Mice infected intranasally (IN) or intradermally (ID) with 100 PFU of either huRVFV or mosRVFV were serially euthanised on a daily basis. Graphs indicate viral titers at the infection site such as skin (A) and lung (C) and their draining lymph nodes ALN (B) and MLN (D), respectively. Viral titer values are presented as mean ± SEM. Dotted lines indicate viral detection limits. Statistical significance was determined using Mixed-effect model with Tukey's multiple comparisons test. (ns – not significant, *p ≤ 0.05).

The initial viral replication in the lung was however different: no virus was detected in any samples from mice infected with mosRVFV. There was no detectable virus in the lungs of animals at 1 DPI with huRVFV either, but there was at least one sample/day positive during the following days from both, intradermally and intranasally huRVFV-infected groups as well. Interestingly, not every intranasally infected animals had detectable amount of virus in their lungs. There was no significant difference in terms of viral load between the groups based on

their infection route (Figure 26. C). Only a fraction of the mice infected with huRVFV had virus in their mediastinal lymph nodes. These cases were confined to the intranasally infected animals with one exception at day 3 post-infection. None of the animals infected with the mosquito isolate had detectable virus in their MLNs (Figure 26. D).

Given that endpoint viral titers determined in the previous experiments can offer insights only into the viral presence at the final disease stage, assessment of the viral load of the organs distant from the infection site harvested through serial euthanasia, can shed light on when these organs became infected. Additionally, whether organs initially considered free of the virus at the time of necropsy were maybe transiently invaded by the virus before.
These remote organs, including the blood, remained to be undetectable for viral presence at any timepoint collected from animals exposed to mosRVFV via either ID or IN route (Figure 27.). Two out of three animals infected intradermally with the human isolate had viremia as early as 1 DPI, in accordance with the viremia data from the previous experiment (see Figure 17.), and most of the intradermally infected animals had viremia in the following days too (with two exceptions). In contrast to this, only one or two blood sample(s)/day were positive for viremia following IN exposure with huRVFV starting at day 2 post-infection (Figure 27. A). A similar dissemination pattern could be observed in the spleen. While all spleen samples from intradermally infected huRVFV animals were positive starting from 2 DPI, only one of the intranasally exposed animals was positive at days 3 and 4 post-infection (Figure 27. B).

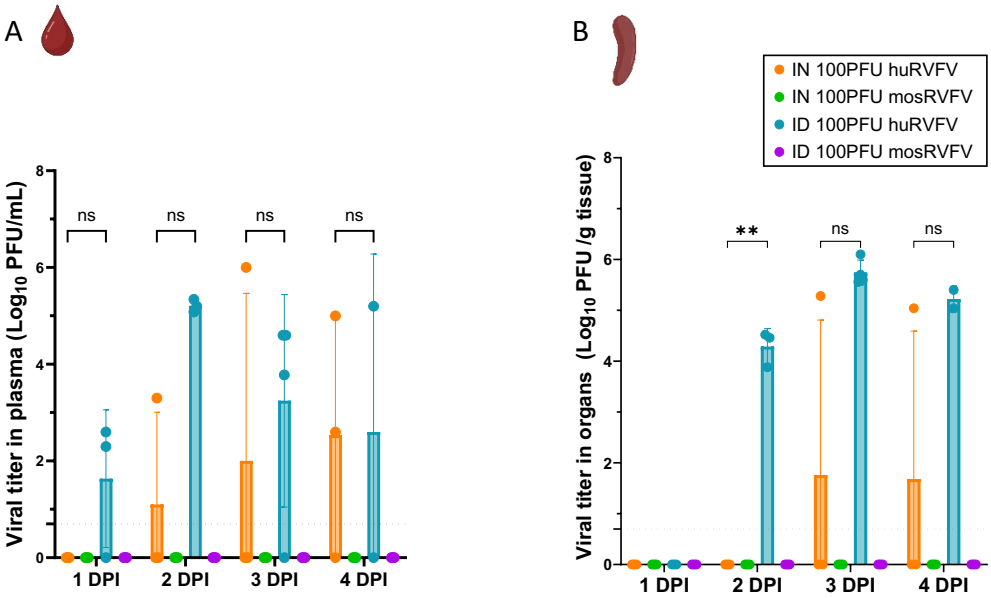

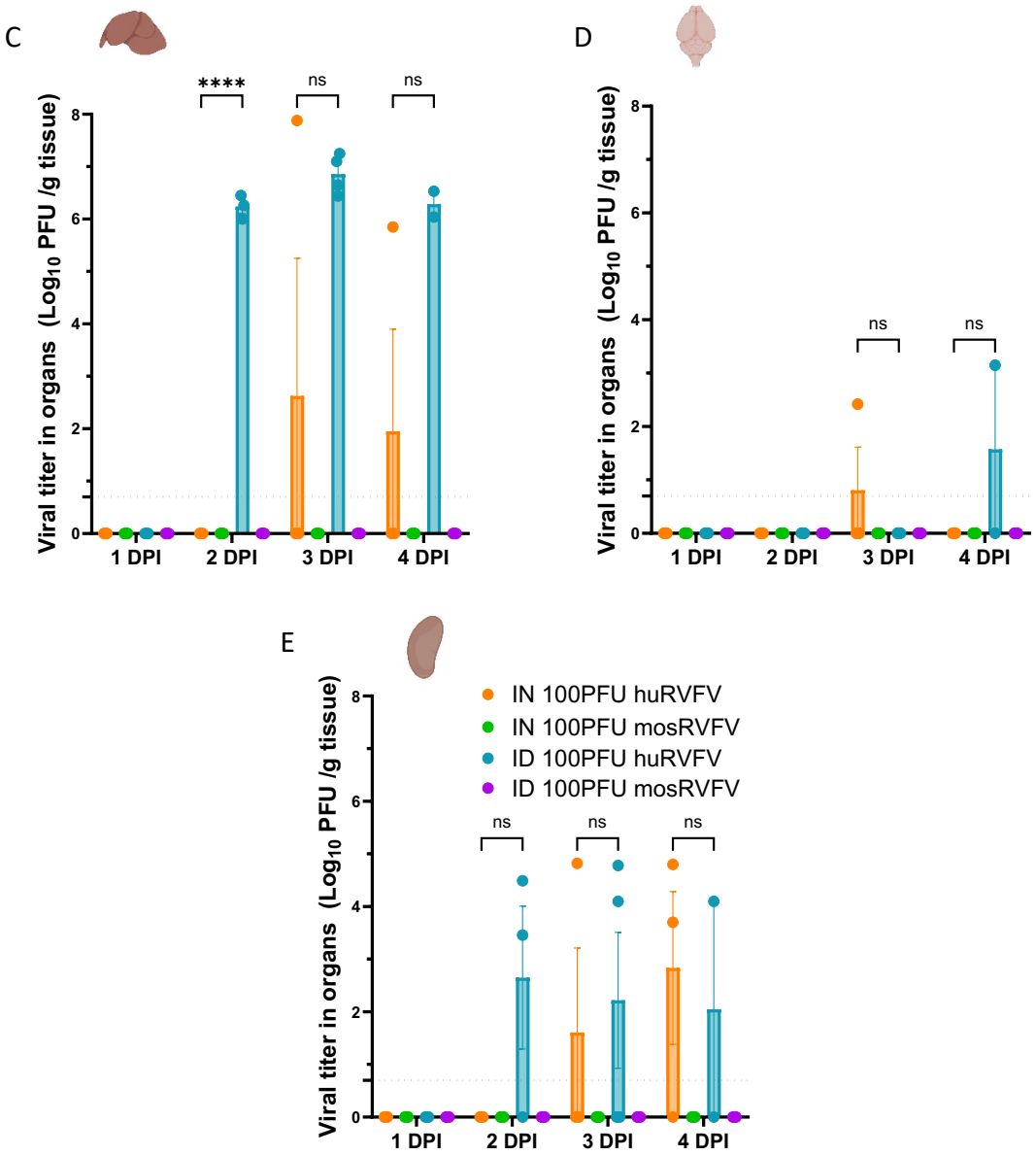

Figure 27. The mosquito isolate of RVFV remains undetectable in all remote organs examined in the early stages of infection, in contrast to the widespread dissemination of the human isolate.

Mice infected intranasally (IN) or intradermally (ID) with 100 PFU of either huRVFV or mosRVFV were serially euthanised on a daily basis. Graphs indicate viral titers in remote organs such as blood (A), spleen (B), liver (C), brain (D), and kidney (E). Viral titer values are presented as mean ± SEM. Dotted lines indicate viral detection limits. Statistical significance was determined using Mixed-effect model with Tukey's multiple comparisons test. (ns – not significant, **p ≤ 0.01, ****p ≤ 0.0001).

The viral dissemination pattern towards the liver was the same as that observed in the spleen (Figure 27. C). Infection in the brain was limited to only two samples, one collected at 3 DPI (IN infection) the other one collected at 4 DPI (ID infection) (Figure 27. D). The kidney was reached by the virus 2 DPI after ID and 3 DPI after IN infection, but only one or two samples/day were virus-positive in both routes of infection (Figure 27. E).

4.3.1.1. Confirmation of viral dissemination via IHC analysis

For biosafety reasons animals were not perfused before dissection, thus viral particles in the circulation may give a false positive result in highly vascularised organs when viral loads are determined via plaque-forming assay. To rule out these potentially false positive by-products, organs were split in two, and one half of the organs was processed for plaque assay, while the other half was analysed by IHC. IHC can provide only semi-quantitative results, but it is useful to locate virus-infected cells inside the tissue.

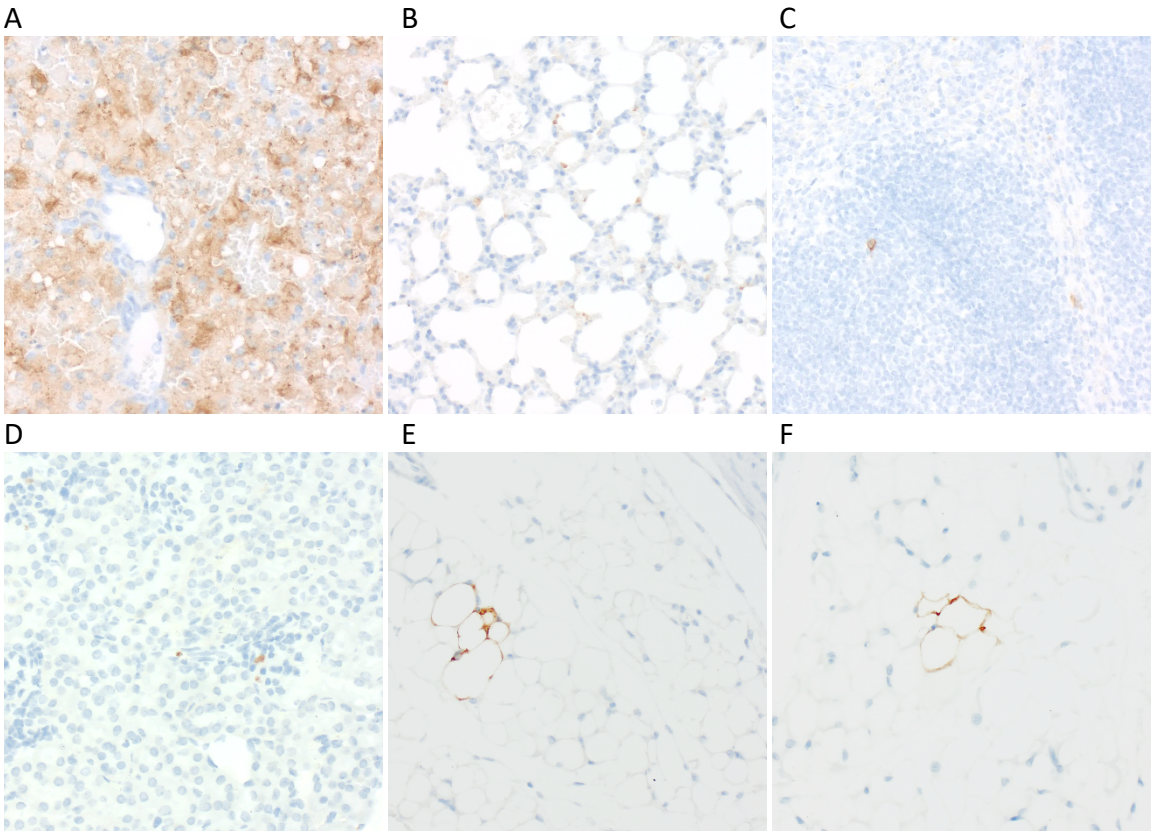

Figure 28. Immunolabelling of RVFV confirmed the parenchymal distribution of RVFV.
Organs were collected at 3 DPI and were stained using polyclonal antibody against RVFV-Gn (brown), and haematoxylin as counterstain (blue). Representative pictures of liver (A), lung (B), spleen (C), kidney (D) and adipose tissues found around the small intestine (E), and kidney (F). Pictures were taken at 20X magnification.

IHC analyses of liver tissue for RVFV-Gn demonstrated a uniform, diffuse staining of the viral antigen throughout the whole tissue (Figure 28. A). Positive immunolabelling in the other organs was absent in the blood vessels or at the perivascular area but was located in the organ parenchyma (Figure 28. B-F).

4.4. Viral dissemination in the late phase of mosRVFV infection

Since mice infected with mosRVFV at the previous experiment only started to show symptoms of the disease during the second week of infection (see Figure 21.), there was a chance that viral dissemination could not be detected until day 4 post-infection, due to a slower disease course of this isolate. To circumvent this, mice were infected intradermally or intranasally with mosRVFV, and were serially euthanised on later time points (5, 7, 14 and 18 DPI) and the same organs were harvested as were in the previous experiment. These time points were chosen on

the basis of the greatest weight loss previously observed on these days. Viral loads were assessed via plaque-forming assay. The experimental design is shown in Figure 29. Since mice infected with huRVFV succumb to the disease within 4 days, these later time points could not be applied for this isolate.

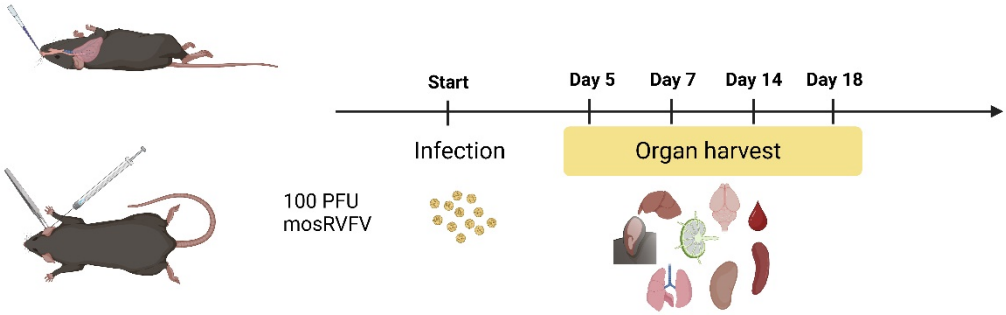

Figure 29. Experimental design for late phase serial euthanasia experiment.
Female WT mice (n=12) were infected IN or ID with 100 PFU of mosRVFV. Mice were monitored daily until the end of experiment. 3 mice per group were humanely euthanised on the indicated days, and their ear, ALN, lung, MLN, liver, brain, spleen, lung, kidney and blood were collected to determine organ viral titers via plaque-forming assay. Blood was also tested for seroconversion too.

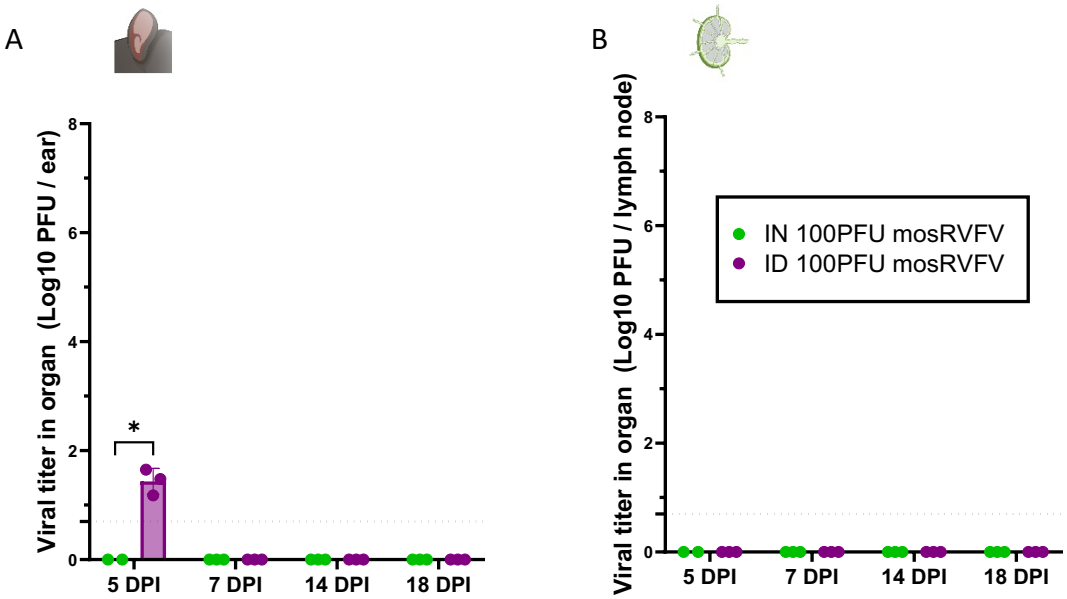

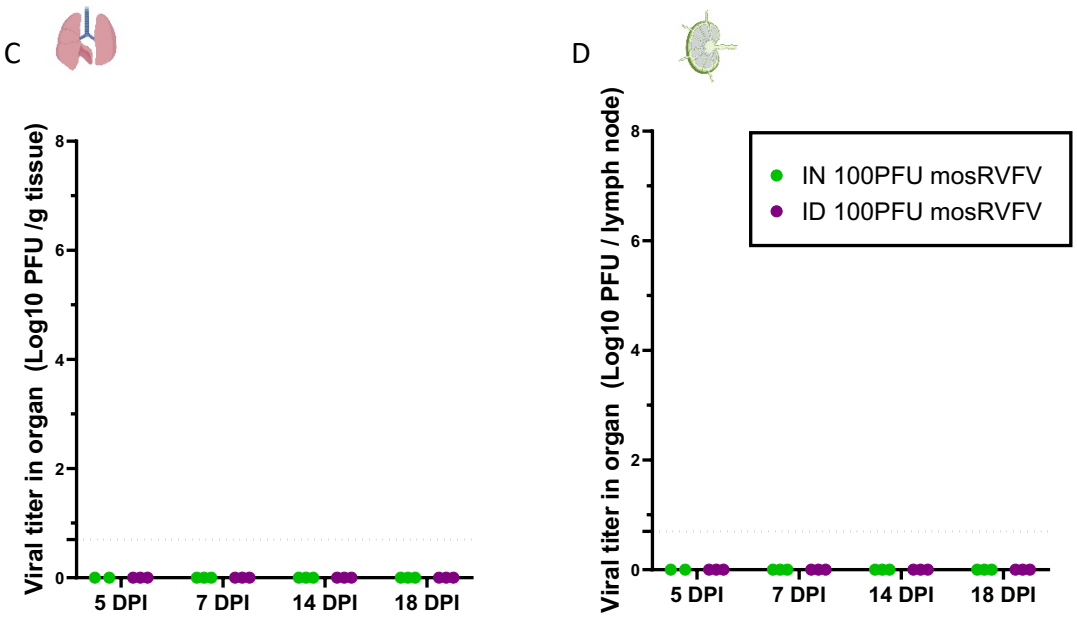

Figure 30. Mosquito isolate of RVFV was cleared from the skin by the first week of infection and remained to be undetectable in the lung.
Mice infected intranasally (IN) or intradermally (ID) with 100 PFU of mosRVFV were serially euthanised on different time points. Graphs indicate viral titers at the infection site such as skin (A) and lung (C) and their draining lymph nodes ALN (B) and MLN (D). Viral titer values are presented as mean ± SEM. Dotted lines indicate viral detection limits. Statistical significance was determined using Mixed-effect model with Tukey's multiple comparisons test. (ns – not significant, *p ≤ 0.05).

Although mosRVFV was still present in the skin of all intradermally infected individuals at 5 DPI, samples collected at later time points became negative. (Figure 30. A). Lungs and draining lymph nodes were negative at all time points regardless of the infection route.

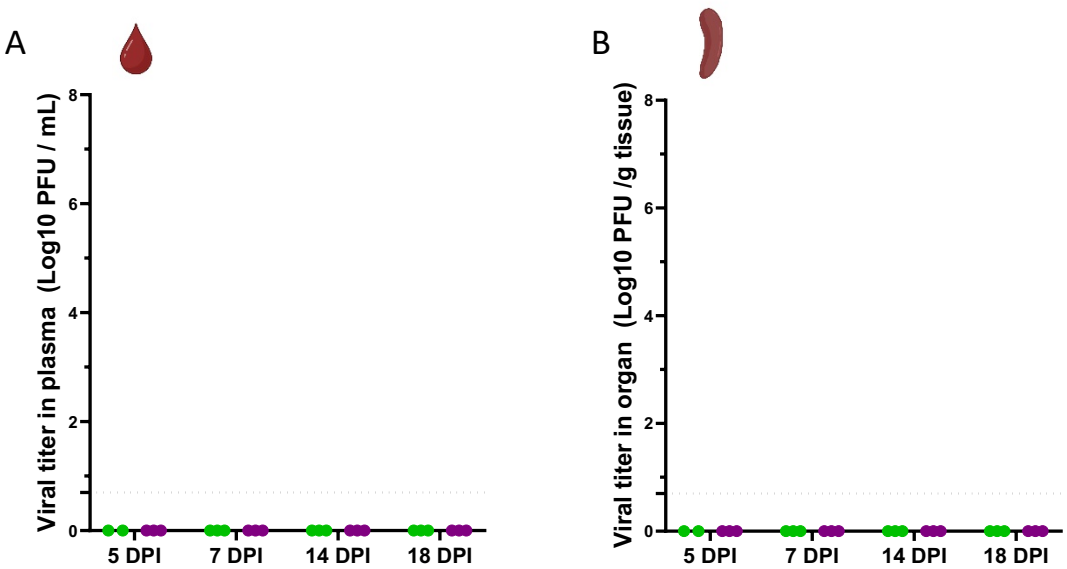

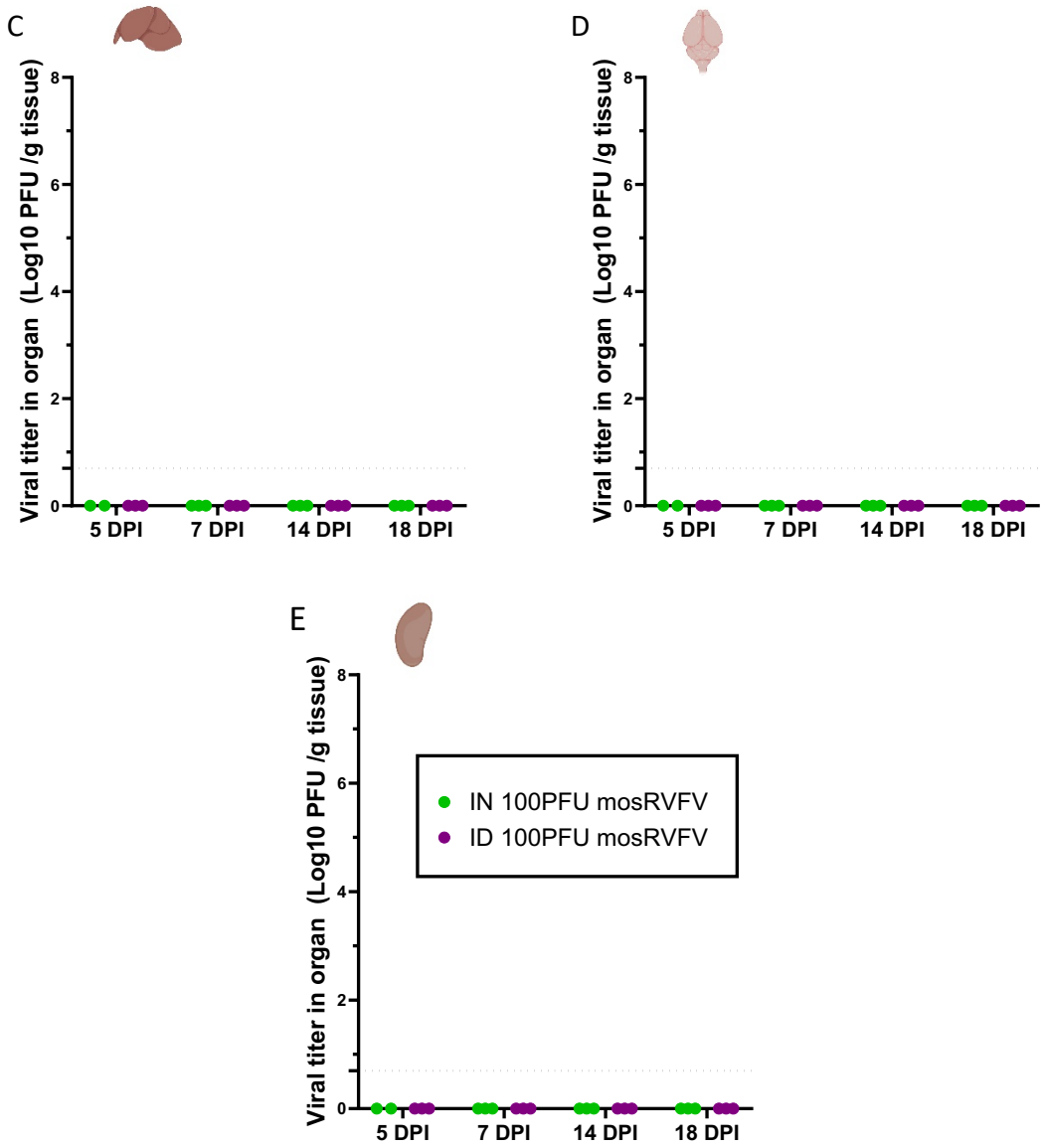

Figure 31. mosRVFV is not detectable in any of the examined remote organs during the late phase of infection.
Mice infected intranasally (IN) or intradermally (ID) with 100 PFU of mosRVFV were serially euthanised at different time points. Graphs indicate viral titers in remote organs such as blood (A), spleen (B), liver (C), brain (D), and kidney (E). Viral titer values are presented as mean ± SEM. Dotted lines indicate viral detection limits. Statistical significance was not performed, as all values were identical.

The mosquito isolate of RVFV remained undetectable in all the investigated remote organs collected at any time points from both intradermally or intranasally challenged animals, as shown in Figure 31.

4.4.1. Seroconversion is confined to infection with mosRVFV

As earlier, assessment of seroconversion was used to determine whether negative results for viral dissemination was the consequence of unsuccessful infection or successful virus control. Also, serially collected blood samples may give information about when antibody production against RVFV has started.

No blood samples collected at early time points (up until 4 DPI) contained RVFV-specific IgG antibodies (Figure 32. A). A slight increase in virus-specific antibodies could be seen at day 7 following ID infection with mosRVFV, and all but one sample had seroconverted by 14 DPI following mosRVFV exposure in both the IN and ID infected groups. (Figure 32. B).

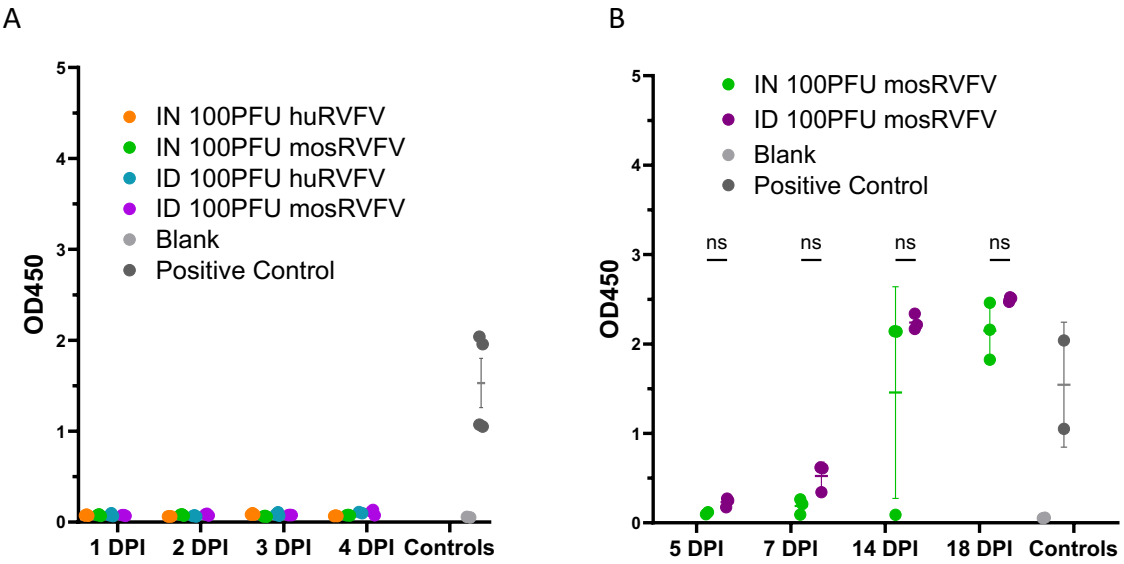

Figure 32. Seroconversion is only detectable during the late phase of RVFV infection by the mosquito isolate.
Blood collected during the early (A) and late (B) phase (refer to Figure 25 and Figure 29) of RVFV infection was screened for RVFV Np-specific IgG antibodies via indirect ELISA method. Monoclonal mouse anti-RVFV Np IgG antibody was used as positive control. Graphs represent the corresponding OD450 values as mean ± SEM. Statistical significance was determined using Kruskal-Wallis test. (ns – not significant).

4.5. The effect of mosquito saliva on mosRVFV infection

Several studies indicate that the saliva of arthropod vectors does not only acts as a vehicle for different pathogens but can also actively promote the viral fitness and/or dissemination via multiple ways (Guerrero et al., 2020). Since data from previous experiments showed a generally less severe disease profile following mosRVFV infection compared to the human isolate of the virus, it leaves room for speculation whether the mosquito isolate of RVFV still relies heavily on the synergistic effect of mosquito saliva. To test whether the morbidity or mortality, as well as viral dissemination can be enhanced by the presence of vector's saliva, mice were infected intradermally with 100 PFU of mosRVFV alone or in the presence of *Aedes aegypti* PAEA mosquito's saliva. As before, venous blood was collected at early time points to check for viremia, and organs were collected at times of death or at the end of experiment (at 24 DPI) to test for the viral presence via plaque-forming assay. Experimental design is shown in Figure 33.

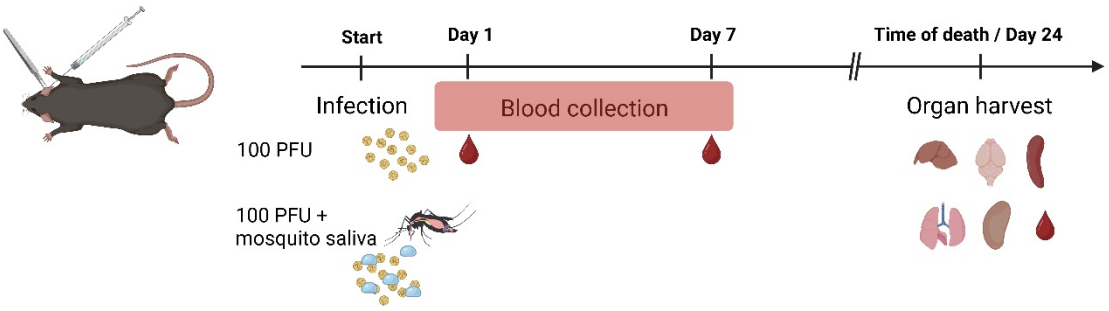

Figure 33. Experimental design for investigating the effect of mosquito saliva on the infection with mosRVFV.
Female WT mice (n=9) were infected ID with 100 PFU of mosRVFV with or without the presence of mosquito saliva. Mice were monitored daily for 24 days. Venous blood was collected at day 1 and day 7 post-infection. At the end of the experiment or in case mice succumb to the disease, liver, brain, spleen, lung, kidney and blood were collected to determine endpoint viral loads.

4.5.1. Mortality and morbidity are unaffected by the presence of mosquito saliva

In both groups, one animal reached humane endpoint criteria at 3 DPI, followed by another fatality in the group infected without the presence of vector saliva at 7 DPI, and one animal infected with additional saliva had to be humanely euthanised due to hind limb paralysis at day-15 post-infection. These events resulted in a ~22% mortality rate in both groups (Figure 34. A). All fatal cases were accompanied by weight loss, and in most cases (three out of four) by hypothermia as well (Figure 34. B-D).

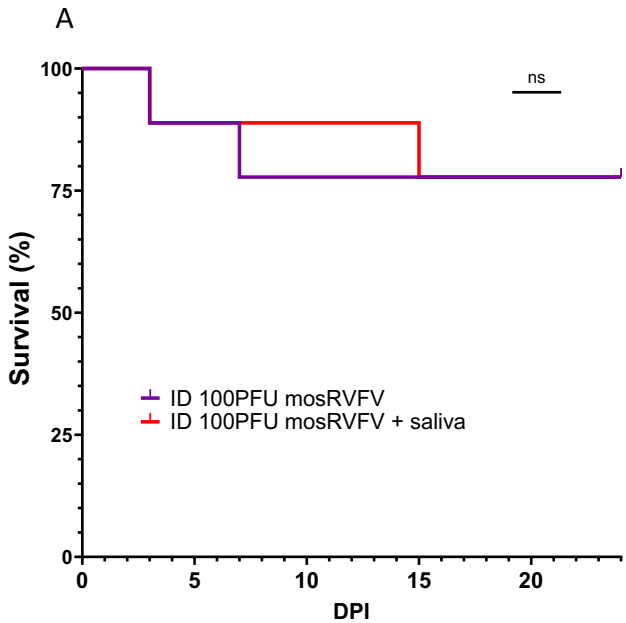

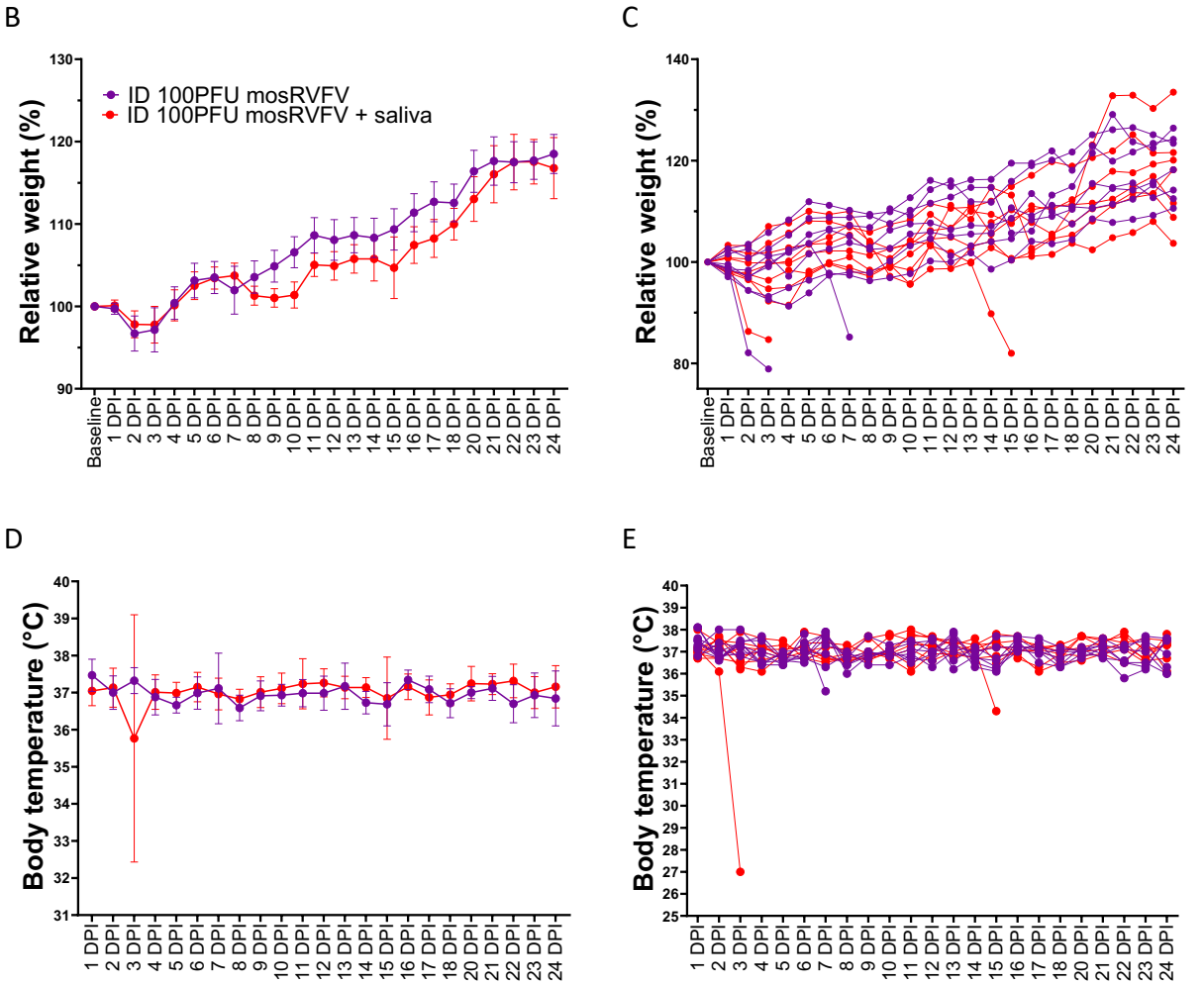

Figure 34. Mosquito saliva does not influence the mortality or morbidity of mosRVFV infection.

Graphs show Kaplan-Meier survival curves (A), relative body weight (B-C) and body temperature (D-E) of mice exposed to 100 PFU of mosRVFV in the presence or the absence of mosquito saliva. Values are reported either as mean ± SEM (B and D) or as individual readings (C and E). Statistical significance was determined using Mantel-Cox test (A) or Mann-Whitney test (B-E).

The mean relative body weight of mice infected in the presence of mosquito saliva showed a trend towards a decrease between 8-21 DPI compared to the virus-only group, but this difference was not significant.

4.5.2. Mosquito saliva does not promote viremia or viral dissemination during mosRVFV infection

Blood collected during the first week of infection was tested for viremia, to see whether the presence of saliva may promote this form of viral dissemination. However, the virus was undetectable in all tested samples, regardless of the time of collection or the presence of mosquito saliva during infection. (Figure 35).

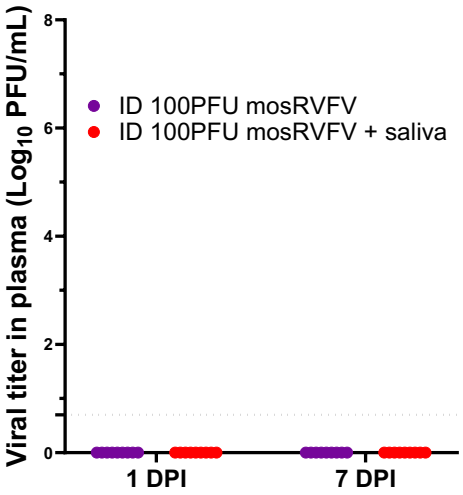

Figure 35. Neither infection route of mosRVFV leads to early viremia.
Blood collected on day 1 and day 7 after infection with mosRVFV in the absence or the presence of mosquito saliva was analysed for virus titer using plaque-forming assay. Graph shows viral load values as mean ± SEM. Dotted line indicates viral detection limit. Due to identical values no statistical analysis was performed.

Despite viremia was not promoted, viral dissemination towards other organs could have been aided by the saliva, thus endpoint viral titers in different organs were measured once again using plaque-forming assay. Plaques were detected only in the brain samples of the animals that reached humane endpoint criteria during the later phase of the disease (Figure 36.).

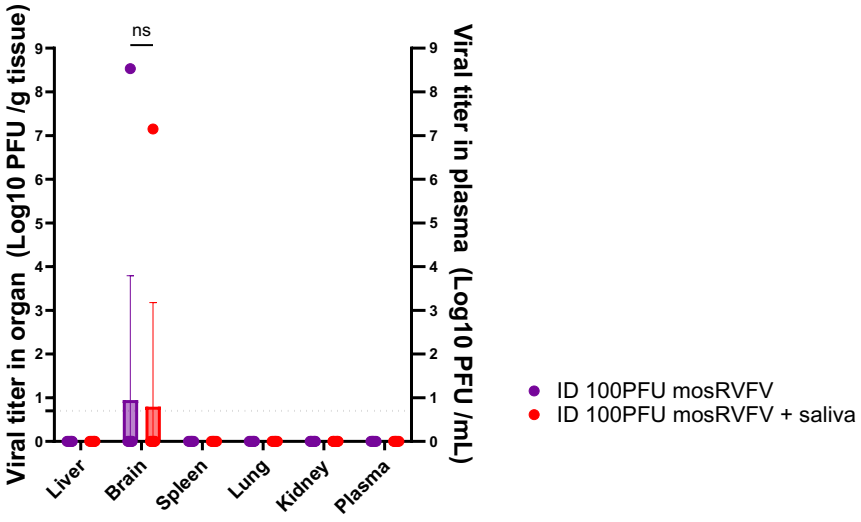

Figure 36. Mosquito saliva did not facilitate viral dissemination of mosRVFV.
Graph represents endpoint viral titers in various organs (liver, brain, spleen, lung, kidney, and blood) collected at the end of the experiment or in case of mice reaching euthanasia criteria

following ID infection with mosRVFV in the absence or the presence of mosquito saliva. Values are reported as mean ± SEM. Dotted line indicates viral detection limit. Statistical significance was determined using multiple Mann-Whitney test. (ns – not significant).

4.5.3. Mosquito saliva has no effect on seroconversion following intradermal mosRVFV infection

Lastly, the effect of the mosquito saliva on the seroconversion was also evaluated. The presence of RVFV Np-specific IgG antibodies in the endpoint blood samples was detected via indirect ELISA. Seroconversion was confirmed in all animals surviving at least for 7 days, although no significant difference was observed in the amount of virus-specific IgG antibodies, as indicated by OD450 values, as shown in Figure 37. The OD450 values of samples obtained from animals reaching endpoint criteria at 7 DPI or 15 DPI are lower compared to those of survivors. Note, sample from animal diseased at 3 DPI following infection without mosquito saliva was not available.

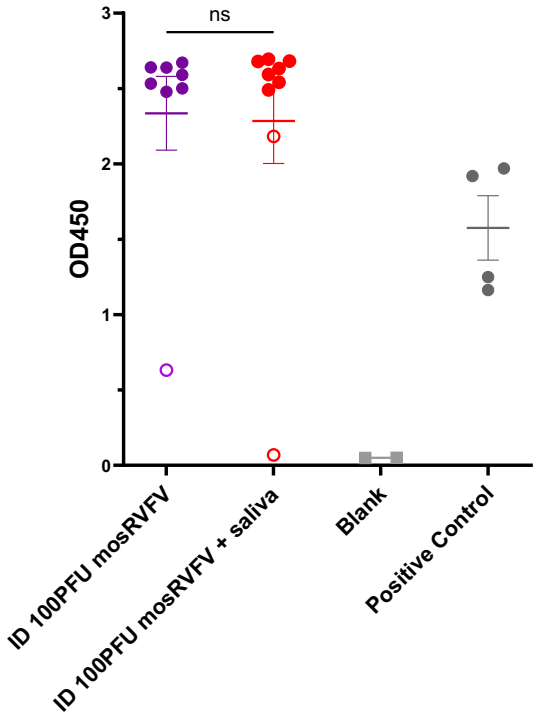

Figure 37. Mosquito saliva did not interfere with antibody production.
Endpoint blood samples from mice infected with mosRVFV, with or without the presence of mosquito saliva, were screened for RVFV Np-specific IgG antibodies by indirect ELISA. Graph represents OD450 values as mean ± SEM. Monoclonal mouse anti-RVFV Np IgG antibody was used as positive control. Values from fatal cases are represented by open symbols. Statistical significance was determined using Mann-Whitney test. (ns – not significant).

4.5.4. Histopathology of the brain

As mosRVFV was only detected in the brain, histological analysis of virus-infected brains was performed using H&E and virus-specific IHC staining to assess the pathomorphological changes induced by the virus together with the affected cell types, respectively. Identifying the areas of the brain affected and the cell types infected may help to understand, or at least speculate on the possible entry mechanisms used by this virus to reach the brain and the

subsequent pathology of this organ. General H&E staining of the section of the brain stem revealed microhaemorrhages due to the disintegration of blood vessels and pronounced cell death characterised with the destruction of cell nuclei. The olfactory bulb and its neighbouring tissue were free of pathological changes, as shown in Figure 38.

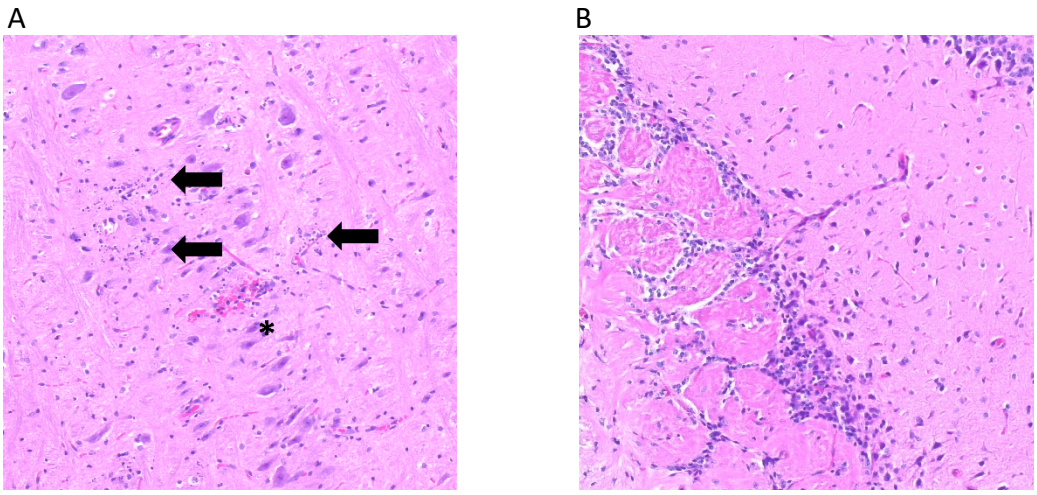

Figure 38. Pathomorphological alterations are almost limited to the brain stem.
Virus positive brain of mosRVFV infected mouse, confirmed via plaque assay, were fixed and embedded to paraffin blocks followed by sectioning and H&E staining. Representative picture of the brain stem (A) showed fragmentation of cell nuclei (arrows) and disintegration of blood vessels accompanied by micro bleeding (asterisk). The olfactory bulb (B) is free from signs of pathology (20x magnification).

4.5.5. Target cells in the brain

Immunolabelling of brain sections using polyclonal antibody against RVFV Gn allowed us to identify - to some extent - the cell types inside the brain that were targeted by the virus based on their morphology. Viral antigen was detected mostly in the neurons, oligodendrocytes and Bergmann glia, but occasionally, astrocytes, and Purkinje cells stained positively as well, as shown in Figure 39.

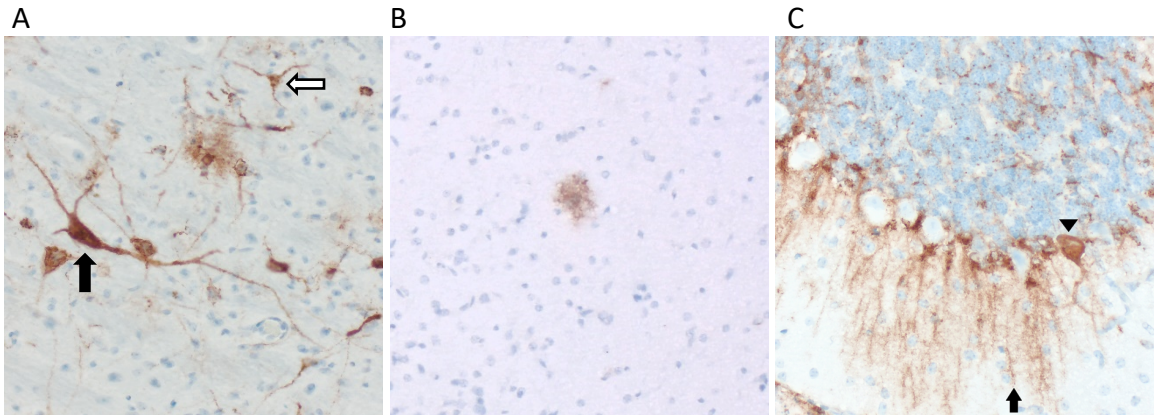

Figure 39. mosRVFV targets distinct cell types in the brain.
IHC staining was performed on the brain collected from mouse with lethal case of mosRVFV infection. Virus-infected cells were identified by positive immunolabelling for RVFV Gn (brown). Virus antigen was detected in neurons (A, black arrow), oligodendrocytes (A, white arrow), astrocytes (B), Bergmann glia (C, arrow) and Purkinje cell (C, arrowhead).

4.5.6. Affected areas in the brain

To suggest the potential entry site of mosRVFV into the brain, the most common brain entry sites, known for other viruses, were analysed for the presence of RVFV antigen by IHC. In the olfactory bulb (Figure 40. A) only a few cells bared the viral antigen, and these cells were most likely astrocytes based on their morphology. The choroid plexus (Figure 40. B) is located in the brain ventricles and its main purpose is to produce the cerebrospinal fluid (Lun et al., 2015). This area showed negative immunolabelling.

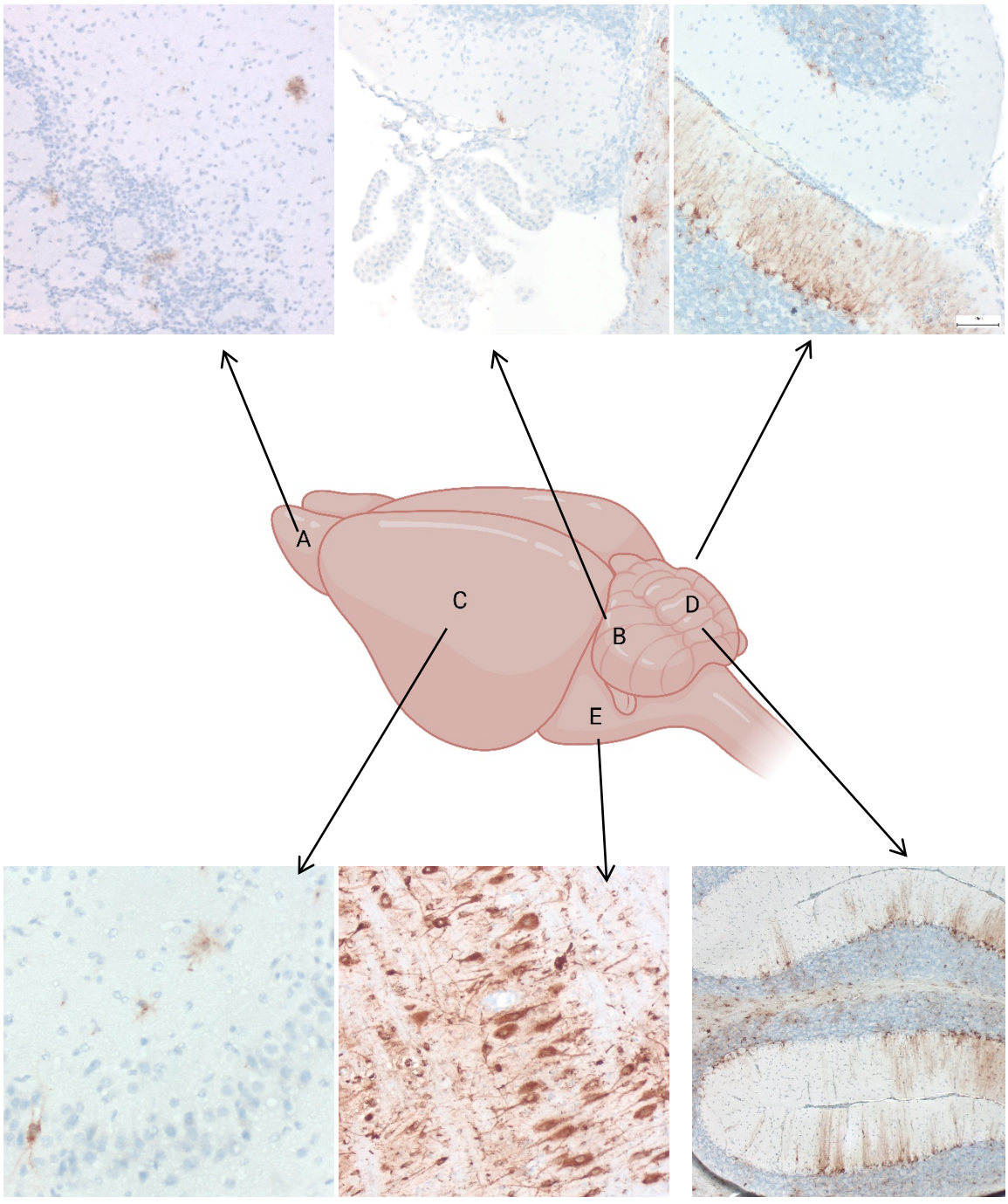

Figure 40. Brainstem and cerebellum are the most virus affected areas in the brain.
IHC staining was performed on the brain collected from mouse with lethal case of mosRVFV infection. Virus infected cells were determined via the positive immunolabelling for RVFV-Gn

(brown) in the following brain areas: olfactory bulb (A), choroid plexus (B), hippocampus (C), cerebellum (D) and brainstem (E). The brain schematic was made with BioRender.

The hippocampus is located in the mid-section of the mouse brain below the cerebral cortex. Virus antigen was sporadically detected in cells with morphology resembling to oligodendrocytes and astrocytes, see in Figure 40. C. Strong positive staining of Bergmann glia with radial morphology and extended processes was located in the molecular layer of the cerebellum. Purkinje cells, astrocytes, and other cells in the granular layer and the white matter were also positively labelled. Notably, Bergmann glia were not uniformly positive in all lobes, despite the positive cells in the granular zone, see Figure 40. D. Massive viral antigen staining was found in the brain stem. Almost all cells in this region were found positive (Figure 40. E). Endothelial cells of blood vessels remained to be negative. (Figure 41. A and B). Virus antigen was not detected in the pia mater's cells either (Figure 41. C).

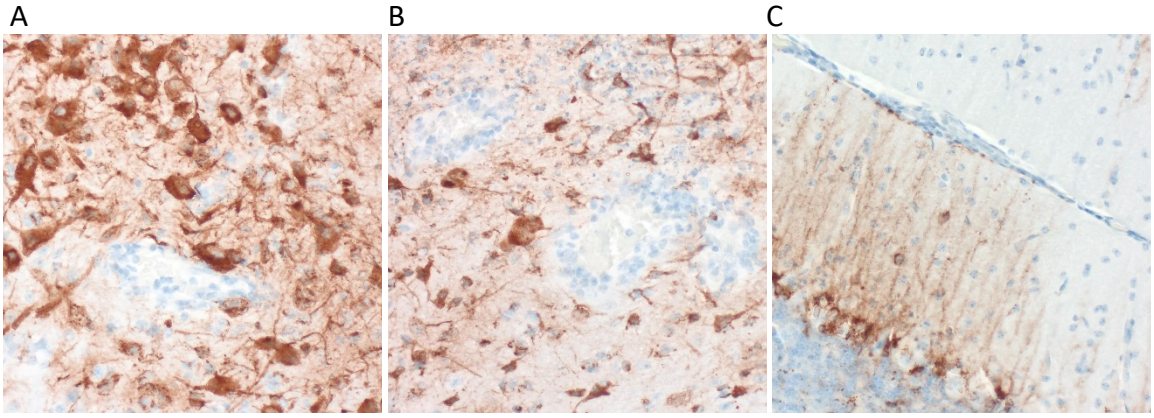

Figure 41. Endothelial and pia cells are negative in mosRVFV infected brain.
IHC staining was performed on the brain collected from mouse with lethal case of mosRVFV infection. Virus infected cells were determined via the positive immunolabelling for RVFV-Gn (brown). Section from the brainstem indicates negative labelling of the endothelial cell (A-B). The pia mater of the cerebellum is also negative for RVFV antigen (C).

4.6. Molecular differences between the two isolates

To understand if the difference in survival, morbidity and dissemination between the two RVFV isolates could be explained by potential changes in their viral proteins, the genetic material of both isolates was sequenced. The nucleotide code was translated to amino acid level and the amino acid sequences of the two isolates were compared. The list of amino acid differences between huRVFV and mosRVFV as well as the reference strain ZH-501 is shown in Table 12. Blue tint highlights the mutations occurring between the isolates used in this study.

Table 12. Differences in the amino acid sequences of huRVFV and mosRVFV

Segment	Gene	Position of difference	Amino acid		
			huRVFV	mosRVFV	ZH-501
S	NSs	23	Isoleucine	Isoleucine	Phenylalanine
		50	Histidine	Tyrosine	Histidine
		155	Methionine	Lysine	Methionine
		156	Valine	Isoleucine	Isoleucine
		157	Valine	Valine	Alanine
		210	Valine	Alanine	Valine
		217	Alanine	Alanine	Valine
		226	Arginine	Cysteine	Arginine
		242	Valine	Valine	Isoleucine
		251	Glycine	Glutamic acid	Glutamic acid
	Np	159	Glutamic acid	Glutamic acid	Glycine
M	NSm	138	Valine	Alanine	Valine
	Gn	266	Methionine	Valine	Methionine
		397	Phenylalanine	Serine	Phenylalanine
		428	Arginine	Glutamine	Glutamine
		598	Isoleucine	Threonine	Isoleucine
		602	Isoleucine	Isoleucine	Valine
		631	Valine	Valine	Isoleucine
	Gc	860	Threonine	Serine	Threonine
		987	Aspartic acid	Glutamic acid	Aspartic acid
		1059	Threonine	Threonine	Serine
L	RdRp	23	Tyrosine	Tyrosine	Phenylalanine
		269	Isoleucine	Threonine	Isoleucine
		278	Asparagine	Asparagine	Serine
		288	Valine	Alanine	Alanine
		302	Isoleucine	Isoleucine	Valine
		663	Threonine	Threonine	Alanine
		1121	Serine	Serine	Glycine
		1333	Isoleucine	Isoleucine	Valine
		1743	Valine	Isoleucine	Valine
		1922	Lysine	Lysine	Arginine
		1984	Asparagine	Asparagine	Aspartic acid
		2072	Serine	Glycine	Serine

The sequencing data revealed 6 amino acid difference on the NSs protein encoded on the S segment. There were 7 amino acids different regarding the M segment: 1 on the NSm, 4 on the Gn and 2 on the Gc protein. There were also 4 changes when considering the L segment.

The available tertiary structures of the RVFV proteins are limited, therefore not all of these mutations' position could be located in a 3-dimensional space. However, the analyses revealed that some of the mutations on the M segment (at the position 397 and 428) are located on the outer surface of the glycoprotein (Gn), as shown in Figure 42.

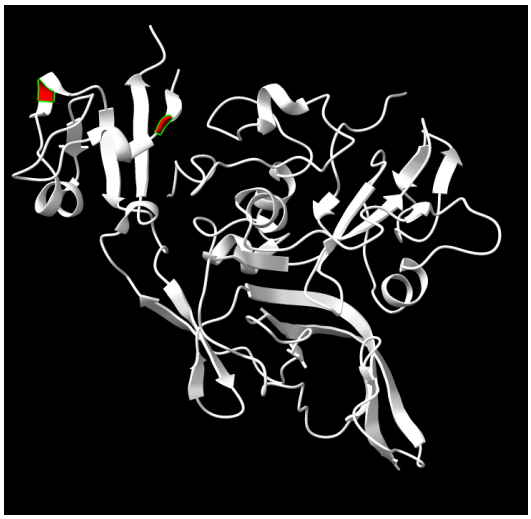

Figure 42. Some amino acid mutations are located on the surface of the glycoprotein.
Tertiary structure of RVFV strain ZH-548 M12 Gn protein was obtained from the Protein Data Bank (ID: 6F8P), based on the original publication from (Halldorsson et al., 2018). Alteration in the amino acid sequence at position 397 and 428 is highlighted with red colouring, using ChimeraX software (Meng et al., 2023).

4.7. In vitro replication capacity of the two isolates is comparable in various cell types

To test whether the identified alterations on the glycoproteins and polymerase influence the infection potential and replication capacity, viral growth kinetics was evaluated, as shown in Figure 43. A549-Npro (lung carcinoma), SH-S5Y5 (neuroblastoma), and Huh7 (hepatocarcinoma), cell lines were kept in culture and infected with either huRVFV or mosRVFV. Virus content of the supernatant was collected daily and was measured via plaque-forming assay.

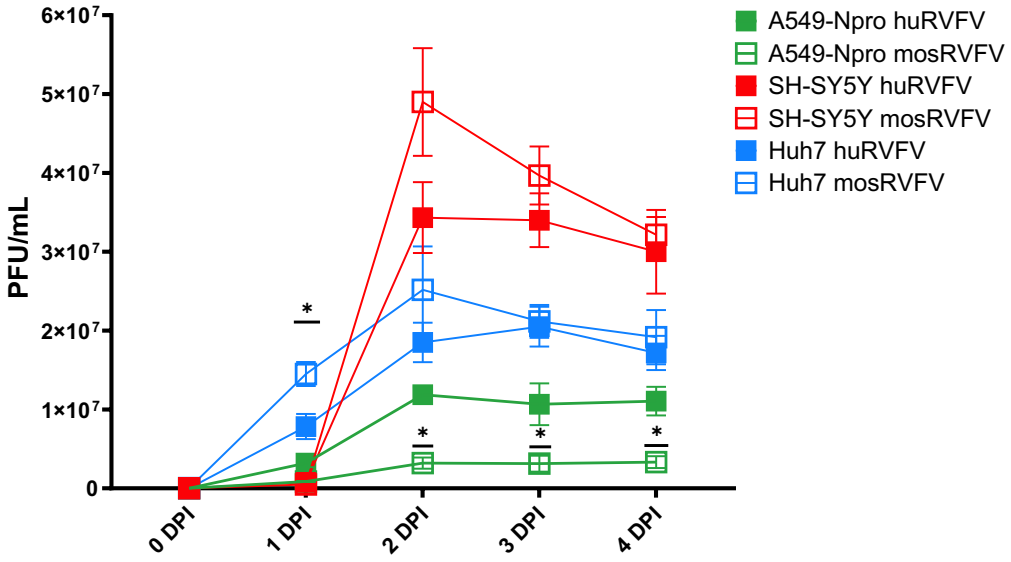

Figure 43. Replication efficiency of RVFV is determined by the host cell type not the virus' origin.
The *in vitro* viral growth kinetics assay was performed on various cell types with lung (green), liver (blue), or brain (red) origin. Cell culture supernatant was collected daily and tested for viral load via plaque-forming assay. Viral load values are represented as mean ± SEM. Statistical

significance was determined using 2-way ANOVA with Tukey's multiple comparison test. (*≤ 0.05).

Both isolates were able to infect and replicate successfully in all 3 types of cells. At 1 DPI mosRVFV produced significantly more virus in the liver cell line than in the other 2 cell lines. Starting from 2 DPI, mosRVFV exhibited significantly lower replication in the lung cell line compared to huRVFV or the same isolate in the other two cell lines. There was no significant difference in the replication of the two isolates in the liver or in the neuroblastoma cell lines. From 2 DPI, both isolates replicated to the highest titers in neuroblastoma cells, followed by the liver cells and the lung cells gave the lowest RVFV titers.

4.7.1. The two isolates show different cytopathic effect (CPE) in cell culture monolayers

A marked difference in plaque morphology was observed depending on the origin of the virus. While plaque diameters were comparable between the two isolates, plaques induced by huRVFV were clear and well-defined, whereas mosRVFV produced turbid plaques characterised by reduced contrast from the monolayer when stained with crystal violet.

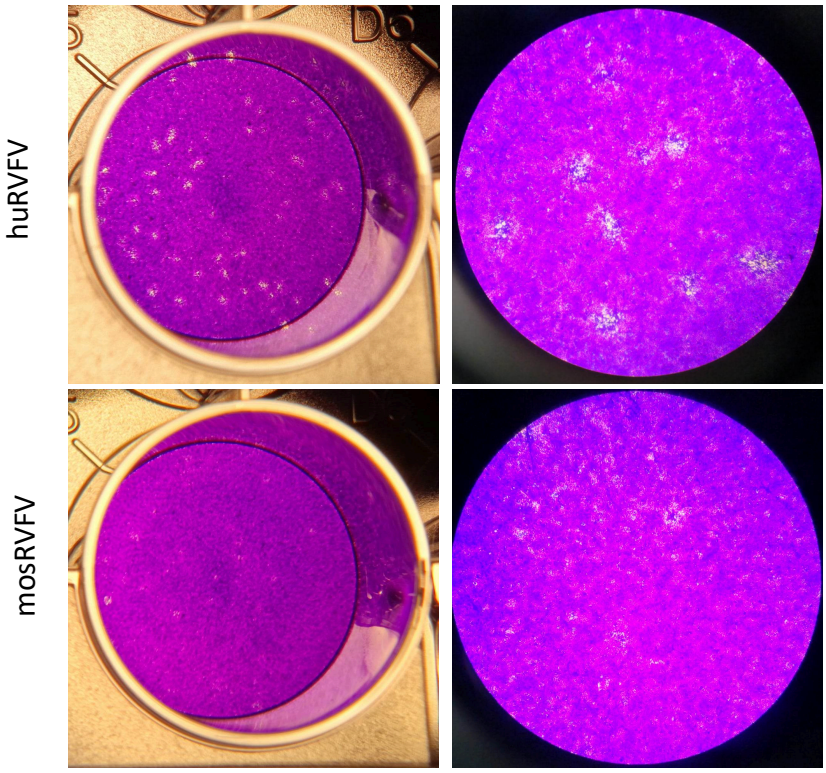

Figure 44. CPE was less prominent in cells infected with mosRVFV

Representative images of crystal violet-stained A549-Npro cell monolayers, used to determine viral load by plaque formation assay, showed different morphologies of plaques depending on the origin of the virus. Clear, well-defined plaques were observed following infection with huRVFV, whereas turbulent plaques with reduced contrast were formed by mosRVFV. Images were taken by using stereo microscope.

4.8. Identifying the early target cells for RVFV

As previous experiments demonstrated, the infection route is a major factor regarding the outcome of RVFV infection. It can be hypothesized that the cell types locally available may provide a unique environment, affecting virus replication, infection and dissemination. This

idea is endorsed by the previous viral load data where virus was more often detected in the skin than in the lung (compare Figure 26. A and C). The lung and the skin have a distinct cell composition. Besides the obvious parenchymal components, there are immune cells (e.g., Langerhans cell or alveolar macrophage) which are exclusively located in one or the other organ (Hartl et al., 2018; Kashem et al., 2017) which may explain the difference in infection efficacy between infection routes. It is believed and for some pathogens it is already proven that arboviruses use the locally available or recently recruited antigen presenting cells or other immune cells as their initial replication site. These infected immune cells, which have the ability to migrate, then spread the virus through the lymphatic system (Visser et al., 2023). This mechanism has not yet been proven for RVFV, but such cells, for example, dendritic cells, macrophages, granulocytes, and moDCs have already been confirmed as possible and susceptible targets. However, these results were reported in studies using either a virus lacking its virulence factors (NSs) and expressing reporter gene protein (green fluorescent protein) (Gommet et al., 2011) or performed only in cell culture (McElroy & Nichol, 2012b).
As the absence of NSs could potentially affect the permissiveness of cells for the virus, the following experiment aimed to identify and further characterise the immune cells that are targeted at the early stage of infection by wild type RVFV. For this, mice were infected ID or IN with the human or mosquito isolate and their skin with ALN or lung with MLN were collected at 2 DPI according to the infection route, see Figure 45. A. Preparation of single-cell suspension was followed by the immuno-labelling of the different immune populations using fluorescent conjugated antibodies specific for various differentiation markers. Infected cells were detected by the use of fluorescence-labelled oligos, complementary to the mRNA of the RVFV Np using the PrimeFlow™ method. For the identification of infected immune cell population, the probe-positive population of the immune cells ($CD45.2^+$) was overlayed to the total immune cell population and was analysed for the expression of various phenotypic markers as shown in Figure 45. B.

4.8.1. Experimental design and gating strategy

A

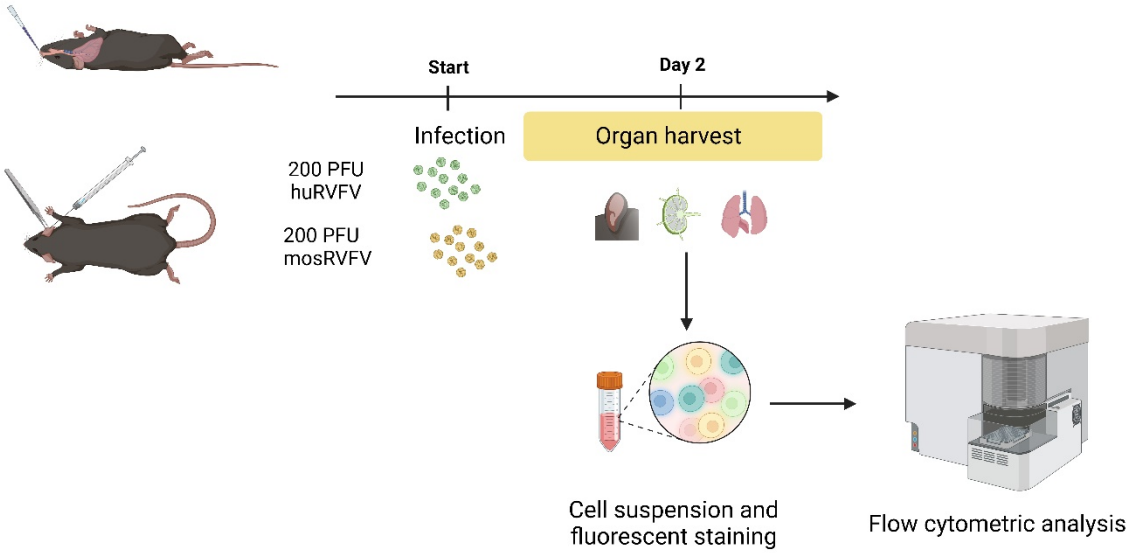

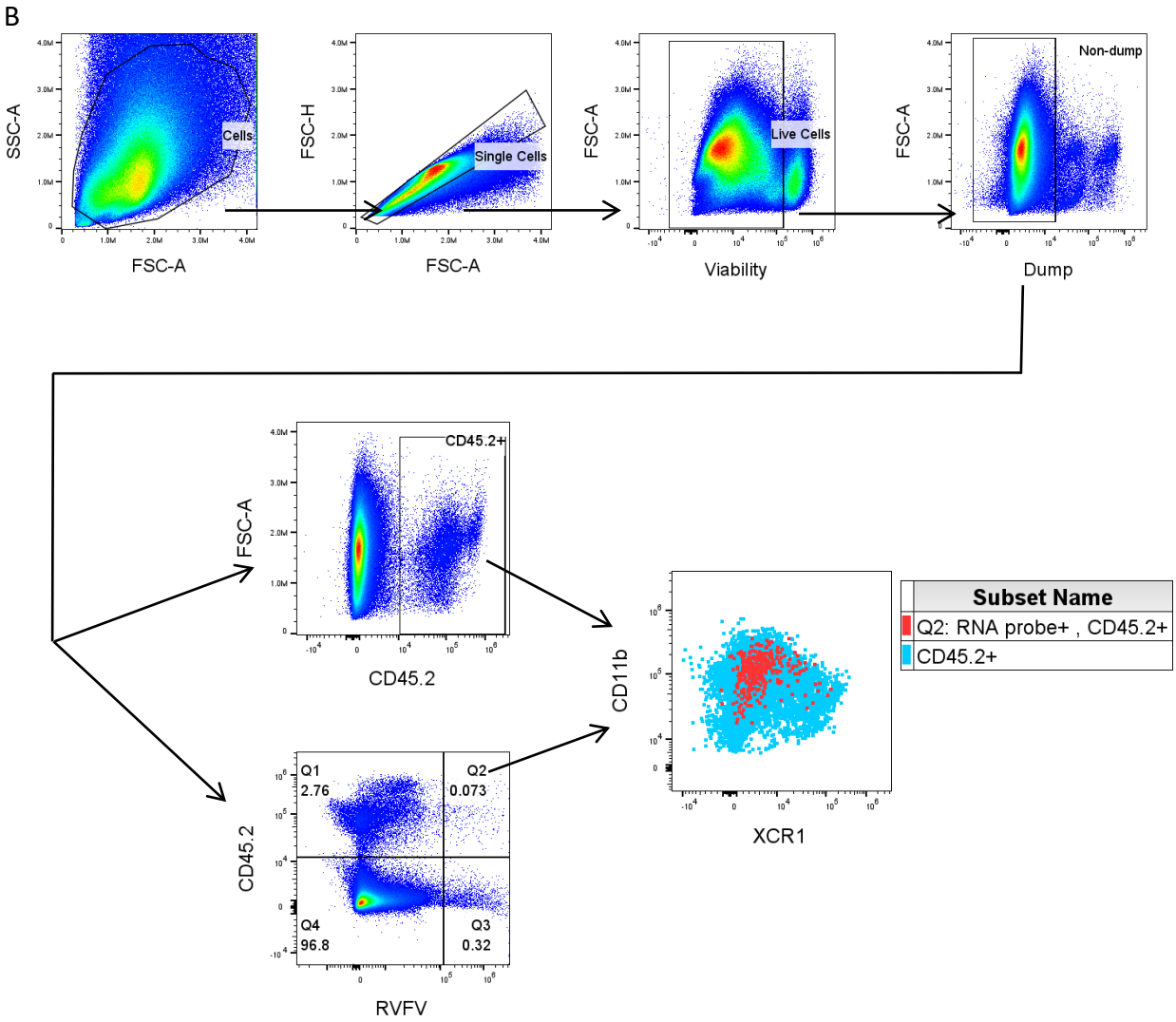

Figure 45. Experimental design and gating strategy for flow cytometric analysis
Female WT mice (n=2-4) were infected ID or IN with mock or 200 PFU of either huRVFV or mosRVFV. At 2 DPI, mice were humanely sacrificed and skin with ALN from ID infected animals and lung together with MLN from IN infected animals were collected and processed for single-cell analyses using a fluorescent flow cytometer (A). A representative figure (B) shows that the gating strategy to identify RVFV-infected cells was performed as follows: after excluding cell debris, cell aggregates, dead cells and cell types of no interest (Dump), RVFV and CD45.2 double positive cells (red) were overlaid on the total CD45.2+ population (blue). FSC, forward scatter; SSC, side scatter

4.8.2. Target cells for RVFV in the skin

The characterisation of the infected immune populations using cell surface phenotypic markers can be used to identify the targets of wild type RVFV in the skin after ID infection. Furthermore, by comparing the distribution of these infected cells in the skin and in the corresponding draining lymph nodes, it is possible to deduce which cell subsets are responsible, at least in part, for viral dissemination in the lymphatics.
PrimeFlow™ analysis revealed that RVFV mostly targets non-immune cells in the skin. The ratio of infected non-immune cells vs infected immune cells was an average of 6:1 in case of huRVFV and similarly 5,6:1 in case of mosRVFV. In contrast, this ratio could not be observed in the

draining lymph nodes, as these secondary lymphoid organs consist mostly immune cells. There was also a notable difference between the isolates regarding their infection efficacy observed in the skin and its draining lymph node in favour of huRVFV (see Figure 46. A, and Supplementary table 1).

A

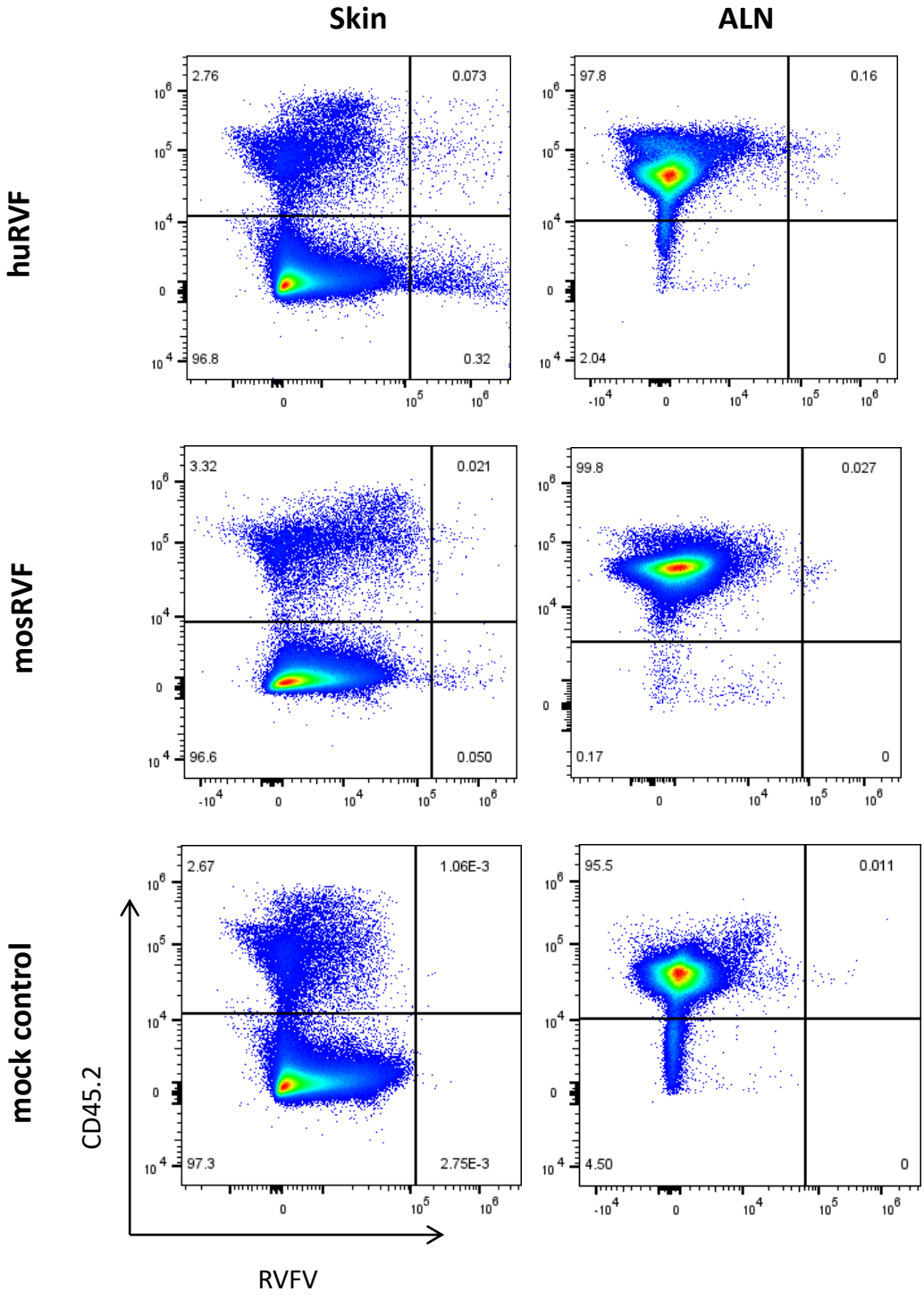

B

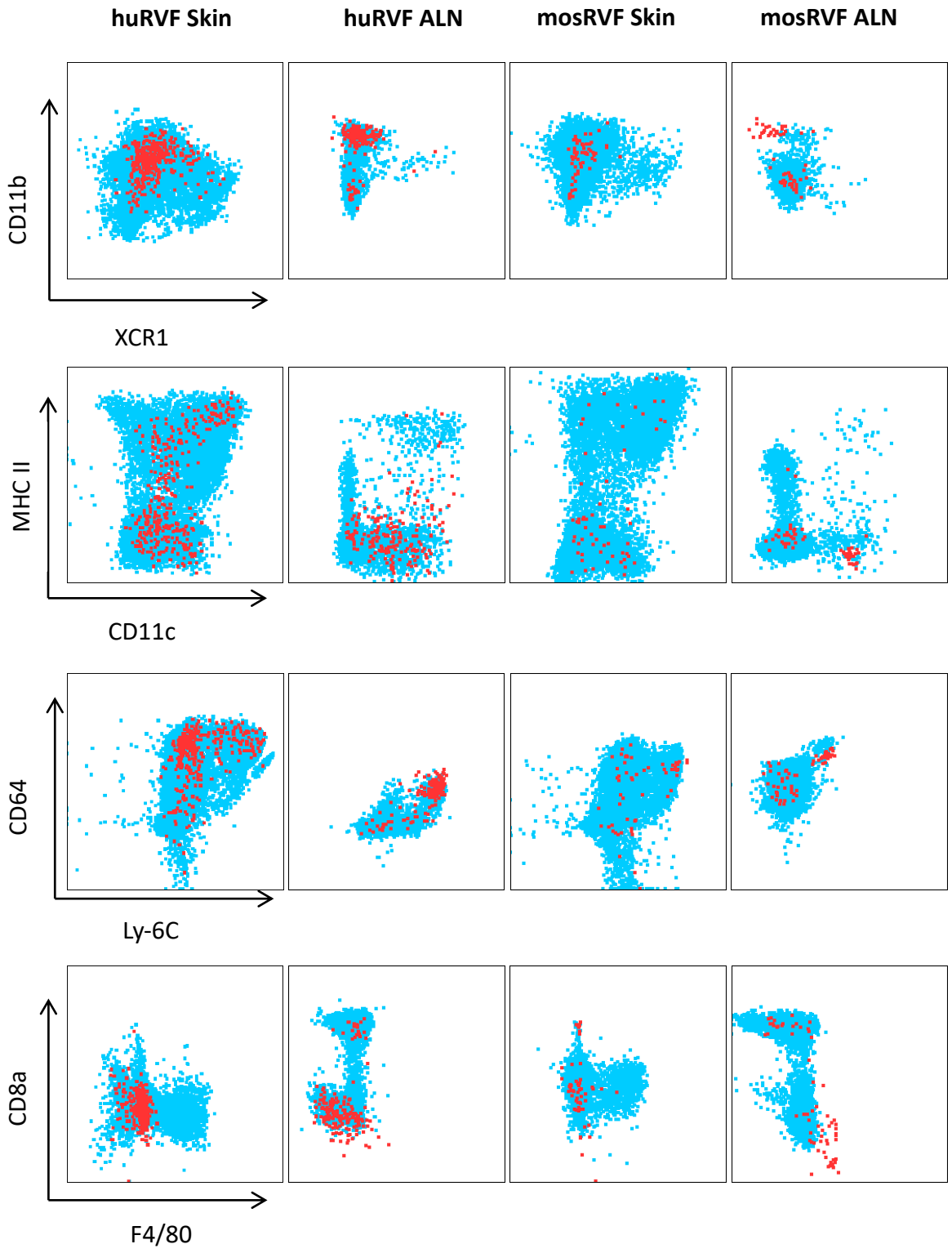
huRVF Skin
huRVF ALN
mosRVF Skin
mosRVF ALN
CD11b
XCR1
MHC II
CD11c
CD64
Ly-6C
CD8a
F4/80

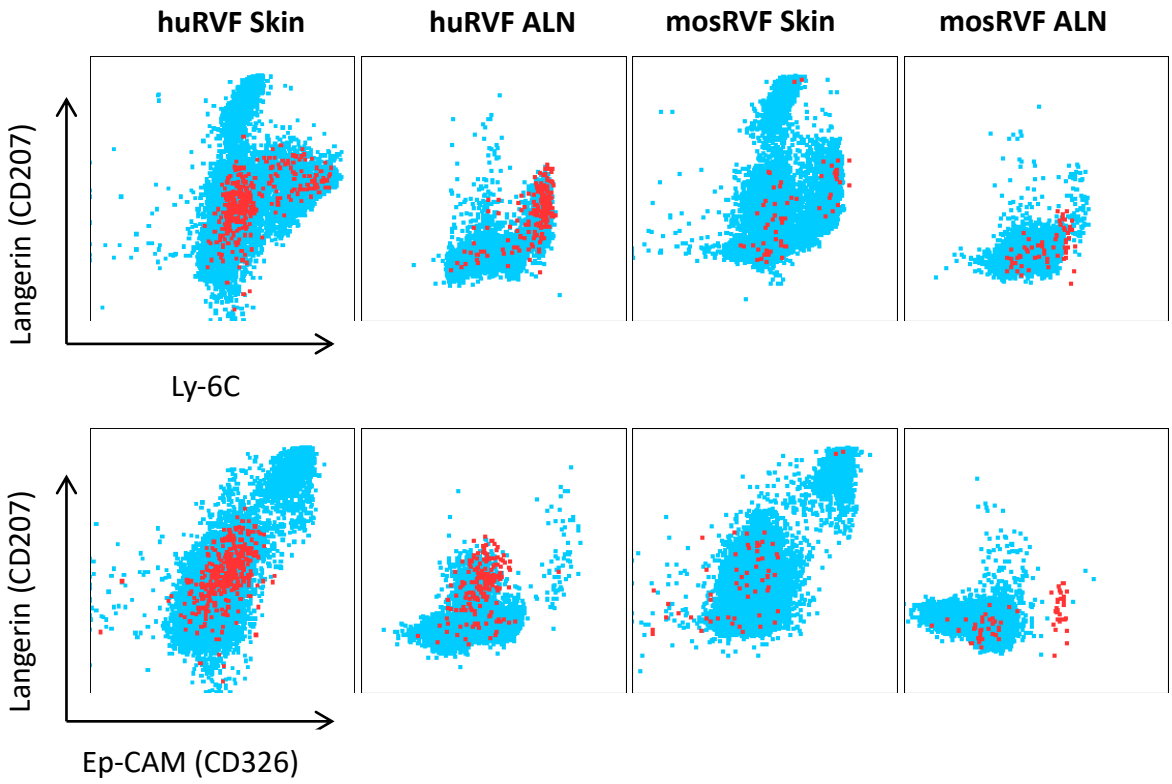

Figure 46. Human isolate of RVFV exhibited similar target cells but higher infection potential in comparison to the mosquito isolate.
Mice were infected ID with 200 PFU (100 PFU/ear) of either huRVFV or mosRVFV, along with mock control. Two days after infection, cells were obtained from the skin of the ears and their draining lymph nodes and were stained for flow cytometry. (A) Representative dot plots indicate the distinct populations' percentage within the non-dump population. (B) Distribution of the RVFV-infected cells (red) among the total CD45.2^{+} population (blue) is displayed as representative dot plot overlays (B).

Flow cytometric data analysis showed that the RVFV infected cells were mostly negative for XCR1, CD8a, F4/80, and Ep-CAM. Only around half of them expressed MHCII, meanwhile most of them were positive for CD11b, CD64, Ly-6C, and Langerin. Infected cells in the draining lymph nodes had similar phenotype, however there was a noticeable decrease in their MHCII expression, and there was a great accumulation of the Ly-6C^{+} population. Interestingly there was no pronounced difference in the phenotype of the infected cells between the two RVFV isolates, as shown in Figure 46. B.

4.8.3. Target cells for RVFV in the lung

The same approach was used to identify early target cells of RVFV in the lung; however, none of the 6 intranasally infected lungs collected 2 DPI showed positivity for RVFV, regardless of the isolates used see Figure 47.

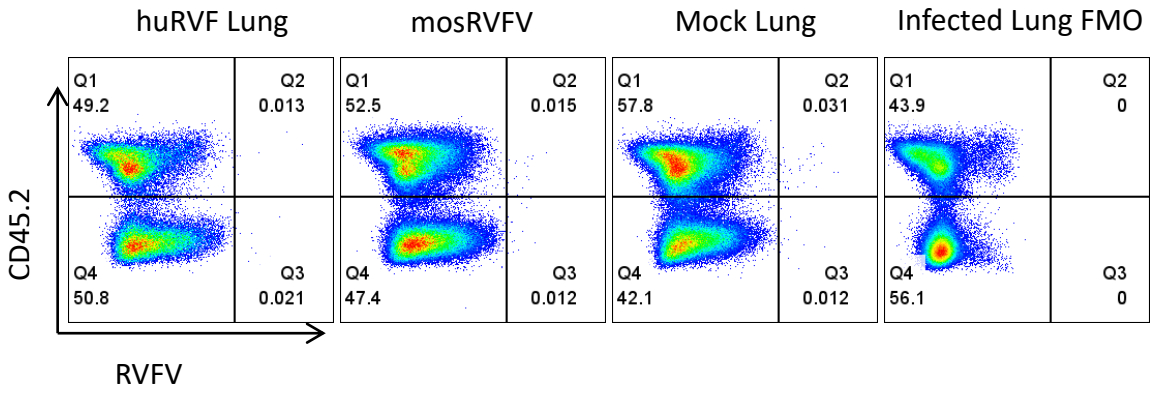

Figure 47. Flow cytometric analyses failed to detect virus infected cells in the lung.
Mice were infected IN with 200 PFU of either huRVFV or mosRVFV. Two days after infection, cells were obtained from the lung and its draining lymph node and were stained for flow cytometry. Representative dot plots indicate the distinct populations's percentage within the non-dump population.

4.8.4. Responsiveness of target cell population during RVFV infection

The previous experiment identified the $CD11b^{+}CD64^{+}Ly\text{-}6C^{+}Langerin^{Mid}$ cell subsets as the major targets for WT RVFV, but it did not provide insight into the behaviour and availability of this population during RVFV infection. To investigate the responsiveness of these cells, their representation in the skin and the corresponding ALN was compared between mock and virus-infected animals, using the same samples as were used for the target cell identification.
Flow cytometric data shows that this cell population is underrepresented in the mock skin but became a well-defined population upon RVFV infection. These cells are virtually absent in the ALN of uninfected animals but became overrepresented following infection (see in

Figure **48**. A). The same population did not expand in the lung following RVFV infection, however in one subject the expression of Langerin and Ly-6C was increased on the $CD11b^{+}CD64^{+}$ cells upon exposure to mosRVFV, but not to huRVFV (

Figure **48**. B). Unfortunately, the number of cells gained from the mediastinal lymph nodes was not enough for flow cytometric analyses.

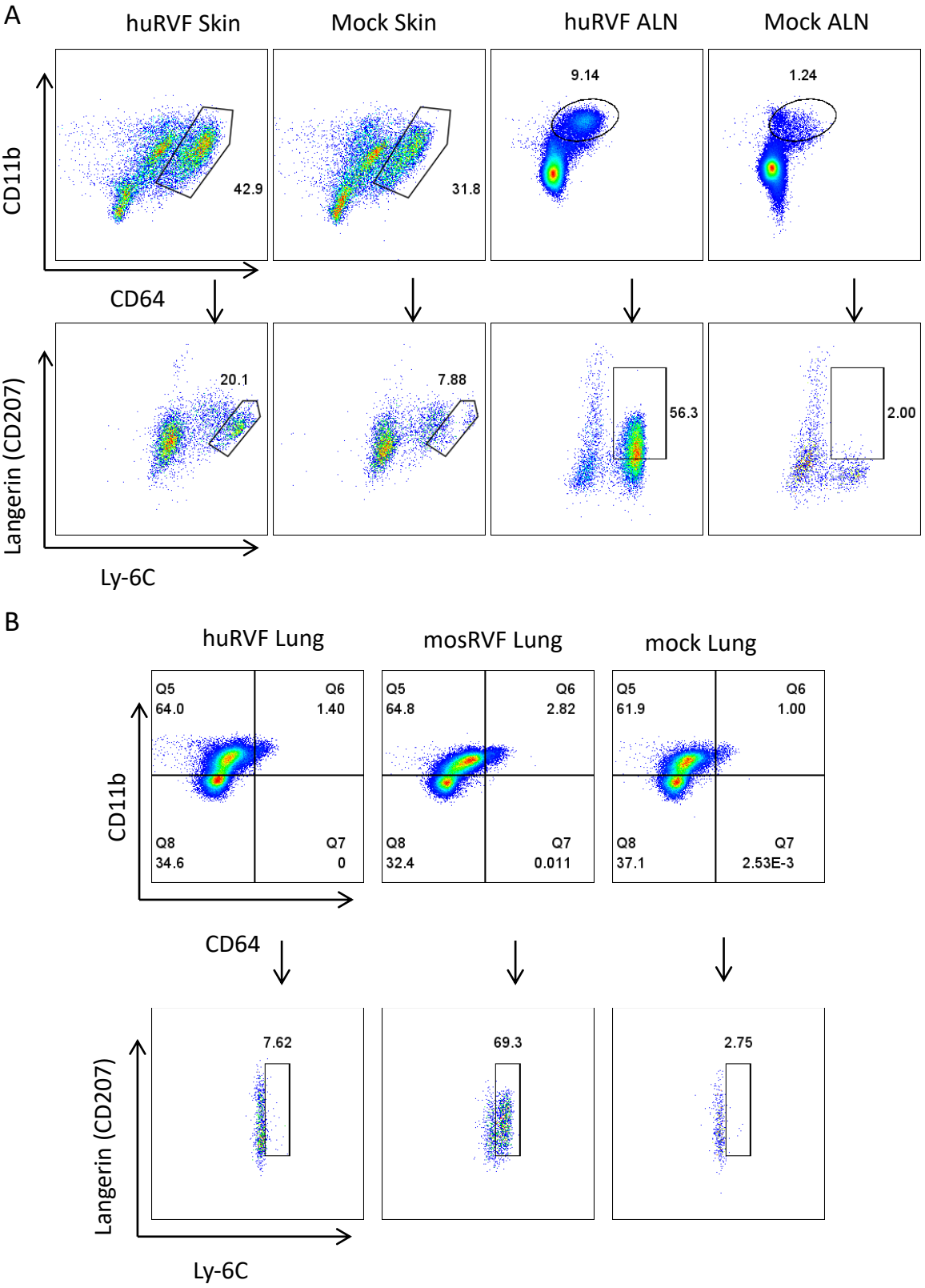

Figure 48. Recruitment of monocytes/monocyte-derived cells upon ID RVFV infection is more pronounced compared to IN route.

Mice were infected ID (A) or IN (B) with mock or 200 PFU of huRVFV or mosRVFV. At 2 DPI, cells were harvested from skin, ALN and lung and stained for flow cytometry. Representative dot plots show the percentage distribution of CD11b and CD64 within the total immune cells, while the same distribution of Langerin and Ly-6C is shown within the $CD64^{+}CD11b^{+}$ cells.

5. Discussion

5.1. Pathogenesis of the human and mosquito isolate of RVFV

Fatality of C57Bl/6J mice following huRVFV infection manifested rapidly. Intradermally infected mice started to reach humane endpoint criteria after 3 days of infection without prior significant weight loss or change in body temperature. While ID infection resulted in death of all individuals, mice infected with higher dose (100 PFU) succumbed to the disease one day sooner, at 3 DPI, in contrast to some case of infection with 10 PFU. A different survival curve characterises the intranasally infected groups, as only 4/6 or 1/6 of the animals died following infection with 100 PFU or 10 PFU of huRVFV, respectively. Animals also began to succumb to the disease at a later time point following IN infection: 4 DPI or 6 DPI depending on the infection dose (higher dose associated with earlier time of death). This disease course including the time of death and the lack of decreased body weight and body temperature prior death are comparable to what researchers have found for the same inbred mice infected with the WT RVFV strain ZH501 (Cartwright et al., 2020; Gray et al., 2012).

Delayed time of death following huRVFV infection was associated with lower infection dose independent of the infection route. Dose-dependent disease progression following infection with RVFV ZH501 was observed by others too (Cartwright et al., 2020; Gowen et al., 2013). We noticed that some animals showed no signs of disease after IN infection with huRVFV, despite being exposed to the full intended infection dose. These animals had no detectable virus in any of their organs, presented with no viremia or elevated liver enzymes in their blood, nor did they produce virus-specific antibodies as a sign of seroconversion. (shown in Figure 17. and Figure 19.). These results suggest that the exposure of these mice to huRVFV did not result in successful infection, therefore these individuals cannot be considered as real survivors. Similar abortive infection following low dosage of ZH501 strain was reported by McElroys's group as well (Cartwright et al., 2020).

As mentioned in the introduction, various factors influence the outcome of RVFV infection. Because no comprehensive study has been published on the effects of the infection route, specifically comparing intranasal and intradermal exposure in C57Bl/6J mice, the currently available reports are not directly applicable to this study. However, several reports indicate a more severe pathogenesis when RVFV is administered through the respiratory tract compared to the dermal route. IN infection route caused higher and longer viremia and more wide-spread tissue infection in cattle when compared to intradermal administration (A. L. Kroeker et al., 2020). IN infection of marmosets with ZH501 resulted in increased mortality rate compared to SC administration (D. R. Smith et al., 2012). When ZH501 strain was administered in an aerosolized form or via SC to BALB/c mice, no difference in survival was observed between the groups, however early and more aggressive brain invasion was found in mice received aerosolised RVFV particles (Reed et al., 2013). Furthermore, SC administration of vaccine strain Smithburn or Clone-13 (Lacote et al., 2022), or ZH501 strain lacking NSs (Dodd et al., 2014b), was sublethal to mice, while IN administration of these attenuated strains caused lethal encephalitis. Similar findings were reported following IN or ID infection of ferrets with RVFV ZH501. While some reports suggest that SC infection leads to faster viral dissemination compared to the IN route (Gowen et al., 2013), our results with huRVFV are the first to identify ID route as associated with a significantly higher mortality rate when compared to IN exposure.

The haemorrhagic form of huRVF disease was observed in mice reaching humane endpoint criteria, affecting multiple organs, especially the liver, regardless of the infection route (shown in Figure 16). While liver damage and subsequent haemorrhaging in mice after RVFV infection

have been reported in several studies, external haemorrhaging, such as in the claws after huRVFV infection, has not been documented in the literature reviewed for this dissertation.
The measurement of the liver enzyme (AST) in the plasma and viremia during the course of infection with huRVFV indicated that the disease progressed faster in case of ID infection, as both – serum AST and viremia – peaked at 3 DPI, while these parameters reached similar levels only at 5 DPI upon IN infection (Figure 17.). Furthermore, viremia was detectable as early as 1 DPI in the majority of the intradermally infected animals receiving 100 PFU. In contrast, the plasma of the mice receiving the same amount of virus intranasally, remained to be virus free up until 3 DPI. The previously mentioned work from Ikegami's group also compared the daily virus load and the presence of another liver enzyme - alanine transaminase - in the blood. They also found that these parameters began to rise earlier following SC infection than in the IN group, although, the time of death was comparable in both groups (Gowen et al., 2013).
Analyses of the endpoint viral loads showed wide dissemination of the virus. The presence of huRVFV was higher in the liver than in any other tested organs (including the spleen, lung, kidney and blood plasma), but the viral loads in the same organs were comparable between IN- or ID-infected animals. Only one individual, infected intranasally, was detected with virus in the brain (see Figure 18.). A similar broad virus dissemination of other WT virus isolates (like ZH501 or ZH548) have been reported by others (Reed et al., 2012; D. R. Smith et al., 2010). It is not clear why most of the huRVFV-infected mice had no detectable virus in the brain. It is possible that huRVFV lacks time to reach the brain due to the very rapid fatal outcome. However, other studies using the ZH501 strain reported the presence of RVFV in the brain of most infected mice already at 2 or 3 DPI, depending on the infection route (Cartwright et al., 2020; Gowen et al., 2013). This indicates that other strains can invade the CNS in such a short time, although researchers used a higher infection dose, which could potentially result in faster viral dissemination, thus earlier brain invasion in those studies.
Monitoring the morbidity and mortality of the mice following ID or IN infection with mosRVFV provided unexpected results. Administering the same amount of virus showed decreased mortality comparing to the infection with huRVFV. Furthermore, mosRVFV did not cause fatal outcome in any of the individuals infected intradermally in this experiment, meanwhile IN infection of mosRVFV was lethal to 1/3 of the animals. Another difference between the human and mosquito isolates was that mice succumbed within 5 days following infection with 100 PFU of huRVFV, whereas mice reached euthanasia criteria much later, on day 14 and 18 after infection with mosRVFV (Figure 21.).
Surprising results emerged from the body weight data too. Mice succumbed to mosRVFV were characterized by steep weight loss 2-3 days prior death. However, one intradermally and two intranasally infected animals lost considerable amount of weight, but all three animals regained and later exceeded their original body weight (refer to Figure 21.). Remarkably, testing the endpoint blood samples for RVFV-specific antibodies revealed that not only these three recovered and the two euthanised animals were seroconverted, but all other virus exposed animals, regardless of the infection route, too (Figure 24.). This implies that not only recovery from mosRVFV infection was possible, but that the majority of the infection was asymptomatic. Both, recovery and asymptomatic infection of mice with WT RVFV is not simply uncharacteristic but rather unprecedented. There is only a single mouse reported in the literature to survive infection with WT RVFV (strain ZH501) (Cartwright et al., 2020). This mouse, however, belong to the inbred strain NZO/HILtJ, which shows a polygenic syndrome of hyper obesity and is often used as a model for Type 2 diabetes (Igel et al., 1997). Therefore, it is safe to state that WT mice being asymptomatic or recovered following by WT RVFV infection is novel.

Sequencing data revealed 6 amino acid differences identified between the two isolates affecting the main virulence factor, NSs, which is encoded on the small segment. Although this study did not focus on the virulence mechanisms of NSs, reduced CPE of mosRVFV was observed in cell culture. Makino's group has reported that partial or complete deletion of the NSs gene resulted in decreased CPE, as indicated by turbulent virus plaque morphology observed in Vero E6 cells, compared to the clear plaques induced by the MP-12 strain (Ikegami et al., 2006). Similar differences in plaque morphology between huRVFV and mosRVFV were observed in this study as well (shown in Figure 44.), suggesting that the amino acid differences found in the NSs between the two isolates might influence the direct CPE of the virus. However, this hypothesis requires further verification, for example, through the use of a reverse genetic system. It is important to remember, that NSs contribute to viral pathogenesis via multiple ways beside direct cytopathic effect, therefore the reduced CPE may not be the only reason for the attenuated phenotype of mosRVFV. Additionally, currently there is no identified genotype linked to these different virulence mechanisms, therefore it is impossible to tell, whether these amino acid differences could be responsible for the different pathogenesis observed between the two isolates. However, it has been reported that the RVFV strain ZH-501 lacking its virulence gene (also known as the delta-NSs strain) was attenuated and caused sublethal infection in rat model following SC administration (Bird et al., 2008). Similar observations were made in mice and hamsters when researchers assessed the pathogenicity of the vaccine strain, Clone-13, which contains a large deletion on its NSs gene (M. Turell et al., 1995).

While there are similarities in pathogenesis between the delta-NSs strain and mosRVFV when used in mouse model, there are several differences between the two strains, as well. C57Bl/6J mice exhibited mortality upon infection with RVFV delta-NSs only when administered IN, but not when administered ID (Dodd et al., 2014b). Mice succumbed to the disease between 6-11 DPI, depending on the infection dose of RVFV delta-NSs administered IN but did not reach euthanasia criteria until 14-18 DPI following mosRVFV infection by the same route. Furthermore, the similar infection dose of delta-NSs to that of mosRVFV was sublethal to mice. Interestingly, while weight loss and occasional mortality were observed when mice were infected intradermally with mosRVFV, no fatal cases were reported when researchers infected mice subcutaneously with RVFV delta-NSs, despite using more than 3 log more virus for infection than was used in this study. Dodd and her colleagues suggested that the earlier adaptive immune response observed following footpad inoculation, compared to IN, contributed to the survival after RVFV delta-NSs infection. This was characterised by a robust pro-inflammatory T-cell response and more rapid and enhanced antibody production against the virus. While the T cell response was not investigated in this current study, the generation of virus-specific antibodies against the same antigen was assessed - and in contrast to Dodd's findings - no significant differences were found between the groups based on the infection route (as shown in Figure 32.).

No mosRVFV was detectable in any of the blood samples processed in this study (shown in Figure 22. and in Figure 31. A) which is in contrast to what was observed for huRVFV, which was present in the blood of all infected animals. In addition, Dodd et al. also reported that RVFV delta-NSs was viraemic regardless of the administration route (Dodd et al., 2014b). This leaves room for speculation that mosRVFV either does not have a viraemic phase, or if it does, it is either very short and occurs at a different time from the sample collection or is at a low level that does not exceed the detection limit. Assessment of viral load in various organs collected at the endpoint did not indicate a wide-spread dissemination, in contrast to what was observed for huRVFV or for other attenuated RVFV strains. None of the organs tested

positive for mosRVFV in any of the animals, except for the brains of the two animals that succumbed to the disease (Figure 23.). The reduced dissemination of mosRVFV and its confinement to the brain is novel. Researchers have previously reported that mice succumbed to encephalitis after IN infection with RVFV delta-NSs, showing significantly higher amounts of virus in their brains, while the virus was also present in their livers (Dodd et al., 2014b). Similarly, the vaccine strain MP-12, was also detectable in the spleen, liver and brain of infected animals despite causing only sublethal infection (Lang et al., 2016). It is unclear whether the organs were only transiently infected with mosRVFV but tested negative because the virus had been cleared by the time the samples were harvested, or whether they were never invaded by the virus at all.

As it was described in detail in the Introduction chapter, mosquito saliva has major effect on arbovirus infections, and it was already reported that saliva from Aedes aegypti positively influences RVFV pathogenesis in mice (Le Coupanec et al., 2013). Surprisingly, no significant changes could be observed by comparing ID mosRVFV infection with or without the presence of mosquito saliva; as both groups had the same mortality rate. While the group receiving additional saliva at the infection had a slightly lower mean body weight, during the second and third weeks of infection, compared to the group without saliva, this difference was not significant at any days. Seroconversion, again, was confirmed in all but one animal (shown in Figure 37.), indicating asymptomatic infection in most of the animals when infected with mosRVFV.
Interestingly, one animal in both groups reached humane endpoint criteria at 3 DPI, similar to the first pathogenesis experiment performed with mosRVFV, in which an ID infected animal lost weight during the first four days of infection, but later recovered (refer to Figure 21. and Figure 34) However, there was one animal in both groups that reached humane endpoint criteria at 7 DPI and 15 DPI following mosRVFV infection in the absence and presence of mosquito saliva, respectively. This delayed onset of symptoms following ID infection was not observed in the first pathogenesis experiment. This discrepancy involved only one animal/group and is believed to be due to the variable nature of in vivo systems, given the relatively small number of animals involved in this study, in accordance with the 3Rs principle. Interestingly, animals needed to be euthanised at the later time points, had high viral loads confined to their brains, however, the virus was undetectable in any of the organs collected from the animals euthanised at 3 DPI. This is interesting, because it is highly unlikely that viral clearance could have taken place in such a short time. While skin samples were not collected in this experiment, therefore it is possible that the virus was still present in the skin, however infection confined to the skin alone, should not induce such morbidity in these animals. Further experiments are needed to explain this scenario, including the harvest of additional tissues and the assessment of acute inflammatory markers.

Despite McKimmie's group reported that sialokinin in *Aedes spp*. saliva induces vascular leakage which favours arboviruses with tropism towards the brain to cross the BBB (Lefteri et al., 2022), the frequency of mosRVFV in the brain was unaffected by the presence of mosquito saliva. Furthermore, additional saliva at the time of inoculation did not promote the viral dissemination into any other tested organs either.
It is difficult to find definitive answers why mosquito saliva has not promoted the virulence of mosRVFV in mice based on the available experimental data. As mentioned in the Introduction, the main effect of mosquito saliva on virus spread is by 1. recruitment of susceptible immune cells (Pingen et al., 2016); 2. modulation of the cytokine milieu towards an inadequate immune

response against viruses (Guerrero et al., 2020; Visser et al., 2023); and 3. disruption of the BBB (Lefteri et al., 2022).
As these parameters were not examined in this study, it is impossible to tell whether these events took place here, however, some of the available results suggest, that even if they were, they may have not promoted viral dissemination anyways. For example, mosRVFV infected immune cells in the skin less frequently as huRVFV did, despite that the influx of the same immune cell population, targeted by the virus, was observable in both groups (Figure 48. and Supplementary Figure 1.). Furthermore, the spread of mosRVFV to the skin draining lymph nodes was also less frequent compared to huRVFV (as shown in Figure 26.), suggesting that this isolate may rely its spread less on recruited immune cells than other strains. Therefore, a potentially increased influx of the immune cells would have not increased mosRVFV dissemination. Additionally, the analyses of the histological sections of the brain suggests, that the virus reached the brain parenchyma via neuronal transport and not through the circulation. General H&E-stained sections of the brain following ID infection with mosRVFV showed pathomorphological changes characteristic to RVF encephalitis (Barbeau et al., 2020; Boyles et al., 2021; D. R. Smith et al., 2010), including nuclei fragmentation and blood vessel disintegration accompanied by micro bleeding, as observed in the brainstem. The anterior part of the brain, including the *bulbus olfactorius*, was free of pathological changes (as shown in Figure 38.). There was an observable gradient in the staining intensity decreasing towards the anterior part of the brain too. Scattered viral antigen was confined to glial, but not neuronal cells in the olfactory bulb. This is in contrasts with what researchers found using RVFV ZH501, as this isolate was present in the olfactory bulb even when the mice were infected through the dermal route (D. R. Smith et al., 2010; Terasaki & Makino, 2015). Furthermore, olfactory bulb was identified as entry site following IN inoculation of delta-NSs, as well (Dodd et al., 2014b).
Since, the choroid plexus, the meninges, and the endothelial cells were not labelled for RVFV antigen (as shown in Figure 40. and Figure 41.) and the fact that the mosRVFV was undetectable in the blood at any time point in all individuals, it is very likely, that mosRVFV does not invade the brain via the circulation. These findings do not exclude that the virus could potentially use the “Trojan horse” strategy to enter the brain parenchyma, although this way of brain invasion has never been observed in any *in vivo* models for RVFV. On the other hand, it is more likely, that mosRVFV infects peripheral neurons and migrates toward the brain through the spinal cord followed by the brainstem, utilizing retrograde axonal transfer. Although spinal cords were not collected in this study, some individuals exhibited hind limb paralysis, indicating neuronal damage in this area of the CNS. Brain invasion through peripheral neurons would partially explain the late-onset occurrence of the neurological symptoms, and why the potential BBB-disruptor effect of the mosquito described by McKimmie’s group (Lefteri et al., 2022) did not facilitate the virus accumulation in the brain. In addition, peripheral nerves were found to be infected sooner than the brain when RVFV delta-NSs was injected SC (Dodd et al., 2014b). Neuronal transport as a means of entry to the brain has been identified by others using other RVFV strains (strain not disclosed) (Reed et al., 2012). However, further experiments are needed to confirm this for mosRVFV as well.

5.2. Longitudinal viral dissemination

Both isolates were present in the skin following ID administration, however the viral load of mosRVFV was continuously declining after 2 DPI in contrast to huRVFV load, which was increasing and showed no signs of clearance (Figure 26. A).
The viral load in the skin draining lymph nodes exhibited a similar pattern to that in the skin. In the case of ID administration of huRVFV, all ALN samples were positive. However, when mice

were infected via the same route with mosRVFV, only one out of three daily samples tested positive. This tissue also tested virus free after 4 DPI. These results indicate that huRVFV had a better fitness in the skin than mosRVFV, although the latter one was still able to replicate and establish local infection with some limited dissemination to the draining lymph nodes.
Despite the higher mortality rate of mosRVFV upon IN infection compared to the ID route, the virus was undetectable in the lung at any time point, suggesting that this isolate either does not use the lung for its initial replication or its replication in this tissue is so low that it is not detectable via plaque forming assay. Whether this isolate targets cells in the upper respiratory tract or directly infects the olfactory or other peripheral nerves is impossible to tell, as these samples were not collected. It was also interesting, that the lung of the mice infected intranasally with huRVFV were not always positive for the virus either. In fact, intradermally infected animals with huRVFV had virus in their lung just as frequently as their IN counterpart (shown in Figure 26.). This may suggest that the fitness of huRVFV is higher in the skin than it is in the lung, which would explain the abortive infections observed in some IN-infected individuals in the pathogenesis experiment (refer to Figure 15.). The viral load in other organs indicates a faster dissemination of huRVFV following ID administration compared to IN administration, as the virus was detected one day earlier in ID-infected mice, except in the brain, where one IN-infected individual was positive at 3 DPI, while one ID-infected animal tested positive at 4 DPI. One possible explanation for the earlier detection of viral particles in organs in the case of ID infection is the presence of viral particles in the blood vessels of the organs. However, IHC analyses confirmed that the infected cells were located distal from the capillaries in all tested tissues (shown in Figure 28.). These findings indicate that the earlier presence of the virus in remote organs in the case of ID infection, was not due to viremia in these highly vascularized organs. However, it is very likely that huRVFV has reached remote organs earlier when administered intradermally, because it entered the blood and the lymphatics sooner, which probably facilitated its spread. Similarly, faster dissemination of RVFV ZH501 was reported following SC infection compared to IN infection by others (Gowen et al., 2013).
All organs (except the previously mentioned skin and ALN) were free from mosRVFV at all time points in this experiment as well, despite one animal has lost weight and all but one was seroconverted. Seroconversion indicates some level of viral replication following mosRVFV administration, because the same amount of huRVFV was not sufficient to generate antibody response. The initial replication of mosRVFV in the skin is evident, however, it is not clear where the virus was replicating in the IN-infected animals, as no virus could be detected in any of the tested samples at any time points. Some possible explanation could be: 1. the virus replicated in the upper respiratory tract - from which samples were not collected – and was cleared similarly to skin; 2. The virus replicated in the lung but with very low efficiency, hence it remains below the detection limit; 3. The virus infected periphery nerves but became eliminated before reaching the brain; 4. the virus may have reached the brain between 7 and 14 DPI and were eliminated but samples were not collected during this period. It is also possible that the virus was under tight control by the immune system, and the viral load remained below the detection limit in asymptomatic cases. There was one IN-infected animal sacrificed at 14 DPI, which almost reached the humane endpoint criteria by losing >19% of its original body weight, which indicates progressed morbidity, yet every sample collected from this individual was virus-free. It is possible that the virus was below the detection limit in the tested organs, or it was present in other tissues that were not harvested. Additionally, prominent weight loss could have resulted from a severe pro-inflammatory immune response, identified as a cause of death during other haemorrhagic fever virus infections (Jain et al.,

2020). However, the measurements recorded during this experiment do not provide sufficient data to confirm any of these possible explanations.

The fact that mosRVFV was not detectable at any time point in any remote organs despite the successful infection indicated by the seroconversion is surprising, because others reported that even RVFV delta-NSs was detectable in the brain following IN inoculation as early as 2 DPI, and was present in the blood, liver and spleen at 1 DPI upon SC or IN infection as well (Dodd et al., 2014b). This indicates that the altered amino acid sequence of the mosRVFV NSs alone should not prevent the virus from spreading to other organs in the host, even if these substitutions would lead to the dysfunction of the NSs. This suggests that other mechanisms are also involved and influence the pathogenesis of RVFV. In the hope of finding additional differences in their gene products that might be associated with the different disease phenotypes, the amino acid sequences of the two isolates were compared (see Table 12.). Despite clear association between the genotype and pathogenic phenotype of RVFV has not yet been established; Bird et al. identified numerous mutations between RVFV isolates causing lethal or sub-lethal infection in rats. These mutations were mostly affecting the Gn, NSs and the polymerase, but one mutation was found on the Gc and the Np too (Bird et al., 2007). Interestingly, the amino acid differences between huRVFV and mosRVFV were not located at the same position, observed by Bird and his colleagues.
Seven amino acid substitutions were detected between the proteins encoded on the M segment of the two isolates. A study conducted by Morrill et al., identified a single nucleotide and consequent amino acid substitution on the M segment associated with a more virulent phenotype (Morrill et al., 2010). At the position M847, G encodes a glycine, while A encodes a glutamic acid. Researchers found that the virus expressing Gn with the glutamic acid residue, caused mortality in mice quicker, and induced faster viral dissemination with higher viral loads compared to virus carrying glycine residue. Interestingly, the two isolates used in this study both encode the same glutamic acid. However, alterations found between huRVFV and mosRVFV at positions M397 and M428 are located on the surface of the Gn (as shown in Figure 42.). These amino acid differences affect the domain B of the protein. Since this domain is partially responsible for the attachment of the virus to cell surface receptors, it is theoretically possible that these mutations may influence how effectively the virus infects certain types of cells and, consequently, determine the tropism of the isolates. This hypothesis requires further investigation by using reverse genetics system. Additionally, one amino acid difference on the NSm was identified too. While NSm is dispensable for viral replication, it is identified as a minor virulence factor due to its antiapoptotic effect (Won et al., 2007), therefore the mutation of this protein can potentially result in altered pathogenesis, however specific genetic variance of NSm linked to virulence has not been identified yet.
Additionally, four amino acid differences were found in the L segment, which encodes the polymerase. Mutations affecting this gene may result in changes in the replication potential of the virus. However, the viral growth kinetics conducted in this study showed that the two isolates replicated in brain- and liver-derived cells to a mostly a similar extent (shown in Figure 43.), suggesting that the variance of the RdRp does not significantly affect viral replication capacity.

It was most surprising to see that despite the pronounced difference in the dissemination profile of the two isolates, displayed in mice; when propagated *in vitro*, using cells with liver, lung or brain origin; both isolates were capable of infecting and replicating in all three cell types to a mostly similar extent. Despite being immortalised cell lines of human origin, these

are commonly used in virological studies as alternatives to primary cells or animals and are widely accepted to represent their tissue of origin (Chang et al., 2022; Mignolet et al., 2023; Sainz et al., 2009; Shipley et al., 2017; C. D. Smith et al., 1986; Ujie et al., 2019; Q. Wang et al., 2019). These, like most *in vitro* systems, have their limitations too. For example, they can only represent a single cell type of the corresponding tissue. In the case of A549 cells, which correspond to type II alveolar epithelial cells (Lieber et al., 1976), their permissiveness for RVFV may or may not align with that of their type I counterparts. Additionally, SH-SY5Y cells used in this study were undifferentiated, resembling to unpolarised neuroblastoma cells, rather than differentiated neurons. Although, no indication was found in the available literature about whether differentiation of these cells would affect their permissivity to RVFV, or to any other viral pathogens. Transcriptomic analyses of the undifferentiated versus differentiated forms of these cells have identified genes mostly related to neuronal functions (Kovalevich & Langford, 2013; J. Li et al., 2015). Thus, absolute correlations between this experiment and *in vivo* results should not be assumed, but it is believed that the use of these cell lines is sufficient to test whether the two RVFV isolates have exclusive tropism for any of these cell types.
huRVFV and mosRVFV exhibited a similar cell type preference, with the highest viral replication was observed in the following order: neuronal cells, hepatocytes, and AECII cells (see Figure 46.). These findings are unexpected, because huRVFV showed pronounced tropism towards the liver and other visceral organs and was rarely detected in the brain. The robust replication of huRVFV in neuronal cells may support the theory that mice succumb to huRVFV infection before the virus would have had a chance to reach the brain. Notably, mosRVFV consistently yielded significantly lower virus titers compared to huRVFV when the isolates were grown in AECII cells, despite its higher mortality rate following intranasal (IN) infection. It is important to note that A549 cells in this study expressed Npro, which is an IFN antagonist of bovine viral diarrhoea virus, therefore the reduced replication capacity of mosRVFV in these cells is unlikely to be due to the potential lack of IFN inhibitory properties of NSs, related to the amino acid substitutions, identified earlier. This finding may support the theory of that this isolate may not primarily use lung cells for its initial replication. However, the observation that mosRVFV can replicate in all tested cell types in vitro, yet was exclusively found in the skin, ALN and the brain in vivo, suggests the existence of additional mechanisms influencing viral dissemination. These mechanisms cannot be solely explained by variations in cell tropism determined by the Gn protein and are not likely to be identified solely through *in vitro* systems.

5.3. Identification of early target cells

Characterization of APCs in the skin revealed that both isolates showed a higher affinity for non-leukocytic cells, as the majority of the infected cells lacked CD45. However, there was a noticeable difference in the frequency of infected cells between huRVFV and mosRVFV infections. huRVFV represented higher infection rate in both immune and non-immune cell populations. Furthermore, there were more infected cells in the draining lymph nodes in case of the infection with huRVFV than with mosRVFV (Figure 46. A). This is also in accordance with the viral load data gained during the serial euthanasia experiment, in which huRVFV produced higher viral load in the skin and its draining lymph node compared to mosRVFV (Figure 26.). This implies that huRVFV is most likely to establish infection in the skin and to migrate towards the lymphatics.

Interestingly, the two isolates showed no difference in preference among immune cells. They both infected the same types of immune cell (as shown in Figure 46. B). Due to the relative low number of infected cells, methods, such as t-distributed stochastic neighbour embedding

(tSNE), commonly used to visualize population defined by various markers simultaneously, was not suitable for this dataset, therefore a simpler approach was used for phenotyping the infected cell. By overlaying the infected immune cell population onto the whole immune population, allowed the identification of the targeted immune cells. This method has the disadvantage of not allowing the comparison of more than two markers at the same time. This makes the identification of certain subpopulations difficult. However, many immune cell types were successfully identified by focusing on exclusive cell surface markers (as shown in Figure 46. B).

For example, almost no infected cells expressed XCR1, which is the marker for cross-presenting cDC1 population. This indicates that these cells are not targeted by RVFV.

Similarly, no F4/80$^+$ cells – referring to both, tissue-resident and monocyte-derived macrophages – were detected with the virus. This was rather surprising because viral antigen was previously reported – via IHC analysis – in macrophages in several organs (Odendaal et al., 2019), including the skin (Vloet et al., 2017). Furthermore, monocyte-derived macrophages were also reported to be permissive for RVFV *in vitro* (McElroy & Nichol, 2012b). This discrepancy may be, because detection of RVFV via flow cytometry in this study was based on nucleotide probes, complementary to the mRNA of the Np, which requires the replication of the virus in the cell, unlike the detection of viral antigen via IHC, which can provide positive results even when the virion is inactivated. Since, macrophages are well-known for their phagocytic and cell-debris removing role, it is possible that infection of these cells implied by IHC-results are the consequence of macrophages engulfing dead cells containing the virus or virus fragments, but remained negative in this study, because the virus was not actively replicating in these phagocytic cells. Additionally, isolates used in this study could have a different tropism to what researchers used in the referenced publications.

The unique cell population of the skin called Langerhans cells are the local resident-macrophages, however they have exceptional migratory and subsequent antigen-presentation capability (Otsuka et al., 2018). They highly express Langerin and Ep-CAM, but this cell population was also found to be RVFV negative, excluding Langerhans cells as the early targets for RVFV.

Nonetheless, vast majority of the infected cells were CD11b$^+$ and CD64$^+$ double positive, marker, which are commonly found together on monocytes, and monocyte-derived macrophages or monocyte-derived DCs. As discussed above, the macrophage marker was not co-expressed with viral RNA, therefore this study identifies monocytes and possibly other monocyte-derived cells as the immune population mainly targeted by RVFV.

There was a noticeable difference in Ly-6C expression among these cells based on their location. Ly-6C is associated with inflammatory monocytes and moDCs. While in the skin, the majority of the infected cells were Ly-6C$^-$, in the draining lymph node, the infected cells were mostly positive for Ly-6C as well. It is not clear whether the Ly-6C$^-$ population is more targeted in the skin then Ly-6C$^+$ cells, or if the infected Ly-6C$^+$ cells migrated to the draining lymph node, contributing to the infected cell population in the ALNs and resulting in a less frequent population in the skin.

Differentiation between monocytes and moDCs is based on the presence of MHC II, as monocytes lack this marker. However, this analysis indicates that barely any infected cells in the lymph node express MHC II. This either suggests that the cells migrating towards the lymph nodes are not moDCs but rather monocytes, however this is contra-intuitive, given that the homing receptors of undifferentiated monocytes, CCR2 or CX_3CR1, direct them to inflamed or uninflamed tissues, respectively, but not towards the lymph nodes (Geissmann et al., 2003). On the other hand, it was reported that viruses can sometimes inhibit DC maturation and

prevent the upregulation of their MHC II molecules (Forsyth & Eisenlohr, 2016). It is not known whether RVFV has similar effect on APCs, but this could explain why most of the infected cells in the ALN are $CD11b^{+}CD64^{+}Ly\text{-}6C^{+}$ but $MHCII^{-}$.

Another interesting characteristic of these infected cells was their moderate expression of Langerin. The cells analysed in this study can be divided into three groups based on their Langerin expression: $Langerin^{-}$, $Langerin^{Mid}$ and $Langerin^{Hi}$, referring to their lack, medium or high expression of Langerin, respectively. Cells expressing Langerin with high intensity corresponds to Langerhans cells. This population, as mentioned before, is negative for the virus. Although infected cells can be found among the Langerin negative cells, most of the infected cells express Langerin on a moderate level. Furthermore, $Ly\text{-}6C^{+}$ cells in the skin and ALN are almost all $Langerin^{Mid}$. There are two reports about dendritic cell populations expressing Langerin yet being distinct from dermal LCs. Such cells were found in the dermis (Merad et al., 2008), as well as in peripheral lymph nodes (Douillard et al., 2005). However, these cells were characterized by being $CD11b^{Low}$ $MHCII^{+}$ in the skin or $CD11b^{Low}$ $CD8\alpha^{+}$ in the lymph node, meanwhile RVFV infected cells in this study are $CD11b^{+}$ and mostly $MHCII^{-}$ and $CD8\alpha^{-}$, indicating that infected cell in this study are different from the ones mentioned in the above referenced publications. There is no report in the currently available literature whether moDCs express Langerin. However, there is a growing number of evidence that monocytes can differentiate into LC-like population – also called monocyte-derived Langerhans cell (moLC) – under inflammatory circumstances. These cells were found in humans and in murine models, too (Ginhoux et al., 2006; Martínez-Cingolani et al., 2014; Otsuka et al., 2018; Picarda et al., 2016; Singh et al., 2016). Whether RVFV-infected $Langerin^{Mid}$ population corresponds to moLCs is not clear, as the reports are controversial about the Ep-CAM- and Langerin-expression found on moLCs. The current experimental design does not allow the investigation of the ontogeny of the infected cells and more detailed investigations are needed.

Comparison of immune cell populations in the skin and draining lymph nodes collected from infected and mock-treated mice revealed an expansion of immune cell populations that were identified as targets for RVFV. This $CD11b^{+}$ $CD64^{+}$ $Ly\text{-}6C^{+}$ $Langerin^{Mid}$ population was notably more frequent in the skin of infected animals compared to uninfected ones, while this population was virtually absent in the ALN of uninfected animals but was prominent in the infected animals, sown in Figure 48.

Flow cytometric data suggests that the main targets for RVFV in the skin are the local non-leukocytic cells and the recruited immune cells, rather than the local immune cell populations. Target cells for RVFV in the lung remained unidentified, as no virus-positive cells were detected (Figure 47.). The pathogenesis experiments indicated that IN administration of the virus might lead to unsuccessful infections due to unidentified factors. It's unclear whether this unfortunate scenario occurred, when none of the three exposed animals became infected, or if the samples tested negative due to the method's low sensitivity. Another explanation could be that the initial target cells following IN infection are not located in the lung.

Interestingly there was one lung sample harvested from an IN-infected mouse with mosRVFV, which represented some expansion of the $CD11b^{+}CD64^{+}Ly\text{-}6C^{+}Langerin^{Mid}$ population, may imply a possible ongoing infection (Figure 48. B), however, this was observed in only one animal, which can be due to individual differences. Regardless, target cells for RVFV-infection during respiratory-route remains to be identified.

6. Outlook

Although this study aimed to improve our understanding on how different factors influence the outcome of RVFV infection, yet it suggests that our current knowledge may not be universally applicable. By involving new, previously not tested natural RVFV isolates, it became evident that different factors, like infection route, should be placed into context regarding the virus isolate. This study found that different isolates might have adapted to different infection route.

The unexpected exclusive accumulation of the mosquito isolate in the brain, coupled with its previously unprecedented sub-lethal nature, could provide a much-needed “natural” mouse model. This model can not only help us study RVF encephalitis but also shed light on the mechanisms of recovery from this disease. As with all new *in vivo* models, several aspects of the pathogenesis remained to be unanswered, as it is with the currently used models as well. While other mouse models often rely on attenuated viral strains, gene-modified hosts, or a combination of both to study RVF encephalitis, this study identified a natural RVFV strain that exclusively caused neuropathic symptoms in WT mice, without an observable liver phase. Furthermore, this strain may result useful to identify host factors involved in successful viral clearance and recovery from RVFV infection.

Utilization of PrimeFlow™ assay provided information about the early target cells in which RVFV actively replicates following dermal exposure. These preliminary findings surprisingly identified dermal non-immune cells and recruited monocytes or monocyte-derived cells as site of early viral replication, not the local APCs. These monocyte-derived cells resemble to monocyte-derived Langerhans cells, but more research is needed on the ontogeny of this cell population, as well as its role in viral dissemination. As the samples analysed by flow cytometry in this study were collected at a single time point, our understanding on the very early events of RVFV infection is not complete. The same experiment performed longitudinally would help to provide a more detailed picture of the relationship between infection of immediately available and recruited cells.

This study did not investigate the activation and subsequent effector function of the immune cells. Such experiments may reveal whether the immune system responds differently to the isolates used in this study, which may be in association with the different tropism and mortality.

Nevertheless, these findings emphasize the limitations of research models, particularly when the same few virus strains are repeatedly utilized; and underscore the need for more comprehensive investigations involving other isolates from endemic areas.

7. References

Afonso, P. V., Ozden, S., Cumont, M. C., Seilhean, D., Cartier, L., Rezaie, P., Mason, S., Lambert, S., Huerre, M., Gessain, A., Couraud, P. O., Pique, C., Ceccaldi, P. E., & Romero, I. A. (2008). Alteration of blood-brain barrier integrity by retroviral infection. *PLoS Pathogens*, *4*(11). https://doi.org/10.1371/journal.ppat.1000205

Ahmed K, S. (2018). Rift Valley Fever in Chronic Carrier and Liver Manifestations. *Journal of Bioterrorism & Biodefense*, *09*(02). https://doi.org/10.4172/2157-2526.1000161

Akkaya, M., Kwak, K., & Pierce, S. K. (2020). B cell memory: building two walls of protection against pathogens. In *Nature Reviews Immunology* (Vol. 20, Issue 4, pp. 229–238). Nature Research. https://doi.org/10.1038/s41577-019-0244-2

Albe, J. R., Boyles, D. A., Walters, A. W., Kujawa, M. R., McMillen, C. M., Reed, D. S., & Hartman, A. L. (2019). Neutrophil and macrophage influx into the central nervous system are inflammatory components of lethal Rift Valley fever encephalitis in rats. *PLOS Pathogens*, *15*(6), e1007833. https://doi.org/10.1371/journal.ppat.1007833

Alhaj, M. (2016). Safety and Efficacy Profile of Commercial Veterinary Vaccines against Rift Valley Fever: A Review Study. *Journal of Immunology Research*, *2016*. https://doi.org/10.1155/2016/7346294

Alomar, A. A., Campbell, L. P., Mathias, D. K., & Burkett-Cadena, N. D. (2023). Rift Valley fever virus: a contagious pathogen affects human and livestock health. *EDIS*, *2023*(3). https://doi.org/10.32473/edis-in1403-2023

Alshammary, A. F., & Al-Sulaiman, A. M. (2021). The journey of SARS-CoV-2 in human hosts: a review of immune responses, immunosuppression, and their consequences. In *Virulence* (Vol. 12, Issue 1, pp. 1771–1794). Taylor and Francis Ltd. https://doi.org/10.1080/21505594.2021.1929800

Anderson, G. W., Slone, T. W., & Peters, C. J. (1988). The gerbil, Meriones unguiculatus, a model for Rift Valley fever viral encephalitis. In *Arch Virol* (Vol. 102).

Anywaine, Z., Lule, S. A., Hansen, C., Warimwe, G., & Elliott, A. (2022). Clinical manifestations of Rift Valley fever in humans: Systematic review and meta-analysis. *PLOS Neglected Tropical Diseases*, *16*(3), e0010233. https://doi.org/10.1371/journal.pntd.0010233

Ardain, A., Marakalala, M. J., & Leslie, A. (2020). Tissue-resident innate immunity in the lung. In *Immunology* (Vol. 159, Issue 3, pp. 245–256). Blackwell Publishing Ltd. https://doi.org/10.1111/imm.13143

Argentine, J. A., & James, A. A. (1995). Characterization of a salivary gland-specific esterase in the vector mosquito, Aedes aegypti. *Insect Biochemistry and Molecular Biology*, *25*(5), 621–630. https://doi.org/10.1016/0965-1748(94)00103-O

Atkins, C., & Freiberg, A. N. (2017). Recent advances in the development of antiviral therapeutics for Rift Valley fever virus infection. In *Future Virology* (Vol. 12, Issue 11, pp. 651–665). Future Medicine Ltd. https://doi.org/10.2217/fvl-2017-0060

Baer, A., Austin, D., Narayanan, A., Popova, T., Kainulainen, M., Bailey, C., Kashanchi, F., Weber, F., & Kehn-Hall, K. (2012). Induction of DNA Damage Signaling upon Rift Valley Fever Virus Infection Results in Cell Cycle Arrest and Increased Viral Replication. *Journal of Biological Chemistry*, *287*(10), 7399–7410. https://doi.org/10.1074/jbc.M111.296608

Bai, F., Kong, K. F., Dai, J., Qian, F., Zhang, L., Brown, C. R., Fikrig, E., & Montgomery, R. R. (2010). A paradoxical role for neutrophils in the pathogenesis of West Nile virus. *Journal of Infectious Diseases*, *202*(12), 1804–1812. https://doi.org/10.1086/657416

Bales, J. M., Powell, D. S., Bethel, L. M., Reed, D. S., & Hartman, A. L. (2012). Choice of inbred rat strain impacts lethality and disease course after respiratory infection with Rift Valley Fever Virus. *Frontiers in Cellular and Infection Microbiology*, *2*, 105. https://doi.org/10.3389/fcimb.2012.00105

Bamia, A., Marcato, V., Boissière, M., Mansuroglu, Z., Tamietti, C., Romani, M., Simon, D., Tian, G., Niedergang, F., Panthier, J.-J., Flamand, M., Souès, S., Bonnefoy, E., Bamia, C. A., & J-j, P. (2020). The NSs Protein Encoded by the Virulent Strain of Rift Valley Fever Virus Targets the Expression of Abl2 and the Actin Cytoskeleton of the Host, Affecting Cell Mobility, Cell Shape, and Cell-Cell Adhesion. *Journal of Virology*, *95*(1). https://doi.org/10.1128/JVI

Barbeau, D. J., Albe, J. R., Nambulli, S., Tilston-Lunel, N. L., Hartman, A. L., Lakdawala, S. S., Klein, E., Duprex, W. P., & McElroy, A. K. (2020). Rift Valley Fever Virus Infection Causes Acute Encephalitis in the Ferret. *MSphere*, *5*(5). https://doi.org/10.1128/mSphere.00798-20

Barbeau, D. J., Cartwright, H. N., Harmon, J. R., Spengler, J. R., Spiropoulou, C. F., Sidney, J., Sette, A., & McElroy, A. K. (2021). Identification and Characterization of Rift Valley Fever Virus-Specific T Cells Reveals a Dependence on CD40/CD40L Interactions for Prevention of Encephalitis. *Journal of Virology*, *95*(23). https://doi.org/10.1128/jvi.01506-21

Batista, L., Jouvion, G., Simon-Chazottes, D., Houzelstein, D., Burlen-Defranoux, O., Boissière, M., Tokuda, S., do Valle, T. Z., Cumano, A., Flamand, M., Montagutelli, X., & Panthier, J. J. (2020). Genetic dissection of Rift Valley fever pathogenesis: Rvfs2 locus on mouse chromosome 11 enables survival to early-onset hepatitis. *Scientific Reports*, *10*(1). https://doi.org/10.1038/s41598-020-65683-w

Bearer, E. L., Breakefield, X. O., Schuback, D., Reese, T. S., & LaVail, J. H. (2000). Retrograde axonal transport of herpes simplex virus: Evidence for a single mechanism and a role for tegument. *Proceedings of the National Academy of Sciences*, *97*(14), 8146–8150. https://doi.org/10.1073/pnas.97.14.8146

Bermejo-Jambrina, M., Eder, J., Helgers, L. C., Hertoghs, N., Nijmeijer, B. M., Stunnenberg, M., & Geijtenbeek, T. B. H. (2018). C-type lectin receptors in antiviral immunity and viral escape. In *Frontiers in Immunology* (Vol. 9, Issue MAR). Frontiers Media S.A. https://doi.org/10.3389/fimmu.2018.00590

Bird, B. H., Albariño, C. G., Hartman, A. L., Erickson, B. R., Ksiazek, T. G., & Nichol, S. T. (2008). Rift Valley Fever Virus Lacking the NSs and NSm Genes Is Highly Attenuated, Confers Protective Immunity from Virulent Virus Challenge, and Allows for Differential Identification of Infected and Vaccinated Animals. *Journal of Virology*, *82*(6), 2681–2691. https://doi.org/10.1128/jvi.02501-07

Bird, B. H., Khristova, M. L., Rollin, P. E., Ksiazek, T. G., & Nichol, S. T. (2007). Complete Genome Analysis of 33 Ecologically and Biologically Diverse Rift Valley Fever Virus Strains Reveals Widespread Virus Movement and Low Genetic Diversity due to Recent Common Ancestry. *Journal of Virology*, *81*(6), 2805–2816. https://doi.org/10.1128/jvi.02095-06

Bird, B. H., Ksiazek, T. G., Nichol, S. T., & Maclachlan, ; N James. (2009). Rift Valley fever virus. In *JAVMA* (Vol. 234, Issue 7).

Botros, B., Omar, A., Elian, K., Mohamed, G., Soliman, A., Salib, A., Salman, D., Saad, M., & Earhart, K. (2006). Adverse response of non-indigenous cattle of European breeds to live attenuated Smithburn Rift Valley fever vaccine. *Journal of Medical Virology*, *78*(6), 787–791. https://doi.org/10.1002/jmv.20624

Boyles, D. A., Schwarz, M. M., Albe, J. R., Mcmillen, C. M., O'malley, K. J., Reed, D. S., & Hartman, A. L. (2021). Development of Rift valley fever encephalitis in rats is mediated by

early infection of olfactory epithelium and neuroinvasion across the cribriform plate. *Journal of General Virology*, *102*, 1522. https://doi.org/10.1099/jgv.0.001522

Braciale, T. J., Sun, J., & Kim, T. S. (2012). Regulating the adaptive immune response to respiratory virus infection. In *Nature Reviews Immunology* (Vol. 12, Issue 4, pp. 295–305). https://doi.org/10.1038/nri3166

Bradl, M., & Lassmann, H. (2010). Oligodendrocytes: Biology and pathology. In *Acta Neuropathologica* (Vol. 119, Issue 1, pp. 37–53). https://doi.org/10.1007/s00401-009-0601-5

Bryden, S. R., Pingen, M., Lefteri, D. A., Miltenburg, J., Delang, L., Jacobs, S., Abdelnabi, R., Neyts, J., Pondeville, E., Major, J., Müller, M., Khalid, H., Tuplin, A., Varjak, M., Merits, A., Edgar, J., Graham, G. J., Shams, K., & McKimmie, C. S. (2020). Pan-viral protection against arboviruses by activating skin macrophages at the inoculation site. In *Sci. Transl. Med* (Vol. 12). https://www.science.org

Bustos-Arriaga, J., García-Machorro, J., León-Juárez, M., García-Cordero, J., Santos-Argumedo, L., Flores-Romo, L., Méndez-Cruz, A. R., Juárez-Delgado, F. J., & Cedillo-Barrón, L. (2011). Activation of the Innate Immune Response against DENV in Normal Non-Transformed Human Fibroblasts. *PLoS Neglected Tropical Diseases*, *5*(12), e1420. https://doi.org/10.1371/journal.pntd.0001420

Calisher, C. H., & Calzolari, M. (2021). Taxonomy of phleboviruses, emphasizing those that are sandfly-borne†. *Viruses*, *13*(5). https://doi.org/10.3390/v13050918

Calvo-Pinilla, E., Marín-López, A., Moreno, S., Lorenzo, G., Utrilla-Trigo, S., Jiménez-Cabello, L., Benavides, J., Nogales, A., Blasco, R., Brun, A., & Ortego, J. (2020). A protective bivalent vaccine against Rift Valley fever and bluetongue. *Npj Vaccines*, *5*(1). https://doi.org/10.1038/s41541-020-00218-y

Caroline, A. L., Powell, D. S., Bethel, L. M., Oury, T. D., Reed, D. S., & Hartman, A. L. (2014). Broad Spectrum Antiviral Activity of Favipiravir (T-705): Protection from Highly Lethal Inhalational Rift Valley Fever. *PLoS Neglected Tropical Diseases*, *8*(4), e2790. https://doi.org/10.1371/journal.pntd.0002790

Cartwright, H. N., Barbeau, D. J., & McElroy, A. K. (2020). Rift Valley Fever Virus Is Lethal in Different Inbred Mouse Strains Independent of Sex. *Frontiers in Microbiology*, *11*. https://doi.org/10.3389/fmicb.2020.01962

Chambers, T. J., & Diamond, M. S. (2003). Pathogenesis of flavivirus encephalitis. In *Current Topics in Microbiology and Immunology.* (Vol. 43, pp. 273–342). https://doi.org/10.1016/S0065-3527(03)60008-4

Chan, Y. K., & Gack, M. U. (2016). Viral evasion of intracellular DNA and RNA sensing. In *Nature Reviews Microbiology* (Vol. 14, Issue 6, pp. 360–373). Nature Publishing Group. https://doi.org/10.1038/nrmicro.2016.45

Chang, C.-W., Parsi, K., Somasundaran, M., Vanderleeden, E., Liu, P., Cruz, J., Cousineau, A., Finberg, R., & Kurt-Jones, E. (2022). A Newly Engineered A549 Cell Line Expressing ACE2 and TMPRSS2 Is Highly Permissive to SARS-CoV-2, Including the Delta and Omicron Variants. *Viruses*, *14*(7), 1369. https://doi.org/10.3390/v14071369

Choumet, V., Attout, T., Chartier, L., Khun, H., Sautereau, J., Robbe-Vincent, A., Brey, P., Huerre, M., & Bain, O. (2012). Visualizing Non Infectious and Infectious Anopheles gambiae Blood Feedings in Naive and Saliva-Immunized Mice. *PLoS ONE*, *7*(12), e50464. https://doi.org/10.1371/journal.pone.0050464

Chow, K. V., Lew, A. M., Sutherland, R. M., & Zhan, Y. (2016). Monocyte-Derived Dendritic Cells Promote Th Polarization, whereas Conventional Dendritic Cells Promote Th Proliferation.

The Journal of Immunology, *196*(2), 624–636. https://doi.org/10.4049/jimmunol.1501202

Chow, K. V., Sutherland, R. M., Zhan, Y., & Lew, A. M. (2017). Heterogeneity, functional specialization and differentiation of monocyte-derived dendritic cells. In *Immunology and Cell Biology* (Vol. 95, Issue 3, pp. 244–251). Nature Publishing Group. https://doi.org/10.1038/icb.2016.104

Cintolo, J. A., Datta, J., Mathew, S. J., & Czerniecki, B. J. (2012). Dendritic cell-based vaccines: Barriers and opportunities. In *Future Oncology* (Vol. 8, Issue 10, pp. 1273–1299). https://doi.org/10.2217/fon.12.125

Colonna, M., & Butovsky, O. (2017). Microglia function in the central nervous system during health and neurodegeneration. In *Annual Review of Immunology* (Vol. 35, pp. 441–468). Annual Reviews Inc. https://doi.org/10.1146/annurev-immunol-051116-052358

Connors, K. A., & Hartman, A. L. (2022). Advances in Understanding Neuropathogenesis of Rift Valley Fever Virus. *Annu. Rev. Virol*, *2022*, 437–450. https://doi.org/10.1146/annurev-virology-091919

Cristina Lebre, M., Antons, J. C., Kalinski, P., Schuitemaker, J. H. N., van Capel, T. M. M., Kapsenberg, M. L., & de Jong, E. C. (2003). Double-Stranded RNA-Exposed Human Keratinocytes Promote Th1 Responses by Inducing a Type-1 Polarized Phenotype in Dendritic Cells: Role of Keratinocyte-Derived Tumor Necrosis Factor α, Type I Interferons, and Interleukin-18. *Journal of Investigative Dermatology*, *120*(6), 990–997. https://doi.org/10.1046/j.1523-1747.2003.12245.x

Crozat, K., Guiton, R., Contreras, V., Feuillet, V., Dutertre, C.-A., Ventre, E., Vu Manh, T.-P., Baranek, T., Storset, A. K., Marvel, J., Boudinot, P., Hosmalin, A., Schwartz-Cornil, I., & Dalod, M. (2010). The XC chemokine receptor 1 is a conserved selective marker of mammalian cells homologous to mouse CD8α+ dendritic cells. *Journal of Experimental Medicine*, *207*(6), 1283–1292. https://doi.org/10.1084/jem.20100223

Daubney, R., Hudson, J. R., & Garnham, P. C. (1931). Enzootic hepatitis or rift valley fever. An undescribed virus disease of sheep cattle and man from east africa. *The Journal of Pathology and Bacteriology*, *34*(4), 545–579. https://doi.org/10.1002/path.1700340418

Davis, B. M., Rall, G. F., & Schnell, M. J. (2015). Everything You Always Wanted to Know about Rabies Virus (But Were Afraid to Ask). In *Annual Review of Virology* (Vol. 2, pp. 451–471). Annual Reviews Inc. https://doi.org/10.1146/annurev-virology-100114-055157

Debbabi, H., Ghosh, S., Kamath, A. B., Alt, J., deMello, D. E., Dunsmore, S., & Behar, S. M. (2005). Primary type II alveolar epithelial cells present microbial antigens to antigen-specific CD4+ T cells. *American Journal of Physiology-Lung Cellular and Molecular Physiology*, *289*(2), L274–L279. https://doi.org/10.1152/ajplung.00004.2005

Demeure, C. E., Brahimi, K., Hacini, F., Marchand, F., Péronet, R., Huerre, M., St.-Mezard, P., Nicolas, J.-F., Brey, P., Delespesse, G., & Mécheri, S. (2005). Anopheles Mosquito Bites Activate Cutaneous Mast Cells Leading to a Local Inflammatory Response and Lymph Node Hyperplasia . *The Journal of Immunology*, *174*(7), 3932–3940. https://doi.org/10.4049/jimmunol.174.7.3932

den Haan, J. M. M., Arens, R., & van Zelm, M. C. (2014). The activation of the adaptive immune system: Cross-talk between antigen-presenting cells, T cells and B cells. In *Immunology Letters* (Vol. 162, Issue 2, pp. 103–112). Elsevier. https://doi.org/10.1016/j.imlet.2014.10.011

DiPiazza, A., Nogales, A., Poulton, N., Wilson, P. C., Martínez-Sobrido, L., & Sant, A. J. (2017). Pandemic 2009 H1N1 Influenza Venus reporter virus reveals broad diversity of MHC class

II-positive antigen-bearing cells following infection in vivo. *Scientific Reports*, *7*(1), 10857. https://doi.org/10.1038/s41598-017-11313-x

Dodd, K. A., McElroy, A. K., Jones, M. E. B., Nichol, S. T., & Spiropoulou, C. F. (2013). Rift Valley Fever Virus Clearance and Protection from Neurologic Disease Are Dependent on CD4 + T Cell and Virus-Specific Antibody Responses . *Journal of Virology*, *87*(11), 6161–6171. https://doi.org/10.1128/jvi.00337-13

Dodd, K. A., McElroy, A. K., Jones, T. L., Zaki, S. R., Nichol, S. T., & Spiropoulou, C. F. (2014a). Rift Valley Fever Virus Encephalitis Is Associated with an Ineffective Systemic Immune Response and Activated T Cell Infiltration into the CNS in an Immunocompetent Mouse Model. *PLoS Neglected Tropical Diseases*, *8*(6), e2874. https://doi.org/10.1371/journal.pntd.0002874

Dodd, K. A., McElroy, A. K., Jones, T. L., Zaki, S. R., Nichol, S. T., & Spiropoulou, C. F. (2014b). Rift Valley Fever Virus Encephalitis Is Associated with an Ineffective Systemic Immune Response and Activated T Cell Infiltration into the CNS in an Immunocompetent Mouse Model. *PLoS Neglected Tropical Diseases*, *8*(6). https://doi.org/10.1371/journal.pntd.0002874

Dohm, D. J., Rowton, E. D., Lawyer, P. G., O'Guinn, M., & Turell, M. J. (2000). Laboratory Transmission of Rift Valley Fever Virus by *Phlebotomus duboscqi, Phlebotomus papatasi, Phlebotomus sergenti,* and *Sergentomyia schwetzi* (Diptera: Psychodidae). *Journal of Medical Entomology*, *37*(3), 435–438. https://doi.org/10.1093/jmedent/37.3.435

Domínguez, P. M., & Ardavín, C. (2010). Differentiation and function of mouse monocyte-derived dendritic cells in steady state and inflammation. In *Immunological Reviews* (Vol. 234).

Dong, M. B., Rahman, M. J., & Tarbell, K. V. (2016). Flow cytometric gating for spleen monocyte and DC subsets: Differences in autoimmune NOD mice and with acute inflammation. *Journal of Immunological Methods*, *432*, 4–12. https://doi.org/10.1016/j.jim.2015.08.015

Dorner, B. G., Dorner, M. B., Zhou, X., Opitz, C., Mora, A., Güttler, S., Hutloff, A., Mages, H. W., Ranke, K., Schaefer, M., Jack, R. S., Henn, V., & Kroczek, R. A. (2009). Selective Expression of the Chemokine Receptor XCR1 on Cross-presenting Dendritic Cells Determines Cooperation with CD8+ T Cells. *Immunity*, *31*(5), 823–833. https://doi.org/10.1016/j.immuni.2009.08.027

Douillard, P., Stoitzner, P., Tripp, C. H., Clair-Moninot, V., Aït-Yahia, S., McLellan, A. D., Eggert, A., Romani, N., & Saeland, S. (2005). Mouse Lymphoid Tissue Contains Distinct Subsets of Langerin/CD207+ Dendritic Cells, Only One of Which Represents Epidermal-Derived Langerhans Cells. *Journal of Investigative Dermatology*, *125*(5), 983–994. https://doi.org/10.1111/j.0022-202X.2005.23951.x

Doyle, J. D., Barbeau, D. J., Cartwright, H. N., & McElroy, A. K. (2022). Immune correlates of protection following Rift Valley fever virus vaccination. *Npj Vaccines*, *7*(1). https://doi.org/10.1038/s41541-022-00551-4

Dudziak, D., Kamphorst, A. O., Heidkamp, G. F., Buchholz, V. R., Trumpfheller, C., Yamazaki, S., Cheong, C., Liu, K., Lee, H.-W., Park, C. G., Steinman, R. M., & Nussenzweig, M. C. (2007). Differential Antigen Processing by Dendritic Cell Subsets in Vivo. *Science*, *315*(5808), 107–111. https://doi.org/10.1126/science.1136080

Duvaud, S., Gabella, C., Lisacek, F., Stockinger, H., Ioannidis, V., & Durinx, C. (2021). Expasy, the Swiss Bioinformatics Resource Portal, as designed by its users. *Nucleic Acids Research*, *49*(W1), W216–W227. https://doi.org/10.1093/nar/gkab225

Eiz-Vesper, B., & Schmetzer, H. M. (2020). Antigen-Presenting Cells: Potential of Proven und New Players in Immune Therapies. *Transfus Med Hemother*, *47*, 429–431. https://doi.org/10.1159/000512729

El, M., Sabiq, M. El, Omran, M., Abdalkareem, A., El, M. A., Mohamed, G., Elbashir, A., & Khalafala, O. (2009). Acute Renal Failure Associated With the Rift Valley Fever: A Single Center Study. In *Saudi J Kidney Dis Transpl* (Vol. 20, Issue 6). http://journals.lww.com/sjkd

Evans, A., Gakuya, F., Paweska, J. T., Rostal, M., Akoolo, L., Van Vuren, P. J., Manyibe, T., Macharia, J. M., Ksiazek, T. G., Feikin, D. R., Breiman, R. F., & Kariuki Njenga, M. (2008). Prevalence of antibodies against Rift Valley fever virus in Kenyan wildlife. *Epidemiology and Infection*, *136*(9), 1261–1269. https://doi.org/10.1017/S0950268807009806

Faburay, B., Gaudreault, N. N., Liu, Q., Davis, A. S., Shivanna, V., Sunwoo, S. Y., Lang, Y., Morozov, I., Ruder, M., Drolet, B., Scott McVey, D., Ma, W., Wilson, W., & Richt, J. A. (2016). Development of a sheep challenge model for Rift Valley fever. *Virology*, *489*, 128–140. https://doi.org/10.1016/j.virol.2015.12.003

Fakour, S., Naserabadi, S., & Ahmadi, E. (2017). The first positive serological study on rift valley fever in ruminants of Iran. *Journal of Vector Borne Diseases*, *54*(4), 348–352. https://doi.org/10.4103/0972-9062.225840

Forsyth, K. S., & Eisenlohr, L. C. (2016). Giving CD4+ T cells the slip: Viral interference with MHC class II-restricted antigen processing and presentation. In *Current Opinion in Immunology* (Vol. 40, pp. 123–129). Elsevier Ltd. https://doi.org/10.1016/j.coi.2016.03.003

Furuta, Y., Takahashi, K., Kuno-Maekawa, M., Sangawa, H., Uehara, S., Kozaki, K., Nomura, N., Egawa, H., & Shiraki, K. (2005). Mechanism of Action of T-705 against Influenza Virus. *Antimicrobial Agents and Chemotherapy*, *49*(3), 981–986. https://doi.org/10.1128/AAC.49.3.981-986.2005

Furuta, Y., Takahashi, K., Shiraki, K., Sakamoto, K., Smee, D. F., Barnard, D. L., Gowen, B. B., Julander, J. G., & Morrey, J. D. (2009). T-705 (favipiravir) and related compounds: Novel broad-spectrum inhibitors of RNA viral infections. *Antiviral Research*, *82*, 95–102. https://doi.org/10.1016/j.antiviral.2009.02.198

Ganaie, S. S., Schwarz, M. M., McMillen, C. M., Price, D. A., Feng, A. X., Albe, J. R., Wang, W., Miersch, S., Orvedahl, A., Cole, A. R., Sentmanat, M. F., Mishra, N., Boyles, D. A., Koenig, Z. T., Kujawa, M. R., Demers, M. A., Hoehl, R. M., Moyle, A. B., Wagner, N. D., … Hartman, A. L. (2021). Lrp1 is a host entry factor for Rift Valley fever virus. *Cell*, *184*(20), 5163-5178.e24. https://doi.org/10.1016/j.cell.2021.09.001

Gaudreault, N. N., Sabarish, ·, Indran, V., Velmurugan Balaraman, ·, Wilson, W. C., & Richt, J. A. (2019). Molecular aspects of Rift Valley fever virus and the emergence of reassortants. *Virus Genes*, *55*, 1–11. https://doi.org/10.1007/s11262-018-1611-y

Geissmann, F., Jung, S., & Littman, D. R. (2003). Blood Monocytes Consist of Two Principal Subsets with Distinct Migratory Properties. *Immunity*, *19*(1), 71–82. https://doi.org/10.1016/S1074-7613(03)00174-2

GeurtsvanKessel, C. H., & Lambrecht, B. N. (2008). Division of labor between dendritic cell subsets of the lung. *Mucosal Immunology*, *1*(6), 442–450. https://doi.org/10.1038/mi.2008.39

GeurtsvanKessel, C. H., Willart, M. A. M., Van Rijt, L. S., Muskens, F., Kool, M., Baas, C., Thielemans, K., Bennett, C., Clausen, B. E., Hoogsteden, H. C., Osterhaus, A. D. M. E., Rimmelzwaan, G. F., & Lambrecht, B. N. (2008). Clearance of influenza virus from the lung depends on migratory langerin+CD11b- but not plasmacytoid dendritic cells. *Journal of Experimental Medicine*, *205*(7), 1621–1634. https://doi.org/10.1084/jem.20071365

Ginhoux, F., & Jung, S. (2014). Monocytes and macrophages: Developmental pathways and tissue homeostasis. In *Nature Reviews Immunology* (Vol. 14, Issue 6, pp. 392–404). Nature Publishing Group. https://doi.org/10.1038/nri3671

Ginhoux, F., Tacke, F., Angeli, V., Bogunovic, M., Loubeau, M., Dai, X. M., Stanley, E. R., Randolph, G. J., & Merad, M. (2006). Langerhans cells arise from monocytes in vivo. *Nature Immunology*, *7*(3), 265–273. https://doi.org/10.1038/ni1307

Gommet, C., Billecocq, A., Jouvion, G., Hasan, M., Zaverucha do Valle, T., Guillemot, L., Blanchet, C., van Rooijen, N., Montagutelli, X., Bouloy, M., & Panthier, J.-J. (2011). Tissue Tropism and Target Cells of NSs-Deleted Rift Valley Fever Virus in Live Immunodeficient Mice. *PLoS Neglected Tropical Diseases*, *5*(12), e1421. https://doi.org/10.1371/journal.pntd.0001421

Gowen, B. B., Bailey, K. W., Scharton, D., Vest, Z., Westover, J. B., Skirpstunas, R., & Ikegami, T. (2013). Post-exposure vaccination with MP-12 lacking NSs protects mice against lethal Rift Valley fever virus challenge. *Antiviral Research*, *98*(2), 135–143. https://doi.org/10.1016/j.antiviral.2013.03.009

Gowen, B. B., Wong, M.-H., Jung, K.-H., Sanders, A. B., Mendenhall, M., Bailey, K. W., Furuta, Y., & Sidwell, R. W. (2007). In Vitro and In Vivo Activities of T-705 against Arenavirus and Bunyavirus Infections. *Antimicrobial Agents and Chemotherapy*, *51*(9), 3168–3176. https://doi.org/10.1128/AAC.00356-07

Gras, G., & Kaul, M. (2010). Molecular mechanisms of neuroinvasion by monocytes-macrophages in HIV-1 infection. *Retrovirology*, *7*(1), 30. https://doi.org/10.1186/1742-4690-7-30

Gray, K. K., Worthy, M. N., Juelich, T. L., Agar, S. L., Poussard, A., Ragland, D., Freiberg, A. N., & Holbrook, M. R. (2012). Chemotactic and Inflammatory Responses in the Liver and Brain Are Associated with Pathogenesis of Rift Valley Fever Virus Infection in the Mouse. *PLoS Neglected Tropical Diseases*, *6*(2), e1529. https://doi.org/10.1371/journal.pntd.0001529

Griffin, D. E. (2003). Immune responses to RNA-virus infections of the CNS. In *Nature Reviews Immunology* (Vol. 3, Issue 6, pp. 493–502). https://doi.org/10.1038/nri1105

Grobbelaar, A. A., Weyer, J., Leman, P. A., Kemp, A., Paweska, J. T., & Swanepoel, R. (2011). Molecular epidemiology of rift valley fever virus. *Emerging Infectious Diseases*, *17*(12), 2270–2276. https://doi.org/10.3201/eid1712.111035

Guerrero, D., Cantaert, T., & Missé, D. (2020). Aedes Mosquito Salivary Components and Their Effect on the Immune Response to Arboviruses. In *Frontiers in Cellular and Infection Microbiology* (Vol. 10). Frontiers Media S.A. https://doi.org/10.3389/fcimb.2020.00407

Guilliams, M., Lambrecht, B. N., & Hammad, H. (2013). Division of labor between lung dendritic cells and macrophages in the defense against pulmonary infections. In *Mucosal Immunology* (Vol. 6, Issue 3, pp. 464–473). https://doi.org/10.1038/mi.2013.14

Guillot, L., Nathan, N., Tabary, O., Thouvenin, G., Le Rouzic, P., Corvol, H., Amselem, S., & Clement, A. (2013). Alveolar epithelial cells: Master regulators of lung homeostasis. In *International Journal of Biochemistry and Cell Biology* (Vol. 45, Issue 11, pp. 2568–2573). Elsevier Ltd. https://doi.org/10.1016/j.biocel.2013.08.009

Guu, T. S. Y., Zheng, W., & Tao, Y. J. (2012). Bunyavirus: Structure and replication. *Advances in Experimental Medicine and Biology*, *726*, 245–266. https://doi.org/10.1007/978-1-4614-0980-9_11

Halldorsson, S., Li, S., Li, M., Harlos, K., Bowden, T. A., & Huiskonen, J. T. (2018). Shielding and activation of a viral membrane fusion protein. *Nature Communications*, *9*(1), 349. https://doi.org/10.1038/s41467-017-02789-2

Hamel, R., Dejarnac, O., Wichit, S., Ekchariyawat, P., Neyret, A., Luplertlop, N., Perera-Lecoin, M., Surasombatpattana, P., Talignani, L., Thomas, F., Cao-Lormeau, V.-M., Choumet, V., Briant, L., Desprès, P., Amara, A., Yssel, H., & Missé, D. (2015). Biology of Zika Virus Infection in Human Skin Cells. *Journal of Virology*, *89*(17), 8880–8896. https://doi.org/10.1128/JVI.00354-15

Harmon, J. R., Barbeau, D. J., Nichol, S. T., Spiropoulou, C. F., & McElroy, A. K. (2020). Rift Valley fever virus vaccination induces long-lived, antigen-specific human T cell responses. *Npj Vaccines*, *5*(1). https://doi.org/10.1038/s41541-020-0166-9

Harmon, J. R., Spengler, J. R., Coleman-McCray, J. D., Nichol, S. T., Spiropoulou, C. F., & McElroy, A. K. (2018). CD4 T Cells, CD8 T Cells, and Monocytes Coordinate To Prevent Rift Valley Fever Virus Encephalitis. *Journal of Virology*, *92*(24). https://doi.org/10.1128/jvi.01270-18

Hartl, D., Tirouvanziam, R., Laval, J., Greene, C. M., Habiel, D., Sharma, L., Yildirim, A. Ö., Dela Cruz, C. S., & Hogaboam, C. M. (2018). Innate Immunity of the Lung: From Basic Mechanisms to Translational Medicine. In *Journal of Innate Immunity* (Vol. 10, Issues 5–6, pp. 487–501). S. Karger AG. https://doi.org/10.1159/000487057

Hartman, A. (2017). Rift Valley Fever. *Clin Lab Med.*, *37*(2), 285–301. https://doi.org/10.1016/j.cll.2017.01.004

Herbert, J. A., & Panagiotou, S. (2022). Immune Response to Viruses. In *Encyclopedia of Infection and Immunity* (Vol. 1, pp. 429–444). Elsevier. https://doi.org/10.1016/B978-0-12-818731-9.00235-4

Higgins, B. W., McHeyzer-Williams, L. J., & McHeyzer-Williams, M. G. (2019). Programming Isotype-Specific Plasma Cell Function. In *Trends in Immunology* (Vol. 40, Issue 4, pp. 345–357). Elsevier Ltd. https://doi.org/10.1016/j.it.2019.01.012

Hilton, L., Moganeradj, K., Zhang, G., Chen, Y.-H., Randall, R. E., McCauley, J. W., & Goodbourn, S. (2006). The NPro Product of Bovine Viral Diarrhea Virus Inhibits DNA Binding by Interferon Regulatory Factor 3 and Targets It for Proteasomal Degradation. *Journal of Virology*, *80*(23), 11723–11732. https://doi.org/10.1128/jvi.01145-06

Hise, A. G., Traylor, Z., Hall, N. B., Sutherland, L. J., Dahir, S., Ermler, M. E., Muiruri, S., Muchiri, E. M., Kazura, J. W., Labeaud, A. D., King, C. H., & Stein, C. M. (2015). Association of Symptoms and Severity of Rift Valley Fever with Genetic Polymorphisms in Human Innate Immune Pathways. *PLoS Negl Trop Dis.*, *9*(3). https://doi.org/10.1371/journal.pntd.0003584

Hum, N. R., Bourguet, F. A., Sebastian, A., Lam, D., Phillips, A. M., Sanchez, K. R., Rasley, A., Loots, G. G., & Weilhammer, D. R. (2022). MAVS mediates a protective immune response in the brain to Rift Valley fever virus. *PLOS Pathogens*, *18*(5), e1010231. https://doi.org/10.1371/journal.ppat.1010231

Igel, M., Becker, W., Herberg, L., & Joost, H.-G. (1997). Hyperleptinemia, Leptin Resistance, and Polymorphic Leptin Receptor in the New Zealand Obese Mouse*. In *Endocrinology* (Vol. 138). https://academic.oup.com/endo/article/138/10/4234/2987735

Ikegami, T. (2019). Candidate vaccines for human Rift Valley fever. *Expert Opinion on Biological Therapy*, *19*(12), 1333–1342. https://doi.org/10.1080/14712598.2019.1662784

Ikegami, T., & Makino, S. (2011). The pathogenesis of rift valley fever. In *Viruses* (Vol. 3, Issue 5, pp. 493–519). https://doi.org/10.3390/v3050493

Ikegami, T., Narayanan, K., Won, S., Kamitani, W., & Peters, C. J. (2009). Rift Valley Fever Virus NSs Protein Promotes Post-Transcriptional Downregulation of Protein Kinase PKR and Inhibits eIF2a Phosphorylation. *PLoS Pathog*, *5*(2), 1000287. https://doi.org/10.1371/journal.ppat.1000287

Ikegami, T., Won, S., Peters, C. J., & Makino, S. (2006). Rescue of Infectious Rift Valley Fever Virus Entirely from cDNA, Analysis of Virus Lacking the NSs Gene, and Expression of a Foreign Gene. *Journal of Virology*, *80*(6), 2933–2940. https://doi.org/10.1128/jvi.80.6.2933-2940.2006

International Committee on Taxonomy of Viruses. (2023). *Current ICTV Taxonomy Release*. https://ictv.global/taxonomy/taxondetails?taxnode_id=202200163

Jain, S., Khaiboullina, S. F., & Baranwal, M. (2020). Immunological Perspective for Ebola Virus Infection and Various Treatment Measures Taken to Fight the Disease. *Pathogens*, *9*(10), 850. https://doi.org/10.3390/pathogens9100850

Jansen van Vuren, P., Tiemessen, C. T., & Paweska, J. T. (2011). Anti-nucleocapsid protein immune responses counteract pathogenic effects of Rift Valley fever virus infection in mice. *PLoS ONE*, *6*(9). https://doi.org/10.1371/journal.pone.0025027

Javelle, E., Lesueur, A., Pommier De Santi, V., De Laval, F., Lefebvre, T., Holweck, G., Durand, G. A., Leparc-Goffart, I., Texier, G., & Simon, F. (2020a). The challenging management of Rift Valley Fever in humans: Literature review of the clinical disease and algorithm proposal. In *Annals of Clinical Microbiology and Antimicrobials* (Vol. 19, Issue 1). BioMed Central Ltd. https://doi.org/10.1186/s12941-020-0346-5

Javelle, E., Lesueur, A., Pommier De Santi, V., De Laval, F., Lefebvre, T., Holweck, G., Durand, G. A., Leparc-Goffart, I., Texier, G., & Simon, F. (2020b). The challenging management of Rift Valley Fever in humans: Literature review of the clinical disease and algorithm proposal. *Annals of Clinical Microbiology and Antimicrobials*, *19*(1), 1–18. https://doi.org/10.1186/s12941-020-0346-5

Kamal, S. (2009). Pathological studies on postvaccinal reactions of Rift Valley fever in goats. *Virology Journal*, *6*(1), 94. https://doi.org/10.1186/1743-422X-6-94

Kambayashi, T., & Laufer, T. M. (2014). Atypical MHC class II-expressing antigen-presenting cells: Can anything replace a dendritic cell? In *Nature Reviews Immunology* (Vol. 14, Issue 11, pp. 719–730). Nature Publishing Group. https://doi.org/10.1038/nri3754

Kashem, S. W., Haniffa, M., & Kaplan, D. H. (2017). Antigen-Presenting Cells in the Skin. *Annual Review of Immunology*, *35*(1), 469–499. https://doi.org/10.1146/annurev-immunol-051116-052215

Kempkes, R. W. M., Joosten, I., Koenen, H. J. P. M., & He, X. (2019). Metabolic Pathways Involved in Regulatory T Cell Functionality. *Frontiers in Immunology*, *10*. https://doi.org/10.3389/fimmu.2019.02839

Kirsi,', J. J., North, J. A., Mckernan, P. A., Murray, B. K., Canonico, P. G., Huggins, J. W., Srivastava, P. C., & Robins5, R. K. (1983). Broad-Spectrum Antiviral Activity of 2-p-D-Ribofuranosylselenazole-4-Carboxamide, a New Antiviral Agentt. In *ANTiMICROBIAL AGENTS AND CHEMOTHERAPY* (Vol. 24, Issue 3).

Kitandwe, P. K., McKay, P. F., Kaleebu, P., & Shattock, R. J. (2022). An Overview of Rift Valley Fever Vaccine Development Strategies. In *Vaccines* (Vol. 10, Issue 11). MDPI. https://doi.org/10.3390/vaccines10111794

Koch, J., Xin, Q., Tischler, N. D., & Lozach, P. Y. (2021). Entry of phenuiviruses into mammalian host cells. *Viruses*, *13*(2). https://doi.org/10.3390/v13020299

Kovalevich, J., & Langford, D. (2013). Considerations for the use of SH-SY5Y neuroblastoma cells in neurobiology. *Methods in Molecular Biology*, *1078*, 9–21. https://doi.org/10.1007/978-1-62703-640-5_2

Kreher, F., Tamietti, C., Gommet, C., Guillemot, L., Ermonval, M., Failloux, A. B., Panthier, J. J., Bouloy, M., & Flamand, M. (2014). The Rift Valley fever accessory proteins NSm and P78/NSm-GN are distinct determinants of virus propagation in vertebrate and

invertebrate hosts. *Emerging Microbes and Infections*, *3*(10). https://doi.org/10.1038/emi.2014.71

Kroeker, A. L., Smid, V., Embury-Hyatt, C., Collignon, B., Pinette, M., Babiuk, S., & Pickering, B. (2020). Increased Susceptibility of Cattle to Intranasal RVFV Infection. *Frontiers in Veterinary Science*, *7*. https://doi.org/10.3389/fvets.2020.00137

Kroeker, A., Smid, V., Embury-Hyatt, C., Moffat, E., Collignon, B., Lung, O., Lindsay, R., & Weingartl, H. (2018). RVFV Infection in Goats by Different Routes of Inoculation. *Viruses*, *10*(12), 709. https://doi.org/10.3390/v10120709

Lacote, S., Tamietti, C., Chabert, M., Confort, M. P., Conquet, L., Pulido, C., Aurine, N., Baquerre, C., Thiesson, A., Pain, B., De Las Heras, M., Flamand, M., Montagutelli, X., Marianneau, P., Ratinier, M., & Arnaud, F. (2022). Intranasal Exposure to Rift Valley Fever Virus Live-Attenuated Strains Leads to High Mortality Rate in Immunocompetent Mice. *Viruses*, *14*(11). https://doi.org/10.3390/v14112470

Lam, J. H., Smith, F. L., & Baumgarth, N. (2020). B Cell Activation and Response Regulation During Viral Infections. *Viral Immunology*, *33*(4), 294–306. https://doi.org/10.1089/vim.2019.0207

Lang, Y., Henningson, J., Jasperson, D., Li, Y., Lee, J., Ma, J., Li, Y., Cao, N., Liu, H., Wilson, W., Richt, J., Ruder, M., McVey, S., & Ma, W. (2016). Mouse model for the Rift Valley fever virus MP12 strain infection. *Veterinary Microbiology*, *195*, 70–77. https://doi.org/10.1016/j.vetmic.2016.09.009

Lathan, R., Simon-Chazottes, D., Jouvion, G., Godon, O., Malissen, M., Flamand, M., Bruhns, P., & Panthier, J.-J. (2017). Innate Immune Basis for Rift Valley Fever Susceptibility in Mouse Models. *Scientific Reports*, *7*(1), 7096. https://doi.org/10.1038/s41598-017-07543-8

Lau, A. H., & Thomson, A. W. (2003). Dendritic cells and immune regulation in the liver. In *Gut* (Vol. 52, Issue 2, pp. 307–314). https://doi.org/10.1136/gut.52.2.307

Le Borgne, M., Etchart, N., Goubier, A., Lira, S. A., Sirard, J. C., van Rooijen, N., Caux, C., Aït-Yahia, S., Vicari, A., Kaiserlian, D., & Dubois, B. (2006). Dendritic Cells Rapidly Recruited into Epithelial Tissues via CCR6/CCL20 Are Responsible for CD8+ T Cell Crosspriming In Vivo. *Immunity*, *24*(2), 191–201. https://doi.org/10.1016/j.immuni.2006.01.005

Le Coupanec, A., Babin, D., Fiette, L., Jouvion, G., Ave, P., Misse, D., Bouloy, M., & Choumet, V. (2013). Aedes Mosquito Saliva Modulates Rift Valley Fever Virus Pathogenicity. *PLoS Neglected Tropical Diseases*, *7*(6). https://doi.org/10.1371/journal.pntd.0002237

Le May, N., Dubaele, S., Proietti De Santis, L., Billecocq, A., le Bouloy, M., & Egly, J.-M. (2004). TFIIH Transcription Factor, a Target for the Rift Valley Hemorrhagic Fever Virus viremia, and leads to miscarriage in pregnant animals, resulting in economic disaster in African countries. RVFV possesses a single-stranded segmented RNA genome. In *Cell* (Vol. 116).

Le May, N., Gauliard, N., Billecocq, A., & Bouloy, M. (2005). The N Terminus of Rift Valley Fever Virus Nucleoprotein Is Essential for Dimerization. *Journal of Virology*, *79*(18), 11974–11980. https://doi.org/10.1128/jvi.79.18.11974-11980.2005

Le May, N., Mansuroglu, Z., Lé ger, P., Josse, T., Blot, G., Billecocq, A., Flick, R., Jacob, Y., Bonnefoy, E., & le Bouloy, M. (2008). A SAP30 Complex Inhibits IFN-b Expression in Rift Valley Fever Virus Infected Cells. *PLoS Pathog.*, *4*(1). https://doi.org/10.1371/journal.ppat.0040013

Lebre, M. C., van der Aar, A. M. G., van Baarsen, L., van Capel, T. M. M., Schuitemaker, J. H. N., Kapsenberg, M. L., & de Jong, E. C. (2007). Human Keratinocytes Express Functional Toll-Like Receptor 3, 4, 5, and 9. *Journal of Investigative Dermatology*, *127*(2), 331–341. https://doi.org/10.1038/sj.jid.5700530

Lefteri, D. A., Bryden, S. R., Pingen, M., Terry, S., McCafferty, A., Beswick, E. F., Georgiev, G., Van der Laan, M., Mastrullo, V., Campagnolo, P., Waterhouse, R. M., Varjak, M., Merits, A., Fragkoudis, R., Griffin, S., Shams, K., Pondeville, E., & McKimmie, C. S. (2022). Mosquito saliva enhances virus infection through sialokinin-dependent vascular leakage. *Proceedings of the National Academy of Sciences*, *119*(24). https://doi.org/10.1073/pnas.2114309119

Léger, P., Tetard, M., Youness, B., Cordes, N., Rouxel, R. N., Flamand, M., & Lozach, P. Y. (2016). Differential Use of the C-Type Lectins L-SIGN and DC-SIGN for Phlebovirus Endocytosis. *Traffic*, *17*(6), 639–656. https://doi.org/10.1111/TRA.12393

Li, J., Ma, Z., Shi, M., Malty, R. H., Aoki, H., Minic, Z., Phanse, S., Jin, K., Wall, D. P., Zhang, Z., Urban, A. E., Hallmayer, J., Babu, M., & Snyder, M. (2015). Identification of Human Neuronal Protein Complexes Reveals Biochemical Activities and Convergent Mechanisms of Action in Autism Spectrum Disorders. *Cell Systems*, *1*(5), 361–374. https://doi.org/10.1016/j.cels.2015.11.002

Li, Z., Ji, C., Cheng, J., Åbrink, M., Shen, T., Kuang, X., Shang, Z., & Wu, J. (2022). Aedes albopictus salivary proteins adenosine deaminase and 34k2 interact with human mast cell specific proteases tryptase and chymase. *Bioengineered*, *13*(5), 13752–13766. https://doi.org/10.1080/21655979.2022.2081652

Liaskou, E., Wilson, D. V., & Oo, Y. H. (2012). Innate immune cells in liver inflammation. In *Mediators of Inflammation* (Vol. 2012). https://doi.org/10.1155/2012/949157

Lieber, M., Todaro, G., Smith, B., Szakal, A., & Nelson-Rees, W. (1976). A continuous tumor-cell line from a human lung carcinoma with properties of type II alveolar epithelial cells. *International Journal of Cancer*, *17*(1), 62–70. https://doi.org/10.1002/ijc.2910170110

Lim, P.-Y., Behr, M. J., Chadwick, C. M., Shi, P.-Y., & Bernard, K. A. (2011). Keratinocytes Are Cell Targets of West Nile Virus In Vivo. *Journal of Virology*, *85*(10), 5197–5201. https://doi.org/10.1128/JVI.02692-10

Lin, A., & Loré, K. (2017). Granulocytes: New members of the antigen-presenting cell family. In *Frontiers in Immunology* (Vol. 8, Issue DEC). Frontiers Media S.A. https://doi.org/10.3389/fimmu.2017.01781

Linthicum, K. J., Britch, S. C., & Anyamba, A. (2016). Rift Valley Fever: An Emerging Mosquito-Borne Disease∗. In *Annual Review of Entomology* (Vol. 61, pp. 395–415). Annual Reviews Inc. https://doi.org/10.1146/annurev-ento-010715-023819

Lozach, P.-Y., Kühbacher, A., Meier, R., Mancini, R., Bitto, D., Bouloy, M., & Helenius, A. (2011). DC-SIGN as a Receptor for Phleboviruses. *Cell Host & Microbe*, *10*(1), 75–88. https://doi.org/10.1016/j.chom.2011.06.007

Lubisi, B. A., Mutowembwa, P. B., Ndouvhada, P. N., Odendaal, L., Bastos, A. D. S., & Penrith, M. L. (2023). Experimental Infection of Domestic Pigs (Sus scrofa) with Rift Valley Fever Virus. *Viruses*, *15*(2). https://doi.org/10.3390/v15020545

Lun, M. P., Monuki, E. S., & Lehtinen, M. K. (2015). Development and functions of the choroid plexus-cerebrospinal fluid system. In *Nature Reviews Neuroscience* (Vol. 16, Issue 8, pp. 445–457). Nature Publishing Group. https://doi.org/10.1038/nrn3921

MacDonald, G. H., & Johnston, R. E. (2000). Role of Dendritic Cell Targeting in Venezuelan Equine Encephalitis Virus Pathogenesis. *Journal of Virology*, *74*(2), 914–922. https://doi.org/10.1128/JVI.74.2.914-922.2000

Majumdar, S., Pathak, S., & Nandi, D. (2018). Thymus - The syte for Development of Cellular Immunity. *Resonance*, *23*(2), 197–217. https://doi.org/10.1007/s12045-018-0605-3

Makoschey, B., van Kilsdonk, E., Hubers, W. R., Vrijenhoek, M. P., Smit, M., Wichgers Schreur, P. J., Kortekaas, J., & Moulin, V. (2016). Rift Valley Fever Vaccine Virus Clone 13 Is Able to

Cross the Ovine Placental Barrier Associated with Foetal Infections, Malformations, and Stillbirths. *PLOS Neglected Tropical Diseases*, *10*(3), e0004550. https://doi.org/10.1371/journal.pntd.0004550

Malet, H., Williams, H. M., Cusack, S., & Rosenthal, M. (2023). The mechanism of genome replication and transcription in bunyaviruses. In *PLoS Pathogens* (Vol. 19, Issue 1). Public Library of Science. https://doi.org/10.1371/journal.ppat.1011060

Mansuroglu, Z., Josse, T., Gilleron, J., Billecocq, A., Leger, P., Bouloy, M., & Bonnefoy, E. (2010). Nonstructural NSs Protein of Rift Valley Fever Virus Interacts with Pericentromeric DNA Sequences of the Host Cell, Inducing Chromosome Cohesion and Segregation Defects. *Journal of Virology*, *84*(2), 928–939. https://doi.org/10.1128/JVI.01165-09

Marín-López, A., Raduwan, H., Chen, T. Y., Utrilla-Trigo, S., Wolfhard, D. P., & Fikrig, E. (2023). Mosquito Salivary Proteins and Arbovirus Infection: From Viral Enhancers to Potential Targets for Vaccines. In *Pathogens* (Vol. 12, Issue 3). MDPI. https://doi.org/10.3390/pathogens12030371

Martínez-Cingolani, C., Grandclaudon, M., Jeanmougin, M., Jouve, M., Zollinger, R., & Soumelis, V. (2014). Human blood BDCA-1 dendritic cells differentiate into Langerhans-like cells with thymic stromal lymphopoietin and TGF-β. *Blood*, *124*(15), 2411–2420. https://doi.org/10.1182/blood-2014-04-568311

Maximova, O. A., Bernbaum, J. G., & Pletnev, A. G. (2016). West Nile Virus Spreads Transsynaptically within the Pathways of Motor Control: Anatomical and Ultrastructural Mapping of Neuronal Virus Infection in the Primate Central Nervous System. *PLoS Neglected Tropical Diseases*, *10*(9). https://doi.org/10.1371/journal.pntd.0004980

McComb, S., Thiriot, A., Akache, B., Krishnan, L., & Stark, F. (2019). Introduction to the Immune System. In *Methods in Molecular Biology* (Vol. 2024, pp. 1–24). Humana Press Inc. https://doi.org/10.1007/978-1-4939-9597-4_1

McElroy, A. K., & Nichol, S. T. (2012a). Rift Valley fever virus inhibits a pro-inflammatory response in experimentally infected human monocyte derived macrophages and a pro-inflammatory cytokine response may be associated with patient survival during natural infection. *Virology*, *422*(1), 6–12. https://doi.org/10.1016/j.virol.2011.09.023

McElroy, A. K., & Nichol, S. T. (2012b). Rift Valley fever virus inhibits a pro-inflammatory response in experimentally infected human monocyte derived macrophages and a pro-inflammatory cytokine response may be associated with patient survival during natural infection. *Virology*, *422*(1), 6–12. https://doi.org/10.1016/j.virol.2011.09.023

McGavern, D. B., & Kang, S. S. (2011a). Illuminating viral infections in the nervous system. In *Nature Reviews Immunology* (Vol. 11, Issue 5, pp. 318–329). https://doi.org/10.1038/nri2971

McGavern, D. B., & Kang, S. S. (2011b). Illuminating viral infections in the nervous system. In *Nature Reviews Immunology* (Vol. 11, Issue 5, pp. 318–329). https://doi.org/10.1038/nri2971

Méndez-Sánchez, N., Córdova-Gallardo, J., Barranco-Fragoso, B., & Eslam, M. (2021). Hepatic Dendritic Cells in the Development and Progression of Metabolic Steatohepatitis. In *Frontiers in Immunology* (Vol. 12). Frontiers Media S.A. https://doi.org/10.3389/fimmu.2021.641240

Meng, E. C., Goddard, T. D., Pettersen, E. F., Couch, G. S., Pearson, Z. J., Morris, J. H., & Ferrin, T. E. (2023). UCSF ChimeraX : Tools for structure building and analysis. *Protein Science*, *32*(11). https://doi.org/10.1002/pro.4792

Merad, M., Ginhoux, F., & Collin, M. (2008). Origin, homeostasis and function of Langerhans cells and other langerin-expressing dendritic cells. In *Nature Reviews Immunology* (Vol. 8, Issue 12, pp. 935–947). https://doi.org/10.1038/nri2455

Merad, M., Sathe, P., Helft, J., Miller, J., & Mortha, A. (2013). The dendritic cell lineage: Ontogeny and function of dendritic cells and their subsets in the steady state and the inflamed setting. In *Annual Review of Immunology* (Vol. 31, pp. 563–604). https://doi.org/10.1146/annurev-immunol-020711-074950

Mignolet, M., Gilloteaux, J., Halloin, N., Gueibe, M., Willemart, K., De Swert, K., Bielarz, V., Suain, V., Pastushenko, I., Gillet, N. A., & Nicaise, C. (2023). Viral Entry Inhibitors Protect against SARS-CoV-2-Induced Neurite Shortening in Differentiated SH-SY5Y Cells. *Viruses*, *15*(10), 2020. https://doi.org/10.3390/v15102020

Mohamed, M., Mosha, F., Mghamba, J., Zaki, S. R., Shieh, W. J., Paweska, J., Omulo, S., Gikundi, S., Mmbuji, P., Bloland, P., Zeidner, N., Kalinga, R., Breiman, R. F., & Njenga, M. K. (2010). Epidemiologic and clinical aspects of a Rift Valley fever outbreak in humans in Tanzania, 2007. *American Journal of Tropical Medicine and Hygiene*, *83*(2 SUPPL.), 22–27. https://doi.org/10.4269/ajtmh.2010.09-0318

Morrill, J. C., Ikegami, T., Yoshikawa-Iwata, N., Lokugamage, N., Won, S., Terasaki, K., Zamoto-Niikura, A., Peters, C. J., & Makino, S. (2010). Rapid accumulation of virulent rift valley fever virus in mice from an attenuated virus carrying a single nucleotide substitution in the M RNA. *PLoS ONE*, *5*(4). https://doi.org/10.1371/journal.pone.0009986

Murray, P. J., & Wynn, T. A. (2011). Protective and pathogenic functions of macrophage subsets. In *Nature Reviews Immunology* (Vol. 11, Issue 11, pp. 723–737). https://doi.org/10.1038/nri3073

Naik, S. H., Corcoran, L. M., & Wu, L. (2005). Development of murine plasmacytoid dendritic cell subsets. In *Immunology and Cell Biology* (Vol. 83, Issue 5, pp. 563–570). https://doi.org/10.1111/j.1440-1711.2005.01390.x

Nestle, F. O., Di Meglio, P., Qin, J. Z., & Nickoloff, B. J. (2009). Skin immune sentinels in health and disease. In *Nature Reviews Immunology* (Vol. 9, Issue 10, pp. 679–691). https://doi.org/10.1038/nri2622

Nfon, C. K., Marszal, P., Zhang, S., & Weingartl, H. M. (2012). Innate Immune Response to Rift Valley Fever Virus in Goats. *PLoS Negl Trop Dis*, *6*(4), 1623. https://doi.org/10.1371/journal.pntd.0001623

Nickoloff, B. J., & Turka, L. A. (1994). Immunological functions of non-professional antigen-presenting cells: new insights from studies of T-cell interactions with keratinocytes. *Immunology Today*, *15*(10), 464–469. https://doi.org/10.1016/0167-5699(94)90190-2

Odendaal, L., Clift, S. J., Fosgate, G. T., & Davis, A. S. (2019). Lesions and Cellular Tropism of Natural Rift Valley Fever Virus Infection in Adult Sheep. *Veterinary Pathology*, *56*(1), 61–77. https://doi.org/10.1177/0300985818806049/SUPPL_FILE/DS1_VET_10.1177_0300985818806049.PDF

Odendaal, L., Davis, A. S., & Venter, E. H. (2021). Insights into the pathogenesis of viral haemorrhagic fever based on virus tropism and tissue lesions of natural rift valley fever. In *Viruses* (Vol. 13, Issue 4). MDPI AG. https://doi.org/10.3390/v13040709

Ong, R.-Y., Lum, F.-M., & Ng, L. F. (2014). The fine line between protection and pathology in neurotropic flavivirus and alphavirus infections. *Future Virology*, *9*(3), 313–330. https://doi.org/10.2217/fvl.14.6

Otsuka, M., Egawa, G., & Kabashima, K. (2018). Uncovering the Mysteries of Langerhans Cells, Inflammatory Dendritic Epidermal Cells, and Monocyte-Derived Langerhans Cell-Like

Cells in the Epidermis. In *Frontiers in Immunology* (Vol. 9). Frontiers Media S.A. https://doi.org/10.3389/fimmu.2018.01768

Padovan, E., Landmann, R. M., & De Libero, G. (2007). How pattern recognition receptor triggering influences T cell responses: a new look into the system. *Trends in Immunology*, *28*(7), 308–314. https://doi.org/10.1016/j.it.2007.05.002

Pechkovsky, D. V, Goldmann, T., Ludwig, C., Prasse, A., Vollmer, E., Müller-Quernheim, J., & Zissel, G. (2005). CCR2 and CXCR3 agonistic chemokines are differently expressed and regulated in human alveolar epithelial cells type II. *Respiratory Research*, *6*(1), 75. https://doi.org/10.1186/1465-9921-6-75

Pepin, M., Bouloy, M., Bird, B. H., Kemp, A., & Paweska, J. (2010). Rift Valley fever virus (Bunyaviridae: Phlebovirus): An update on pathogenesis, molecular epidemiology, vectors, diagnostics and prevention. In *Veterinary Research* (Vol. 41, Issue 6). https://doi.org/10.1051/vetres/2010033

Phoenix, I., Nishiyama, S., Lokugamage, N., Hill, T. E., Huante, M. B., Slack, O. A. L., Carpio, V. H., Freiberg, A. N., & Ikegami, T. (2016). N-Glycans on the Rift Valley Fever Virus Envelope Glycoproteins Gn and Gc Redundantly Support Viral Infection via DC-SIGN. *Viruses*, *8*(5), 149. https://doi.org/10.3390/v8050149

Picarda, G., Chéneau, C., Humbert, J.-M., Bériou, G., Pilet, P., Martin, J., Duteille, F., Perrot, P., Bellier-Waast, F., Heslan, M., Haspot, F., Guillon, F., Josien, R., & Halary, F. A. (2016). Functional Langerinhigh-Expressing Langerhans-like Cells Can Arise from CD14highCD16− Human Blood Monocytes in Serum-Free Condition. *The Journal of Immunology*, *196*(9), 3716–3728. https://doi.org/10.4049/jimmunol.1501304

Piipponen, M., Li, D., & Landén, N. X. (2020). The Immune Functions of Keratinocytes in Skin Wound Healing. *International Journal of Molecular Sciences*, *21*(22), 8790. https://doi.org/10.3390/ijms21228790

Pingen, M., Bryden, S. R., Pondeville, E., Schnettler, E., Kohl, A., Merits, A., Fazakerley, J. K., Graham, G. J., & McKimmie, C. S. (2016). Host Inflammatory Response to Mosquito Bites Enhances the Severity of Arbovirus Infection. *Immunity*, *44*(6), 1455–1469. https://doi.org/10.1016/j.immuni.2016.06.002

Pingen, M., Schmid, M. A., Harris, E., & McKimmie, C. S. (2017). Mosquito Biting Modulates Skin Response to Virus Infection. In *Trends in Parasitology* (Vol. 33, Issue 8, pp. 645–657). Elsevier Ltd. https://doi.org/10.1016/j.pt.2017.04.003

Piper, M. E., Sorenson, D. R., & Gerrard, S. R. (2011). Efficient Cellular Release of Rift Valley Fever Virus Requires Genomic RNA. *PLoS ONE*, *6*(3), 18070. https://doi.org/10.1371/journal.pone.0018070

Protzer, U., Maini, M. K., & Knolle, P. A. (2012). Living in the liver: Hepatic infections. In *Nature Reviews Immunology* (Vol. 12, Issue 3, pp. 201–213). https://doi.org/10.1038/nri3169

Qu, C., Nguyen, V. A., Merad, M., & Randolph, G. J. (2009). MHC Class I/Peptide Transfer between Dendritic Cells Overcomes Poor Cross-Presentation by Monocyte-Derived APCs That Engulf Dying Cells. *The Journal of Immunology*, *182*(6), 3650–3659. https://doi.org/10.4049/jimmunol.0801532

Raymond, D. D., Piper, M. E., Gerrard, S. R., & Smith, J. L. (2010). Structure of the Rift Valley fever virus nucleocapsid protein reveals another architecture for RNA encapsidation. *PNAS*, *107*(26), 11769–11774. https://doi.org/10.1073/pnas.1001760107/-/DCSupplemental

Reed, C., Lin, K., Wilhelmsen, C., Friedrich, B., Nalca, A., Keeney, A., Donnelly, G., Shamblin, J., Hensley ¤a, L. E., Olinger, G., & Smith, D. R. (2013). Aerosol Exposure to Rift Valley Fever Virus Causes Earlier and More Severe Neuropathology in the Murine Model, which Has

Important Implications for Therapeutic Development. *PLoS Neglected Tropical Diseases*, *7*(4), e2156. https://doi.org/10.1371/journal.pntd.0002156

Reed, C., Steele, K. E., Honko, A., Shamblin, J., Hensley, L. E., & Smith, D. R. (2012). Ultrastructural study of Rift Valley fever virus in the mouse model. *Virology*, *431*(1–2), 58–70. https://doi.org/10.1016/j.virol.2012.05.012

Ribeiro, J. M. C. (2000). Blood-feeding in mosquitoes: probing time and salivary gland anti-haemostatic activities in representatives of three genera (Aedes, Anopheles, Culex). *Medical and Veterinary Entomology*, *14*(2), 142–148. https://doi.org/10.1046/j.1365-2915.2000.00227.x

Riel, D. Van, Verdijk, R., & Kuiken, T. (2015). The olfactory nerve: A shortcut for influenza and other viral diseases into the central nervous system. *Journal of Pathology*, *235*(2), 277–287. https://doi.org/10.1002/path.4461

Rissmann, M., Kley, N., Ulrich, R., Stoek, F., Balkema-Buschmann, A., Eiden, M., & Groschup, M. H. (2020). Competency of amphibians and reptiles and their potential role as reservoir hosts for rift valley fever virus. *Viruses*, *12*(11). https://doi.org/10.3390/v12111206

Rissmann, M., Lenk, M., Stoek, F., Szentiks, C. A., Eiden, M., & Groschup, M. H. (2021). Replication of rift valley fever virus in amphibian and reptile-derived cell lines. *Pathogens*, *10*(6). https://doi.org/10.3390/pathogens10060681

Rissmann, M., Stoek, F., Pickin, M. J., & Groschup, M. H. (2020). Mechanisms of inter-epidemic maintenance of Rift Valley fever phlebovirus. In *Antiviral Research* (Vol. 174). Elsevier B.V. https://doi.org/10.1016/j.antiviral.2019.104692

Ritter, M., Bouloy, le, Vialat, P., Janzen, C., Haller, O., & Frese, M. (2000). Printed in Great Britain Resistance to Rift Valley fever virus in Rattus norvegicus : genetic variability within certain ' inbred ' strains. In *Journal of General Virology* (Vol. 81).

Rock, J. R., & Hogan, B. L. M. (2011). Epithelial Progenitor Cells in Lung Development, Maintenance, Repair, and Disease. *Annual Review of Cell and Developmental Biology*, *27*(1), 493–512. https://doi.org/10.1146/annurev-cellbio-100109-104040

Rostal, M. K., Liang, J. E., Zimmermann, D., Bengis, R., Paweska, J., & Karesh, W. B. (2017). Rift Valley Fever: Does Wildlife Play a Role? *ILAR Journal*, *58*(3), 359–370. https://doi.org/10.1093/ilar/ilx023

Rottstegge, M., Tipton, T., Oestereich, L., Ruibal, P., Nelson, E. V., Olal, C., Port, J. R., Seibel, J., Pallasch, E., Bockholt, S., Koundouno, F. R., Boré, J. A., Rodríguez, E., Escudero-Pérez, B., Günther, S., Carroll, M. W., & Muñoz-Fontela, C. (2022). Avatar Mice Underscore the Role of the T Cell-Dendritic Cell Crosstalk in Ebola Virus Disease and Reveal Mechanisms of Protection in Survivors. *Journal of Virology*, *96*(18). https://doi.org/10.1128/jvi.00574-22

Rusu, M., Bonneau, R., Holbrook, M. R., Watowich, S. J., Birmanns, S., Wriggers, W., & Freiberg, A. N. (2012). An assembly model of Rift Valley fever virus. *Frontiers in Microbiology*, *3*(JUL). https://doi.org/10.3389/fmicb.2012.00254

Sainz, B., Barretto, N., & Uprichard, S. L. (2009). Hepatitis C Virus Infection in Phenotypically Distinct Huh7 Cell Lines. *PLoS ONE*, *4*(8), e6561. https://doi.org/10.1371/journal.pone.0006561

Sato, S., & Kiyono, H. (2012). The mucosal immune system of the respiratory tract. In *Current Opinion in Virology* (Vol. 2, Issue 3, pp. 225–232). https://doi.org/10.1016/j.coviro.2012.03.009

Scharton, D., Bailey, K. W., Vest, Z., Westover, J. B., Kumaki, Y., Van Wettere, A., Furuta, Y., & Gowen, B. B. (2014). Favipiravir (T-705) protects against peracute Rift Valley fever virus infection and reduces delayed-onset neurologic disease observed with ribavirin treatment. *Antiviral Res*, *104*, 84–92. https://doi.org/10.1016/j.antiviral.2014.01.016

Scharton, D., Van Wettere, A. J., Bailey, K. W., Vest, Z., Westover, J. B., Siddharthan, V., & Gowen, B. B. (2015). Rift Valley Fever Virus Infection in Golden Syrian Hamsters. *PLOS ONE*, *10*(1), e0116722. https://doi.org/10.1371/journal.pone.0116722

Schmid, M. A., & Harris, E. (2014a). Monocyte Recruitment to the Dermis and Differentiation to Dendritic Cells Increases the Targets for Dengue Virus Replication. *PLoS Pathogens*, *10*(12). https://doi.org/10.1371/journal.ppat.1004541

Schmid, M. A., & Harris, E. (2014b). Monocyte Recruitment to the Dermis and Differentiation to Dendritic Cells Increases the Targets for Dengue Virus Replication. *PLoS Pathogens*, *10*(12). https://doi.org/10.1371/journal.ppat.1004541

Schneider, B. S., & Higgs, S. (2008). The enhancement of arbovirus transmission and disease by mosquito saliva is associated with modulation of the host immune response. In *Transactions of the Royal Society of Tropical Medicine and Hygiene* (Vol. 102, Issue 5, pp. 400–408). https://doi.org/10.1016/j.trstmh.2008.01.024

Schneider, B. S., Soong, L., Coffey, L. L., Stevenson, H. L., McGee, C. E., & Higgs, S. (2010). Aedes aegypti saliva alters leukocyte recruitment and cytokine signaling by antigen-presenting cells during West Nile virus infection. *PLoS ONE*, *5*(7). https://doi.org/10.1371/journal.pone.0011704

Shin, K. S., Jeon, I., Kim, B. S., Kim, I. K., Park, Y. J., Koh, C. H., Song, B., Lee, J. M., Lim, J., Bae, E. A., Seo, H., Ban, Y. H., Ha, S. J., & Kang, C. Y. (2019). Monocyte-derived dendritic cells dictate the memory differentiation of CD8+ T cells during acute infection. *Frontiers in Immunology*, *10*(AUG). https://doi.org/10.3389/fimmu.2019.01887

Shipley, M. M., Mangold, C. A., Kuny, C. V., & Szpara, M. L. (2017). Differentiated Human SH-SY5Y Cells Provide a Reductionist Model of Herpes Simplex Virus 1 Neurotropism. *Journal of Virology*, *91*(23). https://doi.org/10.1128/JVI.00958-17

Singh, T. P., Zhang, H. H., Borek, I., Wolf, P., Hedrick, M. N., Singh, S. P., Kelsall, B. L., Clausen, B. E., & Farber, J. M. (2016). Monocyte-derived inflammatory Langerhans cells and dermal dendritic cells mediate psoriasis-like inflammation. *Nature Communications*, *7*. https://doi.org/10.1038/ncomms13581

Sizova, O., John, L. S., Ma, Q., & Molldrem, J. J. (2023). Multi-faceted role of LRP1 in the immune system. In *Frontiers in Immunology* (Vol. 14). Frontiers Media S.A. https://doi.org/10.3389/fimmu.2023.1166189

Smith, C. D., Craft, D. W., Shiromoto, R. S., & Yan, P. O. (1986). Alternative cell line for virus isolation. *Journal of Clinical Microbiology*, *24*(2), 265–268. https://doi.org/10.1128/jcm.24.2.265-268.1986

Smith, D. R., Bird, B. H., Lewis, B., Johnston, S. C., McCarthy, S., Keeney, A., Botto, M., Donnelly, G., Shamblin, J., Albariño, C. G., Nichol, S. T., & Hensley, L. E. (2012). Development of a Novel Nonhuman Primate Model for Rift Valley Fever. *Journal of Virology*, *86*(4), 2109–2120. https://doi.org/10.1128/jvi.06190-11

Smith, D. R., Steele, K. E., Shamblin, J., Honko, A., Johnson, J., Reed, C., Kennedy, M., Chapman, J. L., & Hensley, L. E. (2010). The pathogenesis of Rift Valley fever virus in the mouse model. *Virology*, *407*(2). https://doi.org/10.1016/j.virol.2010.08.016

Sofroniew, M. V., & Vinters, H. V. (2010). Astrocytes: Biology and pathology. In *Acta Neuropathologica* (Vol. 119, Issue 1, pp. 7–35). https://doi.org/10.1007/s00401-009-0619-8

Spiegel, M., Plegge, T., & Pöhlmann, S. (2016). The role of phlebovirus glycoproteins in viral entry, assembly and release. In *Viruses* (Vol. 8, Issue 7). MDPI AG. https://doi.org/10.3390/v8070202

Srivastava, B., Błażejewska, P., Heßmann, M., Bruder, D., Geffers, R., Mauel, S., Gruber, A. D., & Schughart, K. (2009). Host Genetic Background Strongly Influences the Response to Influenza A Virus Infections. *PLoS ONE*, *4*(3), e4857. https://doi.org/10.1371/journal.pone.0004857

Steinman, R. M., & Cohn, Z. A. (1973). Identification of a novel cell type in peripheral lymphoid organs of mice. I. Morphology, quantitation, tissue distribution. *The Journal of Experimental Medicine*, *137*(5), 1142–1162. https://doi.org/10.1084/jem.137.5.1142

Ströher, U., West, E., Bugany, H., Klenk, H.-D., Schnittler, H.-J., & Feldmann, H. (2001). Infection and Activation of Monocytes by Marburg and Ebola Viruses. *Journal of Virology*, *75*(22), 11025–11033. https://doi.org/10.1128/JVI.75.22.11025-11033.2001

Sun, M. H., Ji, Y. F., Li, G. H., Shao, J. W., Chen, R. X., Gong, H. Y., Chen, S. Y., & Chen, J. M. (2022). Highly adaptive Phenuiviridae with biomedical importance in multiple fields. In *Journal of Medical Virology* (Vol. 94, Issue 6, pp. 2388–2401). John Wiley and Sons Inc. https://doi.org/10.1002/jmv.27618

Surasombatpattana, P., Hamel, R., Patramool, S., Luplertlop, N., Thomas, F., Desprès, P., Briant, L., Yssel, H., & Missé, D. (2011). Dengue virus replication in infected human keratinocytes leads to activation of antiviral innate immune responses. *Infection, Genetics and Evolution*, *11*(7), 1664–1673. https://doi.org/10.1016/j.meegid.2011.06.009

Terasaki, K., & Makino, S. (2015). Interplay between the Virus and Host in Rift Valley Fever Pathogenesis. *J Innate Immun*, *7*, 450–458. https://doi.org/10.1159/000373924

Tezcan-Ulger, S., Kurnaz, N., Ulger, M., Aslan, G., & Emekdas, G. (2019). Serological evidence of Rift Valley fever virus among humans in Mersin province of Turkey. *Journal of Vector Borne Diseases*, *56*(4), 373–379.

Thangamani, S., & Wikel, S. K. (2009). Differential expression of Aedes aegypti salivary transcriptome upon blood feeding. *Parasites & Vectors*, *2*(1), 34. https://doi.org/10.1186/1756-3305-2-34

Theisen, D., & Murphy, K. (2017). The role of cDC1s in vivo: CD8 T cell priming through cross-presentation. *F1000Research*, *6*, 98. https://doi.org/10.12688/f1000research.9997.1

Turell, M. J., & Perkins, P. V. (1990). Transmission of Rift Valley Fever Virus by the Sand Fly, Phlebotomus duboscqi (Diptera: Psychodidae). *The American Journal of Tropical Medicine and Hygiene*, *42*(2), 185–188. https://doi.org/10.4269/ajtmh.1990.42.185

Turell, M., Saluzzo, J.-F., Dreier, T., Muller, R., Bouloy, M., Smith, J., & Lopez, N. (1995). Characterization of Clone 13, a Naturally Attenuated Avirulent Isolate of Rift Valley Fever Virus, which is Altered in the Small Segment *. *The American Journal of Tropical Medicine and Hygiene*, *53*(4), 405–411. https://doi.org/10.4269/ajtmh.1995.53.405

Ujie, M., Takada, K., Kiso, M., Sakai-Tagawa, Y., Ito, M., Nakamura, K., Watanabe, S., Imai, M., & Kawaoka, Y. (2019). Long-term culture of human lung adenocarcinoma A549 cells enhances the replication of human influenza A viruses. *Journal of General Virology*, *100*(10), 1345–1349. https://doi.org/10.1099/jgv.0.001314

van Furth, R., & Cohn, Z. A. (1968). The origin and kinetics of mononuclear phagocytes. *The Journal of Experimental Medicine*, *128*(3), 415–435. https://doi.org/10.1084/jem.128.3.415

Vialat, P., Muller, R., Vu, T. H., Prehaud, C., & Bouloy, M. (1997). Mapping of the mutations present in the genome of the Rift Valley fever virus attenuated MP12 strain and their putative role in attenuation. *Virus Research*, *52*(1), 43–50. https://doi.org/10.1016/S0168-1702(97)00097-X

Visser, I., Koenraadt, C. J. M., Koopmans, M. P. G., & Rockx, B. (2023). The significance of mosquito saliva in arbovirus transmission and pathogenesis in the vertebrate host. *One Health*, *16*. https://doi.org/10.1016/j.onehlt.2023.100506

Vloet, R. P. M., Vogels, C. B. F., Koenraadt, C. J. M., Pijlman, G. P., Eiden, M., Gonzales, J. L., van Keulen, L. J. M., Wichgers Schreur, P. J., & Kortekaas, J. (2017). Transmission of Rift Valley fever virus from European-breed lambs to Culex pipiens mosquitoes. *PLoS Neglected Tropical Diseases*, *11*(12). https://doi.org/10.1371/journal.pntd.0006145

Vogt, M. B., Lahon, A., Arya, R. P., Kneubehl, A. R., Spencer Clinton, J. L., Paust, S., & Rico-Hesse, R. (2018). Mosquito saliva alone has profound effects on the human immune system. *PLoS Neglected Tropical Diseases*, *12*(5). https://doi.org/10.1371/journal.pntd.0006439

Walters, A. W., Kujawa, M. R., Albe, J. R., Reed, D. S., Klimstra, W. B., & Hartman, A. L. (2019). Vascular permeability in the brain is a late pathogenic event during Rift Valley fever virus encephalitis in rats. *Virology*, *526*, 173–179. https://doi.org/10.1016/j.virol.2018.10.021

Wan, Y. Y., & Flavell, R. A. (2009). How diverse-CD4 effector T cells and their functions. In *Journal of Molecular Cell Biology* (Vol. 1, Issue 1, pp. 20–36). https://doi.org/10.1093/jmcb/mjp001

Wang, J., & Zhang, L. (2021). Retrograde axonal transport property of adeno-associated virus and its possible application in future. In *Microbes and Infection* (Vol. 23, Issue 8). Elsevier Masson s.r.l. https://doi.org/10.1016/j.micinf.2021.104829

Wang, Q., Ma, T., Wu, Y., Chen, Z., Zeng, H., Tong, Z., Gao, F., Qi, J., Zhao, Z., Chai, Y., Yang, H., Wong, G., Bi, Y., Wu, L., Shi, R., Yang, M., Song, J., Jiang, H., An, Z., … Yan, J. (2019). Neutralization mechanism of human monoclonal antibodies against Rift Valley fever virus. *Nature Microbiology*, *4*(7), 1231–1241. https://doi.org/10.1038/s41564-019-0411-z

Wang, X., Hu, C., Ye, W., Wang, J., Dong, X., Xu, J., Li, X., Zhang, M., Lu, H., Zhang, F., Wu, W., Dai, S., Wang, H.-W., & Chen, Z. (2022). Structure of Rift Valley Fever Virus RNA-Dependent RNA Polymerase. *Journal of Virology*, *96*(3), 1713–1734. https://doi.org/10.1128/JVI.01713-21

Wasserman, H. A., Singh, S., & Champagne, D. E. (2004). Saliva of the Yellow Fever mosquito, Aedes aegypti, modulates murine lymphocyte function. *Parasite Immunology*, *26*(6–7), 295–306. https://doi.org/10.1111/j.0141-9838.2004.00712.x

Weingartl, H. M., Zhang, S., Marszal, P., McGreevy, A., Burton, L., & Wilson, W. C. (2014). Rift Valley fever virus incorporates the 78 kDa glycoprotein into virions matured in mosquito C6/36 cells. *PLoS ONE*, *9*(1). https://doi.org/10.1371/journal.pone.0087385

WHO. (n.d.). *Prioritizing diseases for research and development in emergency contexts*. Retrieved August 31, 2023, from https://www.who.int/activities/prioritizing-diseases-for-research-and-development-in-emergency-contexts

WHO. (2019). *Efficacy trials of Rift Valley Fever vaccines and therapeutics Guidance on clinical trial design*. https://cdn.who.int/media/docs/default-source/blue-print/rift-valley-fever-blueprint-trial-design-meeting-report-2019.pdf?sfvrsn=ee74e0fb_3

Wichgers Schreur, P. J., Van Keulen, L., Kant, J., Oreshkova, N., Moormann, R. J. M., & Kortekaas, J. (2016). Co-housing of Rift Valley fever virus infected lambs with immunocompetent or immunosuppressed lambs does not result in virus transmission. *Frontiers in Microbiology*, *7*(MAR). https://doi.org/10.3389/fmicb.2016.00287

Wichit, S., Diop, F., Hamel, R., Talignani, L., Ferraris, P., Cornelie, S., Liegeois, F., Thomas, F., Yssel, H., & Missé, D. (2017). Aedes Aegypti saliva enhances chikungunya virus replication in human skin fibroblasts via inhibition of the type I interferon signaling pathway. *Infection, Genetics and Evolution*, *55*, 68–70. https://doi.org/10.1016/j.meegid.2017.08.032

Wichit, S., Ferraris, P., Choumet, V., & Missé, D. (2016). The effects of mosquito saliva on dengue virus infectivity in humans. In *Current Opinion in Virology* (Vol. 21, pp. 139–145). Elsevier B.V. https://doi.org/10.1016/j.coviro.2016.10.001

Won, S., Ikegami, T., Peters, C. J., & Makino, S. (2006). NSm and 78-Kilodalton Proteins of Rift Valley Fever Virus Are Nonessential for Viral Replication in Cell Culture. *Journal of Virology*, *80*(16), 8274–8278. https://doi.org/10.1128/JVI.00476-06

Won, S., Ikegami, T., Peters, C. J., & Makino, S. (2007). NSm Protein of Rift Valley Fever Virus Suppresses Virus-Induced Apoptosis. *Journal of Virology*, *81*(24), 13335–13345. https://doi.org/10.1128/jvi.01238-07

Wright, D., Kortekaas, J., Bowden, T. A., & Warimwe, G. M. (2019). Rift Valley fever: biology and epidemiology. *J Gen Virol*, *100*(8), 1187–1199. https://doi.org/10.1099/jgv.0.001296

Wynn, T. A., Chawla, A., & Pollard, J. W. (2013). Macrophage biology in development, homeostasis and disease. In *Nature* (Vol. 496, Issue 7446, pp. 445–455). https://doi.org/10.1038/nature12034

Xu, W., Watts, D. M., Costanzo, M. C., Tang, X., & Venegas, L. A. (2013). The Nucleocapsid Protein of Rift Valley Fever Virus Is a Potent Human CD8 + T Cell Antigen and Elicits Memory Responses. *PLoS ONE*, *8*(3), 59210. https://doi.org/10.1371/journal.pone.0059210

Yin, Z., Dai, J., Deng, J., Sheikh, F., Natalia, M., Shih, T., Lewis-Antes, A., Amrute, S. B., Garrigues, U., Doyle, S., Donnelly, R. P., Kotenko, S. V., & Fitzgerald-Bocarsly, P. (2012). Type III IFNs Are Produced by and Stimulate Human Plasmacytoid Dendritic Cells. *The Journal of Immunology*, *189*(6), 2735–2745. https://doi.org/10.4049/jimmunol.1102038

Zhang, C., Merana, G. R., Harris-Tryon, T., & Scharschmidt, T. C. (2022). Skin immunity: dissecting the complex biology of our body's outer barrier. In *Mucosal Immunology* (Vol. 15, Issue 4, pp. 551–561). Springer Nature. https://doi.org/10.1038/s41385-022-00505-y

Zhang, J., Raper, A., Sugita, N., Hingorani, R., Salio, M., Palmowski, M. J., Cerundolo, V., & Crocker, P. R. (2006). Characterization of Siglec-H as a novel endocytic receptor expressed on murine plasmacytoid dendritic cell precursors. *Blood*, *107*(9), 3600–3608. https://doi.org/10.1182/blood-2005-09-3842

Zhu, X., Guan, Z., Fang, Y., Zhang, Y., Guan, Z., Li, S., & Peng, K. (2023). Rift Valley Fever Virus Nucleoprotein Triggers Autophagy to Dampen Antiviral Innate Immune Responses. *Journal of Virology*, *97*(4). https://doi.org/10.1128/jvi.01814-22

8. Appendix

Supplementary table 1. Frequency of infected cells in different cell populations

		huRVFV skin		mosRVFV skin		huRVFV ALN		mosRVFV ALN	
% of infected cells in the parent population	Immune cells	0.022	0.073	0.021	0.03	0.15	0.16	0.012	0.027
	Non-Immune cells	0.17	0.32	0.05	0.025	0	0	0	0

The table contains the frequency of infected cells in different cell populations within the non-dump gate. Data were obtained from all pooled samples of mice infected ID with 200 PFU (100 PFU/ear) of either huRVFV or mosRVFV. Two days after infection, cells were harvested from the skin of the ears and their draining lymph nodes and were stained for flow cytometry.

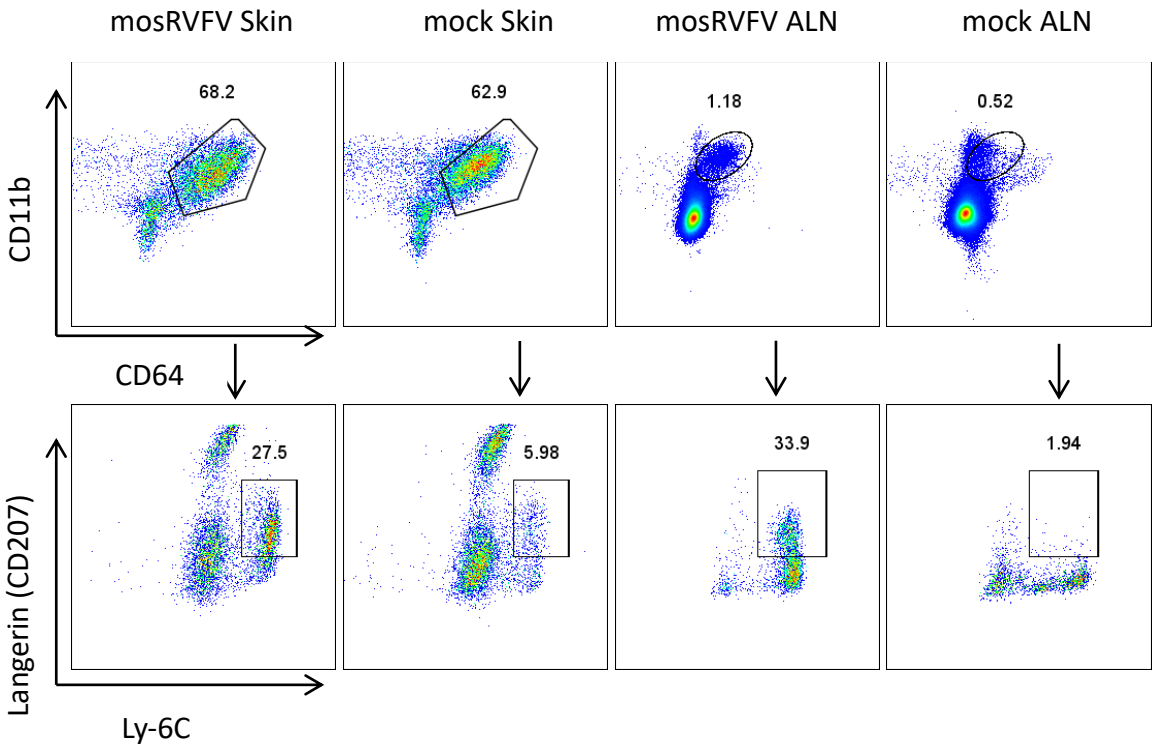

Supplementary Figure 1. Recruitment of monocytes/monocyte-derived cells upon ID mosRVFV infection.

Mice were infected ID mock or 200 PFU of mosRVFV. At 2 DPI cells were harvested from skin, ALN and stained for flow cytometry. Representative dot plots show the percentage distribution of CD11b and CD64 within the total immune cells, while the same distribution of Langerin and Ly-6C is shown within the $CD64^{+}CD11b^{+}$ cells.